Supporting Information for

Helicene-Derived Aggregation-Induced Emission Conjugates with Highly Tunable Circularly Polarized Luminescence

Chengshuo Shen,[a,b] Fuwei Gan,[a] Guoli Zhang,[a] Yongle Ding,[a] Jinghao Wang,[a] Ruibin Wang,[c] Jeanne Crassous,[d] Huibin Qiu*[a,b]

[a]School of Chemistry and Chemical Engineering, State Key Laboratory of Metal Matrix Composites, Shanghai Jiao Tong University, Shanghai 200240, China.

[b]State Key Laboratory for Modification of Chemical Fibers and Polymer Materials, College of Materials Science and Engineering, Donghua University, Shanghai 201620, China.

[c]Instrumental Analysis Center, Shanghai Jiao Tong University, Shanghai 200040, China.

[d]Univ Rennes, Institut des Sciences Chimiques de Rennes, UMR CNRS 6226, Campus de Beaulieu, Rennes 35042, France.

Corresponding author

*hbqiu@sjtu.edu.cn

Table of Contents

General information

All the synthetic experiments were performed using standard Schlenk techniques. Starting materials and reagents were of AR grade quality, which were purchased from commercial sources and used without further purification unless otherwise noted. Chiral resolution of bromohelicenes and ethynylhelicenes were performed at Daicel Chiral Technologies (China) Co., Ltd. NMR spectra were recorded on a Bruker Avance III HD 500 spectrometer or a Bruker Avance III HD 400 spectrometer. Spectra of ^{1}H NMR and ^{13}C NMR were provided in Figures S1–S32. Chemical shifts were determined using residual signals of the deuterated solvents or using TMS as the internal standard and were reported in parts per million (ppm). Due to the rotational barrier from excessive steric hindrance, **4-TH** and **4,13-BTH** showed multiple rotamers in ^{1}H NMR, and by variable temperature NMR, partial merging of the rotamer peaks were observed up to 373 K (Figures S29 and S32). MS spectra of **4-TH** and **4,13-BTH** were recorded on a Bruker SolariX 7.0 T Fourier Transform Ion Cyclotron (Figures S33 and S34). Single crystals of *rac*-2,15- bis(pinacolatoboryl)[6]helicene, *rac*-**2-TEH**, *rac*-**4-TEH**, *P*-**2,15-BTEH**, *M*-**4,13-BTEH**, *rac*-**2-TH**, *rac*-**4-TH**, *rac*-**2,15-BTH** and *P*-**2-TH** were obtained by slow evaporation method (details see Synthetic procedures), and their data were collected on a Bruker SMART APEX II CCD-based X-ray diffractometer with graphite-monochromatic Cu-Kα radiation (λ = 1.54178 Å) or Mo-Kα radiation (λ = 0.71073 Å) (See Tables S1–S3 for the crystal data and structure refinement, and Figures S35–S43 for the structures). UV-vis spectra were recorded using a Lambda 35 UV-vis spectrometer, and ECD spectra were recorded on a JASCO T-815 spectropolarimeter at 293 K in a 1 cm quartz cell. The emission spectra were recorded on a Horiba Fluorolog-3 spectrometer or on a Perkin Elmer LS 55 Luminescence Spectrometer, and the CPL spectra were recorded on a JASCO CPL-300 Spectrophotometer. The emission spectra of all the AIE-helicene conjugates with variation of water fraction were presented in Figures S44–S55.

Theoretical Calculation. For clarity and simplicity, we adopted the *P*-enantiomers for the calculations. Due to the rotations of single bonds on the molecules, *P*-**2-TH** and *P*-**4-TH** contains four reasonable rotamers, namely, (s-*trans*,*P*), (s-*trans*,*M*), (s-*cis*,*P*) and (s-*cis*,*M*) where s-*trans*/s-*cis*

for the stereochemistry of the single bond between helicene and C=C bond of TPE core, while *M*/*P* for the chirality of the TPE unit. Similarly, *P*-**2,15-BTH** and *P*-**4,13-BTH** has 10 reasonable rotamers with part of them possessing the degeneracy number of 2. DFT calculations were performed using Gaussian 09 program.[1] All geometries were optimized at B3LYP/6-311G(d,p) level[2] with SMD continuum solvent model for THF[3] without any symmetry assumptions. Harmonic vibration frequency calculations were performed at the same level for verifying the resulting geometries as local minima (with zero imaginary frequency). Occupancy for each conformation was calculated according to the Gibbs free energy of each conformer following a Boltzmann distribution at 298.15 K according to Eq. 1 for *P*-**2-TH** and *P*-**4-TH**, and Eq. 2 for *P*-**2,15-BTH** and *P*-**4,13-BTH**.

$$p_i = \frac{n_i}{\sum_j n_j} = \frac{e^{-\frac{\Delta G_i}{RT}}}{\sum_j e^{-\frac{\Delta G_j}{RT}}}, \quad (1)$$

$$p_i = \frac{g_i n_i}{\sum_j g_j n_j} = \frac{g_i e^{-\frac{\Delta G_i}{RT}}}{\sum_j g_j e^{-\frac{\Delta G_j}{RT}}}, \quad (2)$$

Where the p is the occupancy for the conformation, ΔG is the relative Gibbs free energy according to the conformation with lowest energy, R is the gas constant, T is the temperature in Kelvin and g is degeneracy of the rotamers. The results of energy calculations were presented in Tables S4–S11. TD-DFT calculations for each conformer were also performed at B3LYP/6-311G(d,p) level with SMD continuum solvent model for THF using optimized structures by Gaussian 09 program. The simulated UV-vis and ECD spectra of **BTEH** and **BTH** were presented in Figures S58–S65.

Synthetic procedures

Synthesis of 4-ethynyl[6]helicene.

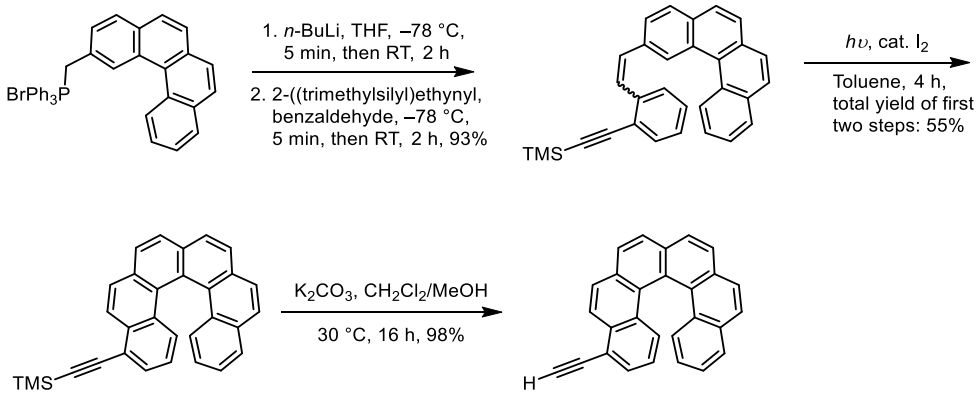

4-(trimethylsilylethynyl)[6]helicene:

1.17 g of (2-[4]helicenyl)triphenylphosphonium bromide[4] (2.0 mmol) was suspended in 20 mL of dry THF under argon and cooled to −78 °C. 1.4 mL of *n*-butyllithium (1.6 mol·L^{-1} in hexane, 2.2 mmol, 1.1 eq.) was added, and the reaction mixture was stirred at −78 °C for 5 min and then at room temperature for 30 min. The reaction mixture turned red during the procedure. Then the reaction mixture was cooled to −78 °C again and 404 mg of 2-((trimethylsilyl)ethynyl)benzaldehyde (2.0 mmol) dissolved in 5 mL of dry THF was added dropwise. The reaction was stirred at −78 °C for 5 min then at room temperature for 2 h. The solvent was removed in vacuum and the product was purified by a short silica column (eluent: CH_2Cl_2) to afford 790 mg of the stilbene derivatives as yellow oil (yield: 93%, mixture of *cis* and *trans* isomers). Then these stilbene derivatives were dissolved in 2 L of toluene and 50 mg of catalytic iodine was added. The solution was irradiated by a mercury lamp for 4 h. Then the solvent was removed, and the residue was purified by silica column chromatography (eluent: heptane) to afford 466 mg of the product as paled yellow solid (total yield: 55%).

^{1}H NMR (500 MHz, $CDCl_3$, 298 K): δ 8.52 (dd, J = 8.8 Hz, J = 0.8 Hz, 1H), 8.05 (d, J = 8.8 Hz, 1H) 8.02 (d, J = 8.1 Hz, 1H), 8.01 (d, J = 8.4 Hz, 1H), 8.00 (d, J = 8.4 Hz, 1H), 7.98 (d, J = 8.1 Hz, 1H), 7.93 (d, J = 8.6 Hz, 1H), 7.91 (d, J = 8.6 Hz, 1H), 7.82 (dd, J = 8.0 Hz, J = 1.4 Hz, 1H), 7.62 (dt, J = 8.6 Hz, J = 1.0 Hz, 1H), 7.53 (d, J = 8.4 Hz, 1H), 7.45 (dd, J = 7.2 Hz, J = 1.1 Hz, 1H), 7.22 (ddd, J = 8.0 Hz, J = 6.8 Hz, J = 1.2 Hz, 1H), 6.72 (ddd, J = 8.4 Hz, J = 6.8 Hz, J = 1.4 Hz, 1H), 6.60 (dd, J = 8.6 Hz, J = 7.2 Hz, 1H), 0.40 (s, 9H). ^{13}C{^{1}H} NMR (125 MHz, $CDCl_3$, 298 K): δ 133.32, 132.14, 131.90, 131.40, 131.36, 130.64, 129.85, 129.77, 128.79, 128.10, 128.09, 128.05, 127.74, 127.70, 127.56, 127.43, 127.30, 127.02, 126.26, 125.81, 125.71, 125.11, 124.16, 123.96, 120.19, 103.90, 99.08, 0.32.

4-ethynyl[6]helicene:

425 mg of 4-(trimethylsilylethynyl)[6]helicene (1 mmol), together with 552 mg of K_2CO_3 (4 mmol), was suspended in a mixture of 20 mL of CH_2Cl_2 and 20 mL of MeOH. The reaction mixture was stirred at 30 °C for 16 hours. Afterwards, 50 mL of H_2O was added into the suspension, and then the reaction mixture was extracted by CH_2Cl_2 and washed with water and brine. The organic layer was dried over Na_2SO_4, concentrated in vacuum and purified with a short silica column (eluent: CH_2Cl_2) to afford 345 mg of the product as paled yellow solid (yield: 98%).

^{1}H NMR (500 MHz, $CDCl_3$, 298 K): δ 8.53 (dd, J = 8.8 Hz, J = 0.8 Hz, 1H), 8.05 (d, J = 8.8 Hz, 1H) 8.03 (d, J = 8.1 Hz, 1H), 8.01 (d, J = 8.4 Hz, 1H), 8.00 (d, J = 8.4 Hz, 1H), 7.99 (d, J = 8.1 Hz, 1H), 7.94 (d, J = 8.6 Hz, 1H), 7.92 (d, J = 8.6 Hz, 1H), 7.83 (dd, J = 7.9 Hz, J = 1.4 Hz, 1H), 7.65 (dt, J = 8.6 Hz, J = 1.1 Hz, 1H), 7.53 (d, J = 8.4 Hz, 1H), 7.47 (dd, J = 7.1 Hz, J = 1.1 Hz, 1H), 7.23 (ddd, J = 7.9 Hz, J = 6.8 Hz, J = 1.2 Hz, 1H), 6.72 (ddd, J = 8.4 Hz, J = 6.8 Hz, J = 1.4 Hz, 1H), 6.62 (dd, J = 8.6 Hz, J = 7.1 Hz, 1H), 3.52 (s, 1H). ^{13}C{^{1}H} NMR (125 MHz, $CDCl_3$, 298 K): δ 133.34, 132.26, 131.93, 131.43, 131.36, 130.95, 129.90, 129.76, 129.03, 128.14, 128.07, 128.03, 127.75, 127.72, 127.61, 127.55, 127.52, 127.26, 127.04, 126.28, 125.75, 125.59, 125.08, 124.14, 123.94, 119.19, 82.55, 81.78.

Synthesis of 4-bromo[6]helicene.

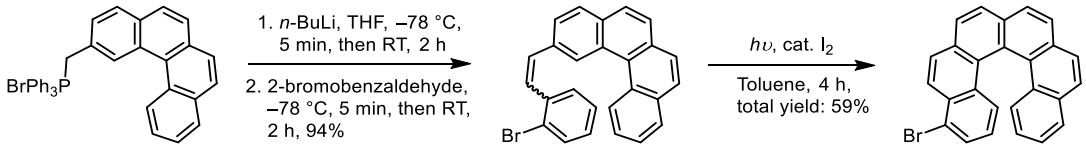

1.17 g of (2-[4]helicenyl)triphenylphosphonium bromide[4] (2.0 mmol) was suspended in 20 mL of dry THF under argon and cooled to −78 °C. 1.4 mL of *n*-butyllithium (1.6 mol·L^{-1} in hexane, 2.2 mmol, 1.1 eq.) was added, and the reaction mixture was stirred at −78 °C for 5 min and then at room temperature for 30 min, and the reaction mixture turned red during the procedure. Then the reaction mixture was cooled to −78 °C again and 370 mg of 2-bromobenzaldehyde (2.0 mmol) dissolved in 5 mL of dry THF was added dropwise. The reaction was stirred at −78 °C for 5 min then at room temperature for 2 h. The solvent was removed in vacuum and the product was purified by short silica column chromatography (eluent: CH_2Cl_2) to afford 766 mg of the stilbene derivatives as yellow oil (yield: 94%, mixture of *cis* and *trans* isomers). Then these stilbene derivatives were dissolved in 2 L of toluene and 50 mg of catalytic iodine was added. The solution was irradiated by a mercury lamp for 4 h. Then the solvent was removed, and the residue was purified by silica column chromatography (heptane : CH_2Cl_2 = 10 : 1, *v*/*v*) to afford 482 mg of the product as paled yellow solid (total yield: 59%).

^{1}H NMR (500 MHz, $CDCl_3$, 298 K): δ 8.40 (dd, J = 8.8 Hz, J = 0.6 Hz, 1H), 8.04 (d, J = 8.8 Hz, 1H), 8.03 (d, J = 8.2 Hz, 1H), 8.01 (d, J = 8.2 Hz, 1H), 8.00 (d, J = 8.2 Hz, 1H), 7.99 (d, J = 8.2 Hz, 1H), 7.93 (d, J = 8.6 Hz, 1H), 7.92 (d, J = 8.6 Hz, 1H), 7.82 (dd, J = 7.9 Hz, J = 1.1 Hz, 1H), 7.61 (dt, J = 8.5 Hz, J = 0.9 Hz, 1H), 7.51 (dt, J = 8.6 Hz, J = 0.6 Hz, 1H), 7.50 (dd, J = 7.5 Hz, J = 1.1 Hz, 1H), 7.23 (ddd, J = 7.9 Hz, J = 6.9 Hz, J = 1.1 Hz, 1H), 6.73 (ddd, J = 8.5 Hz, J = 6.9 Hz, J = 1.4 Hz, 1H), 6.49(dd, J = 8.5 Hz, J = 7.5 Hz, 1H). ^{13}C{^{1}H} NMR (125 MHz, $CDCl_3$, 298 K): δ 133.50, 131.95, 131.73, 131.49, 131.34, 130.26, 129.80, 128.20, 128.06, 127.95, 127.92, 127.85, 127.75, 127.74, 127.69, 127.67, 127.16, 127.02, 126.48, 126.28, 125.80, 125.13, 125.00, 124.15, 122.41.

Synthesis of 4,13-dibromo[6]helicene.

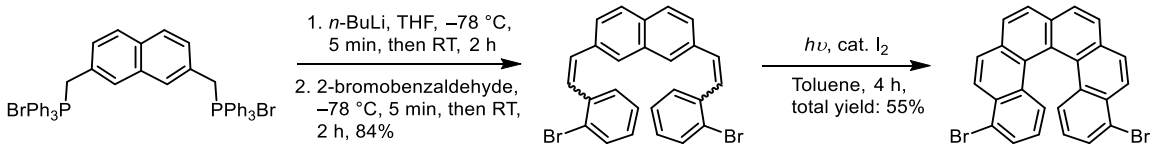

838 mg of 2,7-naphthyldimethyl bis(triphenylphosphonium bromide) (1.0 mmol) was suspended in 20 mL of dry THF under argon and cooled to −78 °C. 1.4 mL of *n*-butyllithium (1.6 mol·L^{-1} in hexane, 2.2 mmol, 1.1 eq.) was added, and the reaction mixture was stirred at −78 °C for 5 min and then at room temperature for 30 min, and the reaction mixture turned red during the procedure. Then the reaction mixture was cooled to −78 °C again and 370 mg of 2-bromobenzaldehyde (2.0 mmol) dissolved in 5 mL of dry THF was added dropwise. The reaction was stirred at −78 °C for 5 min then at room temperature for 2 h. The solvent was removed in vacuum and the product was purified by short silica column chromatography (eluent: CH_2Cl_2) to afford 411 mg of the stilbene derivatives as yellow oil (yield: 84%, mixture of *cis* and *trans* isomers). Then these stilbene derivatives were dissolved in 2 L of toluene and 50 mg of catalytic iodine was added. The solution was irradiated by a mercury lamp for 4 h. Then the solvent was removed, and the residue was purified by silica column chromatography (heptane : CH_2Cl_2 = 10 : 1, *v*/*v*) to afford 265 mg of the product as paled yellow solid (total yield: 55%).

^{1}H NMR (500 MHz, $CDCl_3$, 298 K): δ 8.40 (d, J = 8.8 Hz, 2H), 8.06 – 8.00 (m, 6H), 7.53 – 7.49 (m, 4H), 6.55 (t, J = 8.0 Hz, 2H). ^{13}C{^{1}H} NMR (125 MHz, $CDCl_3$, 298 K): δ 133.76, 131.50, 131.45, 130.32, 129.94, 127.89, 127.86, 127.54, 127.54, 126.69, 125.34, 124.09, 122.52.

Synthesis of 2,15-bis(pinacolatoboryl)[6]helicene.

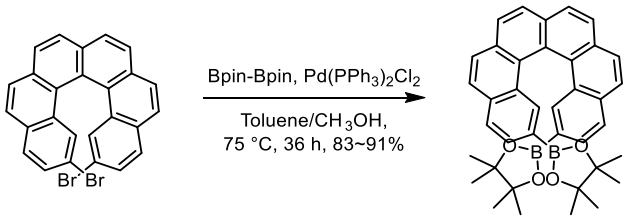

48.6 mg of 2,15-dibromohelicene[5] (0.1 mmol) and 76.2 mg of bis(pinacolato)diboron (Bpin-Bpin, 0.3 mmol), together with 7.0 mg of $Pd(PPh_3)_2Cl_2$ (10 mol %), were suspended in 5 mL of dried mixed solvent (toluene/CH_3OH = 1/1, *v*/*v*) under argon. The reaction was stirred at 75 °C for 36 hours. After the reaction, the solvent was removed, and the residue was purified by silica column chromatography (heptane : ethyl acetate = 15 : 1, *v*/*v*) to obtain the product.

rac-bis(pinacolatoboryl)[6]helicene: Starting with 48.6 mg of *rac*-2,15-dibromo[6]helicene to obtain 48.0 mg of the product as yellow solid (yield: 83%).

P-bis(pinacolatoboryl)[6]helicene: Starting with 48.6 mg of *P*-2,15-dibromo[6]helicene to obtain 52.5 mg of the product as yellow solid (yield: 91%).

M-bis(pinacolatoboryl)[6]helicene: Starting with 48.6 mg of *M*-2,15-dibromo[6]helicene to obtain 49.9 mg of the product as yellow solid (yield: 86%).

^{1}H NMR (500 MHz, $CDCl_3$, 298 K): δ 8.04 (s, 2H), 7.99 (d, J = 8.2 Hz, 2H), 7.97 (d, J = 8.2 Hz, 2H), 7.96 (d, J = 8.5 Hz, 2H), 7.85 (d, J = 8.5 Hz, 2H), 7.70 (d, J = 7.9 Hz, 2H), 7.47 (d, J = 7.9 Hz, 2H), 1.18 (s, 12H), 1.17 (s, 12H). ^{13}C{^{1}H} NMR (125 MHz, $CDCl_3$, 298 K): δ 136.23, 133.97, 133.24, 131.27, 129.96, 128.85, 128.64, 127.51, 127.49, 127.32, 126.79, 126.70, 124.28, 83.43, 25.21, 24.31.

Preparation of single crystals of *rac*-bis(pinacolatoboryl)[6]helicene: 10 mg of *rac*-bis(pinacolatoboryl)[6]helicene was dissolved in 1 mL of CH_2Cl_2 in a small tube which was placed in a closed bottle with 50 mL of pentane. Pale yellow prismatic crystals of *rac*-bis(pinacolatoboryl)[6]helicene, suitable for single crystal X-ray diffraction analysis, were obtained at the bottom of the tube upon solvent diffusion within two days.

Synthesis of **TBTH**.

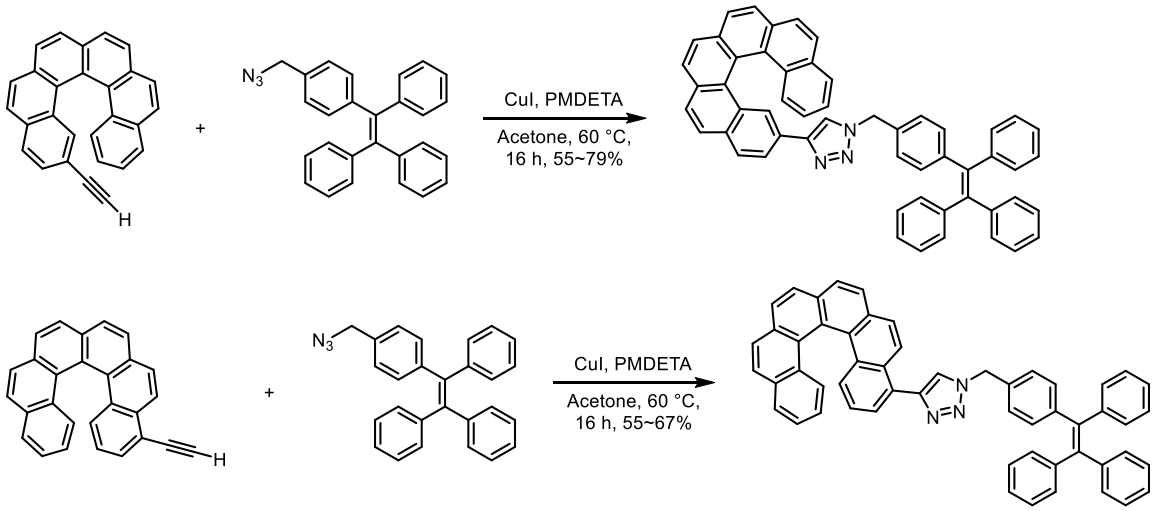

General synthesis procedure for **2-TBTH** and **4-TBTH**

35.2 mg of 2-ethynyl[6]helicene[6] or 4-ethynyl[6]helicene (0.1 mmol) and 38.7 mg of 1-(4-(azidomethyl)phenyl)-1,2,2-triphenylethene (0.1 mmol), together with 1.9 mg of CuI (10 mmol %) and *N*,*N*,*N*′,*N*″,*N*″-pentamethyldiethylenetriamine (PMDETA), were suspended in 4 mL of dried acetone under argon. The mixture was degassed by freeze-pump-thaw method for three time to remove the residual air. Then the reaction was stirred under argon at 60 °C for 16 hours. After the reaction, the solvent was removed, and the residue was purified by silica column chromatography (heptane : ethyl acetate = 5 : 1, *v*/*v*) to obtain the final product.

2-(1-(4-(1,2,2-triphenylvinyl)benzyl)-1*H*-1,2,3-triazol-4-yl)[6]helicene (**2-TBTH**):

rac-**2-TBTH**: Starting with 35.2 mg of *rac*-2-ethynyl[6]helicene (0.1 mmol) to obtain 58.1 mg of the product as yellow solid (yield: 79%).

P-**2-TBTH**: Starting with 35.2 mg of *P*-2-ethynyl[6]helicene (0.1 mmol) to obtain 50.2 mg of the product as yellow solid (yield: 69%).

M-**2-TBTH**: Starting with 35.2 mg of *M*-2-ethynyl[6]helicene (0.1 mmol) to obtain 40.8 mg of the product as yellow solid (yield: 55%).

^{1}H NMR (500 MHz, $CDCl_3$, 298 K): δ 8.02 (d, J = 8.1 Hz, 1H), 8.01 (d, J = 8.2 Hz, 1H), 7.99 (d, J = 8.1 Hz, 1H), 7.97 (d, J = 8.2 Hz, 1H), 7.94 (dt, J = 8.2 Hz, J = 1.2 Hz, 1H), 7.92 (s, 2H), 7.90 (d, J = 8.5 Hz, 1H), 7.88 (d, J = 8.2 Hz, 1H), 7.85 (d, J = 1.2 Hz, 1H), 7.66 (d, J = 8.4 Hz, 1H), 7.61 (d, J = 8.5 Hz, 1H), 7.24 – 7.19 (m, 3H), 7.16 – 7.09 (m, 13H), 7.08 – 7.05 (m, 2H), 7.05 – 6.99 (m, 3H), 6.67 (ddd, J = 8.4 Hz, J = 6.8 Hz, J = 1.4 Hz, 1H), 6.61 (s, 1H), 5.47 (d, J = 15.0 Hz, 1H), 5.19 (d, J = 15.0 Hz, 1H). ^{13}C{^{1}H} NMR (125 MHz, $CDCl_3$, 298 K): δ 148.22, 144.53, 143.58, 143.57, 142.06,

140.16, 133.34, 133.01, 132.13, 131.84, 131.82, 131.79, 131.44, 131.39, 131.37, 129.87, 129.50, 128.42, 128.09, 128.04, 127.92, 127.86, 127.83, 127.68, 127.48, 127.47, 127.39, 127.25, 127.21, 127.18, 127.17, 126.89, 126.83, 126.75, 126.60, 126.26, 125.38, 125.09, 124.14, 123.25, 119.52, 53.84.

4-(1-(4-(1,2,2-triphenylvinyl)benzyl)-1*H*-1,2,3-triazol-4-yl)[6]helicene (**4-TBTH**):

rac-**4-TBTH**: Starting with 35.2 mg of *rac*-4-ethynyl[6]helicene (0.1 mmol) to obtain 44.2 mg of the product as yellow solid (yield: 60%).

P-**4-TBTH**: Starting with 35.2 mg of *P*-4-ethynyl[6]helicene (0.1 mmol) to obtain 49.6 mg of the product as yellow solid (yield: 67%).

M-**4-TBTH**: Starting with 35.2 mg of *M*-4-ethynyl[6]helicene (0.1 mmol) to obtain 40.7 mg of the product as yellow solid (yield: 55%).

^{1}H NMR (500 MHz, $CDCl_3$, 298 K): δ 8.49 (dd, J = 8.8 Hz, J = 0.6 Hz, 1H), 8.03 (d, J = 8.2 Hz, 1H), 8.02 (d, J = 8.2 Hz, 1H), 8.00 (d, J = 8.2 Hz, 1H), 7.99 (d, J = 8.2 Hz, 1H), 7.96 (d, J = 8.8 Hz, 1H), 7.94 (d, J = 8.6 Hz, 1H), 7.92 (d, J = 8.6 Hz, 1H), 7.82 (dd, J = 7.9 Hz, J = 0.9 Hz, 1H), 7.69 (dt, J = 8.5 Hz, J = 0.9 Hz, 1H), 7.64 (s, 1H), 7.62 (d, J = 8.6 Hz, 1H), 7.35 (dd, J = 7.1 Hz, J = 1.1 Hz, 1H), 7.20 (ddd, J = 8.0 Hz, J = 6.9 Hz, J = 1.1 Hz, 1H), 7.14 – 7.00 (m, 19H), 6.71 (ddd, J = 8.6 Hz, J = 6.9 Hz, J = 1.4 Hz, 1H), 6.70 (dd, J = 8.5 Hz, J = 7.1 Hz, 1H), 5.59 (s, 2H). ^{13}C{^{1}H} NMR (125 MHz, $CDCl_3$, 298 K): δ 148.01, 144.68, 143.56, 143.44, 143.34, 141.92, 140.14, 133.36, 132.62, 132.22, 131.90, 131.43, 131.40, 131.37, 131.18, 130.68, 129.86, 129.64, 128.74, 128.20, 128.19, 128.07, 127.93, 127.87, 127.82, 127.73, 127.65, 127.61, 127.49, 127.40, 127.20, 127.13, 127.07, 127.03, 126.79, 126.78, 126.75, 126.31, 125.69, 125.24, 125.03, 124.30, 124.10, 122.73, 54.21.

Synthesis of **TPEH**.

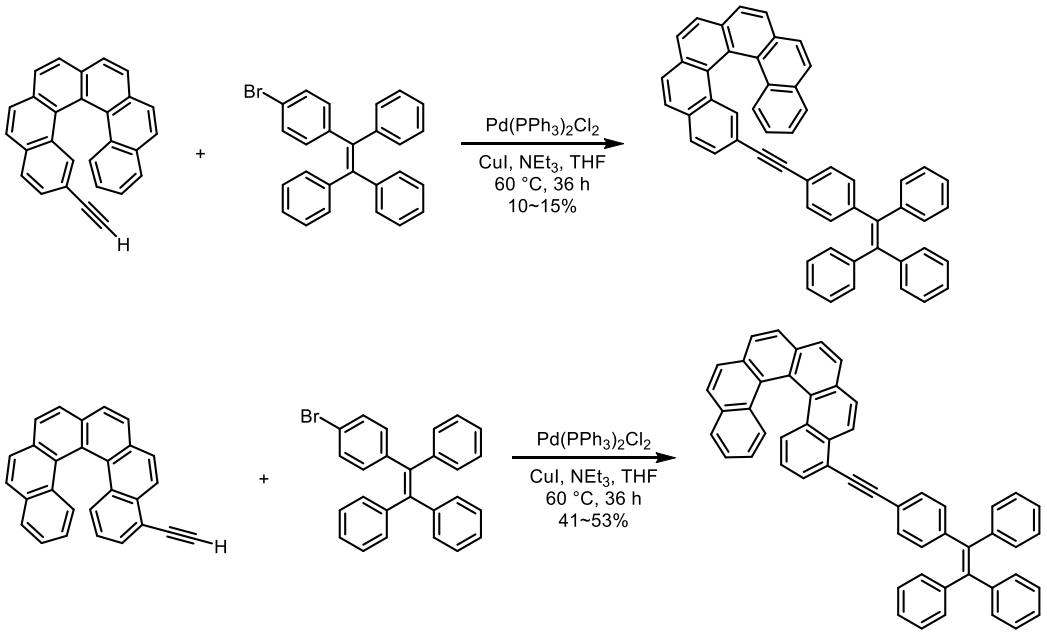

General synthesis procedure for **2-TPEH** and **4-TPEH**

35.2 mg of 2-ethynyl[6]helicene[6] or 4-ethynyl[6]helicene (0.1 mmol) and 41.1 mg of 1-(4-bromophenyl)-1,2,2-triphenylethene (0.1 mmol), together with 3.5 mg of $Pd(PPh_3)_2Cl_2$ (5 mmol %) and 1.9 mg of CuI (10 mmol %), were suspended in 10 mL of dried THF under argon. The mixture was degassed by freeze-pump-thaw method for three time to remove the residual air. Then 200 μL of triethylamine was added and the reaction was stirred at 60 °C for 48 hours. After the reaction, the solvent was removed, and the residue was purified by silica column chromatography (heptane : dichloromethane = 10 : 1, *v*/*v*) to obtain the final product.

2-(2-(1,2,2-triphenylvinyl)ethynyl)[6]helicene (**2-TPEH**):

rac-**2-TPEH**: Starting with 35.2 mg of *rac*-2-ethynyl[6]helicene (0.1 mmol) to obtain 6.8 mg of the product as yellow solid (yield: 10%).

P-**2-TPEH**: Starting with 35.2 mg of *P*-2-ethynyl[6]helicene (0.1 mmol) to obtain 10.3 mg of the product as yellow solid (yield: 15%).

M-**2-TPEH**: Starting with 35.2 mg of *M*-2-ethynyl[6]helicene (0.1 mmol) to obtain 8.2 mg of the product as yellow solid (yield: 12%).

^{1}H NMR (500 MHz, $CDCl_3$, 298 K): δ 8.03 (d, J = 8.2 Hz, 1H), 8.01 (d, J = 8.5 Hz, 1H), 8.00 (d, J = 8.5 Hz, 1H), 7.97 (d, J = 8.2 Hz, 1H), 7.94 (d, J = 8.5 Hz, 1H), 7.93 (d, J = 8.5 Hz, 1H), 7.92 (d, J = 8.5 Hz, 1H), 7.88 (d, J = 8.5 Hz, 1H), 7.80 (dd, J = 8.1 Hz, J = 1.1 Hz, 1H), 7.77 – 7.74 (m, 2H), 7.58 (d, J = 8.5 Hz, 1H), 7.29 – 7.25 (m, 2H), 7.16 – 7.09 (m, 9H), 7.08 – 7.01 (m, 8H), 6.99 – 6.96 (m,

2H), 6.72 (ddd, J = 8.4 Hz, J = 6.9 Hz, J = 1.3 Hz, 1H). $^{13}C\{^{1}H\}$ NMR (125 MHz, $CDCl_3$, 298 K): δ 143.75, 143.69, 143.63, 143.57, 141.73, 140.49, 133.32, 132.24, 132.18, 131.68, 131.54, 131.48, 131.46, 131.37, 131.32, 130.91, 129.82, 129.50, 128.08, 127.97, 127.90, 127.81, 127.78, 127.74, 127.67, 127.55, 127.49, 127.45, 127.28, 127.24, 127.04, 126.80, 126.74, 126.69, 126.34, 126.01, 124.82, 124.18, 121.46, 119.64, 90.18, 89.02.

4-(2-(1,2,2-triphenylvinyl)ethynyl)[6]helicen (**4-TPEH**):

rac-**4-TPEH**: Starting with 35.2 mg of *rac*-4-ethynyl[6]helicene (0.1 mmol) to obtain 27.7 mg of the product as yellow solid (yield: 41%).

P-**4-TPEH**: Starting with 35.2 mg of *P*-4-ethynyl[6]helicene (0.1 mmol) to obtain 36.5 mg of the product as yellow solid (yield: 53%).

M-**4-TPEH**: Starting with 35.2 mg of *M*-4-ethynyl[6]helicene (0.1 mmol) to obtain 34.2 mg of the product as yellow solid (yield: 50%).

^{1}H NMR (500 MHz, $CDCl_3$, 298 K): δ 8.56 (dd, J = 8.6 Hz, J = 0.3 Hz, 1H), 8.03 (d, J = 8.2 Hz, 1H), 8.03 (d, J = 8.8 Hz, 1H), 8.01 (d, J = 8.5 Hz, 1H), 8.00 (d, J = 8.5 Hz, 1H), 7.99 (d, J = 8.2 Hz, 1H), 7.94 (d, J = 8.5 Hz, 1H), 7.92 (d, J = 8.5 Hz, 1H), 7.82 (dd, J = 8.0 Hz, J = 1.0 Hz, 1H), 7.60 (dt, J = 8.6 Hz, J = 0.9 Hz, 1H), 7.54 (d, J = 8.5 Hz, 1H), 7.46 – 7.41 (m, 3H), 7.22 (ddd, J = 7.9 Hz, J = 7.0 Hz, J = 1.0 Hz, 1H), 7.20 – 7.03 (m, 17H), 6.72 (ddd, J = 8.5 Hz, J = 6.9 Hz, J = 1.3 Hz, 1H), 6.62 (dd, J = 8.6 Hz, J = 7.2 Hz, 1H). $^{13}C\{^{1}H\}$ NMR (125 MHz, $CDCl_3$, 298 K): δ 144.22, 143.67, 143.63, 143.52, 141.86, 140.44, 133.34, 131.93, 131.91, 131.64, 131.57, 131.52, 131.47, 131.43, 131.40, 131.12, 130.10, 130.00, 129.81, 128.54, 128.13, 128.08, 128.02, 127.93, 127.83, 127.77, 127.70, 127.58, 127.45, 127.30, 127.29, 127.04, 126.86, 126.78, 126.73, 126.28, 125.88, 125.75, 125.07, 124.21, 124.12, 121.42, 120.43, 94.36, 88.61.

Synthesis of **TEH** and **BTEH**.

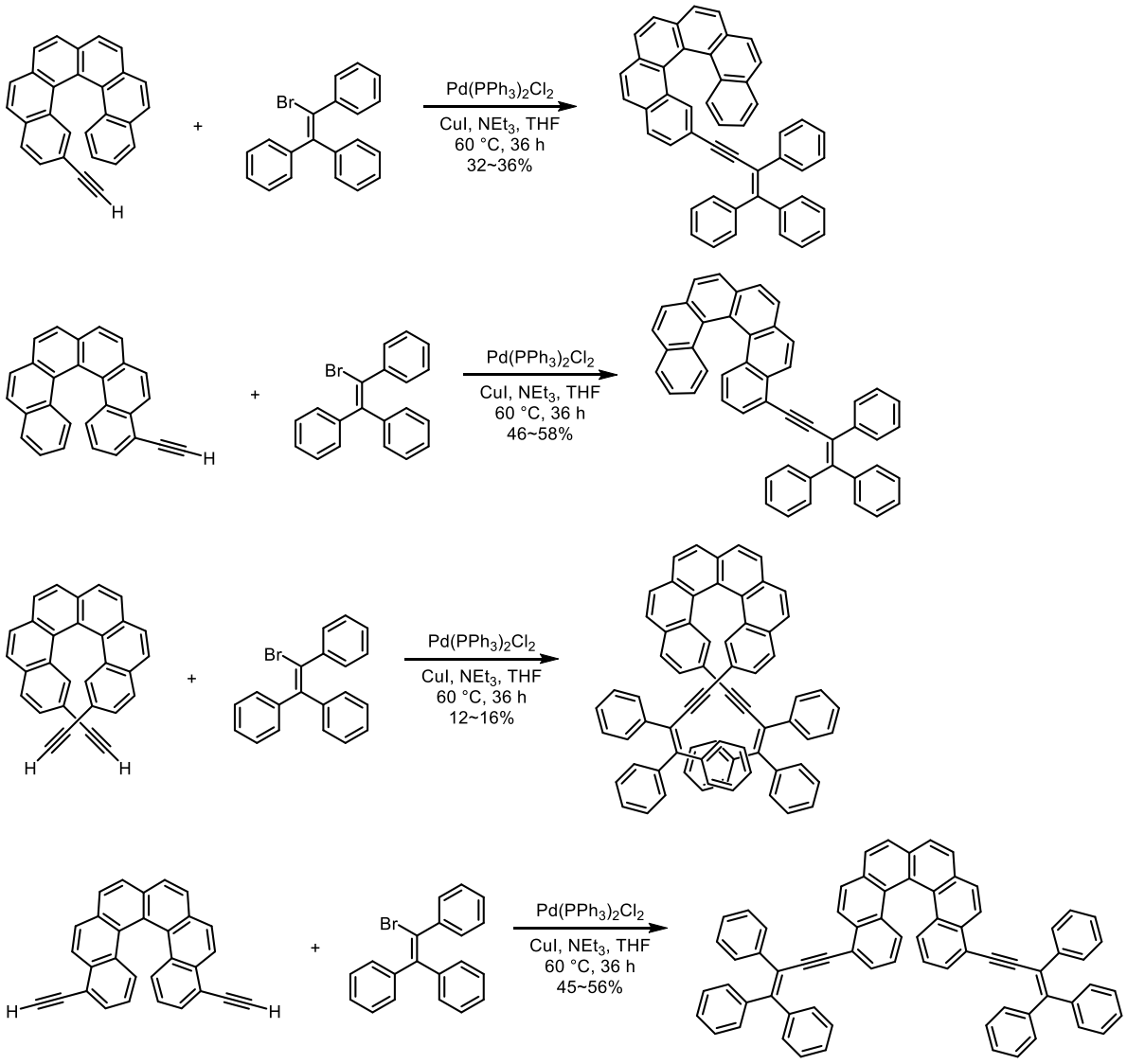

General synthesis procedure for **2-TEH**, **4-TEH**, **2,15-BTEH** and **4,13-BTEH**:

0.1 mmol of monoethynylhelicenes[6] or 0.05 mmol of diethynylhelicenes[6,7] and 33.5 mg of 1-bromo-1,2,2-triphenylethene (0.1 mmol), together with 3.5 mg of $Pd(PPh_3)_2Cl_2$ (5 mmol %) and 1.9 mg of CuI (10 mmol %), were suspended in 10 mL of dried THF under argon. The mixture was degassed by freeze-pump-thaw method for three time to remove the residual air. Then 200 μL of triethylamine was added and the reaction was stirred at 60 °C for 48 hours. After the reaction, the solvent was removed, and the residue was purified by silica column chromatography (heptane : dichloromethane = 5 : 1, *v*/*v*) to obtain the final product.

2-(3,4,4-triphenylbut-3-en-1-yn-1-yl)[6]helicene (**2-TEH**):

rac-**2-TEH**: Starting with 35.2 mg of *rac*-2-ethynyl[6]helicene (0.1 mmol) to obtain 20.4 mg of the

product as yellow solid (yield: 34%).

P-**2-TEH**: Starting with 35.2 mg of *P*-2-ethynyl[6]helicene (0.1 mmol) to obtain 19.2 mg of the product as yellow solid (yield: 32%).

M-**2-TEH**: Starting with 35.2 mg of *M*-2-ethynyl[6]helicene (0.1 mmol) to obtain 21.8 mg of the product as yellow solid (yield: 36%).

^{1}H NMR (500 MHz, $CDCl_3$, 298 K): δ 8.01 (d, J = 8.1 Hz, 1H), 7.99 (s, 2H), 7.95 (d, J = 8.1 Hz, 1H), 7.93 (d, J = 8.2 Hz, 1H), 7.91 (d, J = 8.5 Hz, 1H), 7.90 (d, J = 8.2 Hz, 1H), 7.84 (d, J = 8.5 Hz, 1H), 7.82 (dd, J = 7.9 Hz, J = 0.9 Hz, 1H), 7.68 (d, J = 8.2 Hz, 1H), 7.60 (s, 1H), 7.54 (d, J = 8.5 Hz, 1H), 7.41 – 7.37 (m, 2H), 7.28 – 7.21 (m, 7H), 7.16 – 7.10 (m, 5H), 6.99 – 6.94 (m, 3H), 6.69 (ddd, J = 8.6 Hz, J = 7.0 Hz, J = 1.3 Hz, 1H). ^{13}C{^{1}H} NMR (125 MHz, $CDCl_3$, 298 K): δ 148.22, 142.75, 141.72, 139.81, 133.28, 132.16, 131.63, 131.52, 131.42, 131.35, 131.22, 130.57, 130.12, 129.71, 129.57, 128.21, 127.99, 127.92, 127.88, 127.76, 127.62, 127.60, 127.55, 127.53, 127.51, 127.40, 127.29, 127.24, 127.13, 127.00, 126.98, 126.23, 126.06, 124.76, 124.16, 121.64, 120.07, 93.47, 91.76.

Preparation of single crystals of *rac*-**2-TEH**: 10 mg of *rac*-**2-TEH** was dissolved in 1 mL of CH_2Cl_2 in a small tube which was placed in a closed bottle with 50 mL of pentane. Greenish-yellow prismatic crystals of *rac*-**2-TEH**, suitable for single crystal X-ray diffraction analysis, were obtained at the bottom of the tube upon solvent diffusion within two days.

4-(3,4,4-triphenylbut-3-en-1-yn-1-yl)[6]helicene (**4-TEH**):

rac-**4-TEH**: Starting with 35.2 mg of *rac*-4-ethynyl[6]helicene (0.1 mmol) to obtain 28.0 mg of the product as yellow solid (yield: 46%).

P-**4-TEH**: Starting with 35.2 mg of *P*-4-ethynyl[6]helicene (0.1 mmol) to obtain 35.0 mg of the product as yellow solid (yield: 58%).

M-**4-TEH**: Starting with 35.2 mg of *M*-4-ethynyl[6]helicene (0.1 mmol) to obtain 32.2 mg of the product as yellow solid (yield: 53%).

^{1}H NMR (500 MHz, $CDCl_3$, 298 K): δ 8.00 (d, J = 8.2 Hz, 1H), 7.99 (d, J = 8.1 Hz, 1H), 7.97 (d, J = 8.1 Hz, 1H), 7.96 (d, J = 8.2 Hz, 1H), 7.92 (d, J = 8.5 Hz, 1H), 7.90 (d, J = 8.5 Hz, 1H), 7.81 (dd, J = 7.9 Hz, J = 0.8 Hz, 1H), 7.78 (s, 2H), 7.66 – 7.70 (m, 2H), 7.54 (d, J = 8.5 Hz, 1H), 7.52 – 7.48 (m, 6H), 7.30 – 7.26 (m, 2H), 7.26 – 7.21 (m, 3H), 7.20 – 7.16 (m, 3H), 7.11 – 7.08 (m, 2H), 6.70 (ddd, J = 8.5 Hz, J = 7.0 Hz, J = 1.2 Hz, 1H), 6.55 (dd, J = 8.5 Hz, J = 7.2 Hz, 1H). ^{13}C{^{1}H} NMR (125 MHz, $CDCl_3$, 298 K): δ 149.04, 143.52, 141.48, 139.88, 133.26, 132.04, 131.90, 131.40, 131.35, 131.32, 130.66, 130.26, 130.05, 129.85, 129.83, 128.36, 128.33, 128.19, 128.08, 128.04, 128.01, 127.97, 127.75, 127.67, 127.48, 127.35, 127.33, 127.24, 127.02, 127.00, 126.27, 126.09, 125.70, 125.06, 124.21, 124.03, 122.31, 120.84, 97.09, 92.43.

Preparation of single crystals of *rac*-**4-TEH**: 10 mg of *rac*-**4-TEH** was dissolved in 1 mL of CH_2Cl_2

in a small tube which was placed in a closed bottle with 50 mL of pentane. Greenish-yellow prismatic crystals of *rac*-**4-TEH**, suitable for single crystal X-ray diffraction analysis, were obtained at the bottom of the tube upon solvent diffusion within two days.

2,15-bis(3,4,4-triphenylbut-3-en-1-yn-1-yl)[6]helicene (**2,15-BTEH**):

P-**2,15-BTEH**: Starting with 18.8 mg of *P*-2,15-diethynyl[6]helicene (0.05 mmol) to obtain 5.2 mg of the product as yellow solid (yield: 12%).

M-**2,15-BTEH**: Starting with 18.8 mg of *M*-2,15-diethynyl[6]helicene (0.05 mmol) to obtain 7.0 mg of the product as yellow solid (yield: 16%).

^{1}H NMR (500 MHz, $CDCl_3$, 298 K): δ 7.99 (d, J = 8.1 Hz, 2H), 7.95 (d, J = 8.1 Hz, 2H), 7.90 (d, J = 8.5 Hz, 2H), 7.80 (d, J = 8.5 Hz, 2H), 7.65 (d, J = 8.2 Hz, 2H), 7.55 (s, 1H), 7.39 (m, 4H), 7.25 – 7.18 (m, 12H), 7.16 – 7.10 (m, 10H), 7.00 (d, J = 8.2 Hz, J = 1.6 Hz, 2H), 6.97 (dd, J = 7.5 Hz, J = 2.0 Hz, 4H). ^{13}C{^{1}H} NMR (125 MHz, $CDCl_3$, 298 K): δ 148.26, 142.73, 141.72, 139.82, 133.30, 131.77, 131.49, 131.35, 131.12, 130.58, 130.10, 129.26, 128.41, 127.90, 127.88, 127.87, 127.70, 127.64, 127.62, 127.38, 127.30, 127.28, 127.04, 126.96, 124.09, 121.62, 120.03, 93.56, 91.84.

Preparation of single crystals of *P*-**2,15-BTEH**: 10 mg of *P*-**2,15-BTEH** was dissolved in 1 mL of CH_2Cl_2 in a small tube which was placed in a closed bottle with 50 mL of pentane. Greenish-yellow tabular crystals of *P*-**2,15-BTEH**, suitable for single crystal X-ray diffraction analysis, were obtained at the bottom of the tube upon solvent diffusion within two days.

4,13-bis(3,4,4-triphenylbut-3-en-1-yn-1-yl)[6]helicene (**4,13-BTEH**):

P-**4,13-BTEH**: Starting with 18.8 mg of *P*-4,13-diethynyl[6]helicene (0.05 mmol) to obtain 25.0 mg of the product as yellow solid (yield: 56%).

M-**4,13-BTEH**: Starting with 18.8 mg of *M*-4,13-diethynyl[6]helicene (0.05 mmol) to obtain 20.0 mg of the product as yellow solid (yield: 45%).

^{1}H NMR (500 MHz, $CDCl_3$, 298 K): δ 7.99 (d, J = 8.1 Hz, 2H), 7.94 (d, J = 8.1 Hz, 2H), 7.76 (s, 4H), 7.67 (m, 4H), 7.56–7.46 (m, 10H), 7.43 (d, J = 8.5 Hz, 2H), 7.30 – 7.26 (m, 4H), 7.23 (d, J = 7.1 Hz, 2H), 7.21 (d, J = 7.2 Hz, 2H), 7.19 – 7.13 (m, 6H), 7.12 – 7.07 (m, 4H), 6.56 (dd, J = 8.5 Hz, J = 7.2 Hz, 2H). ^{13}C{^{1}H} NMR (125 MHz, $CDCl_3$, 298 K): δ 149.08, 143.50, 141.46, 139.84, 133.28, 132.03, 131.37, 131.31, 130.65, 130.24, 130.07, 129.66, 128.33, 128.28, 128.20, 128.05, 127.97, 127.92, 127.49, 127.35, 127.34, 126.95, 126.14, 124.30, 124.19, 122.28, 120.87, 97.14, 92.34.

Preparation of single crystals of *M*-**4,13-BTEH**: 10 mg of *M*-**4,13-BTEH** was dissolved in 1 mL of CH_2Cl_2 in a small tube which was placed in a closed bottle with 50 mL of pentane. Greenish-yellow tabular crystals of *M*-**4,13-BTEH**, suitable for single crystal X-ray diffraction analysis, were obtained at the bottom of the tube upon solvent diffusion within two days.

Synthesis of **TH** and **BTH**.

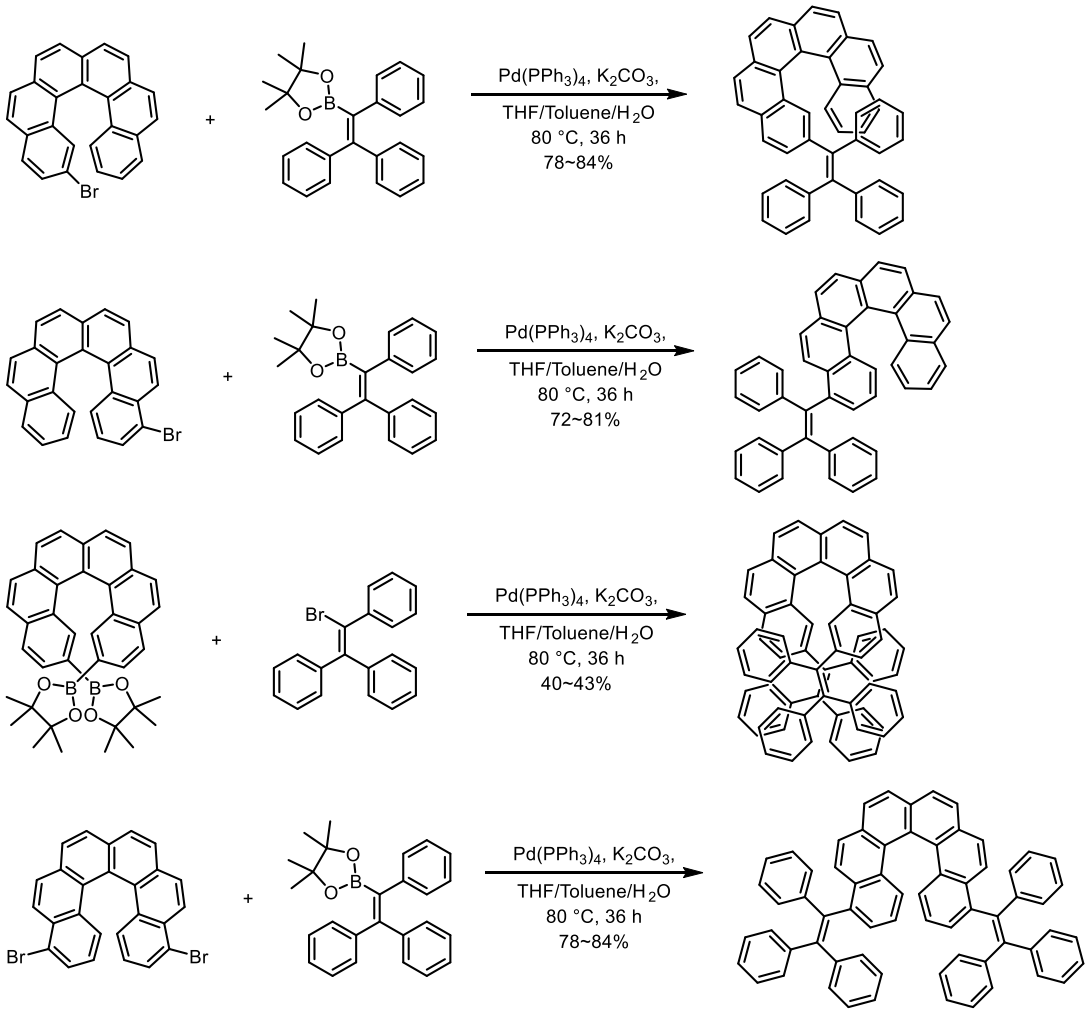

General synthesis procedure for **2-TH**, **4-TH** and **4,13-BTH** starting from bromohelicenes:

0.1 mmol of monobromohelicenes[4] or 0.05 mmol of dibromohelicenes[5] and 57.3 mg of 1-(pinacolatoboryl)-1,2,2-triphenylethene[8] (0.15 mmol), together with 11.6 mg of $Pd(PPh_3)_4$ (10 mmol %) and 28 mg of K_2CO_3 (0.2 mmol), were suspended in 5 mL of mixture solvent of THF/toluene/H_2O (2/2/1, *v*/*v*/*v*) under argon and the reaction was stirred at 80 °C for 48 hours. After the reaction, the reaction mixture was extracted by ethyl acetate and the organic layer was collected and dried over $MgSO_4$. Then the solvent was removed and the residue was purified by silica column chromatography (heptane : ethyl acetate = 20 : 1, *v*/*v*) to obtain the final product.

2-(1,2,2-triphenylvinyl)[6]helicene (**2-TH**):

rac-**2-TH**: Starting with 40.7 mg of *rac*-2-bromo[6]helicene (0.1 mmol) to obtain 49.2 mg of the product as yellow solid (yield: 84%).

P-**2-TH**: Starting with 40.7 mg of *P*-2-bromo[6]helicene (0.1 mmol) to obtain 50.8 mg of the product

as yellow solid (yield: 87%).

M-**2-TH**: Starting with 40.7 mg of *M*-2-bromo[6]helicene (0.1 mmol) to obtain 45.5 mg of the product as yellow solid (yield: 78%).

^{1}H NMR (500 MHz, $CDCl_3$, 298 K): δ 7.93 (dd, J = 8.0 Hz, J = 1.1 Hz, 1H), 7.89 (d, J = 8.2 Hz, 1H), 7.88 (s, 2H), 7.87 (d, J = 8.2 Hz, 1H), 7.85 – 7.82 (m, 3H), 7.77 (d, J = 8.6 Hz, 1H), 7.75 (d, J = 8.2 Hz, 1H), 7.49 (d, J = 8.3 Hz, 1H), 7.46 (ddd, J = 7.9 Hz, J = 6.9 Hz, J = 1.1 Hz, 1H), 7.44 (t, J = 0.9 Hz, 1H), 7.06 – 7.01 (m, 3H), 7.01 – 6.91 (m, 4H), 6.84 (dd, J = 8.3 Hz, J = 1.7 Hz, 1H), 6.80 – 6.75 (m, 5H), 6.51 – 6.45 (m, 4H). ^{13}C{^{1}H} NMR (125 MHz, $CDCl_3$, 298 K): δ 144.13, 143.53, 143.34, 140.71, 140.45, 139.73, 133.03, 132.08, 131.95, 131.44, 131.31, 131.13, 131.10, 130.45, 130.34, 129.25, 128.86, 128.23, 128.07, 127.83, 127.79, 127.59, 127.52, 127.50, 127.45, 127.26, 127.05, 126.75, 126.65, 126.50, 126.33, 126.32, 126.16, 126.15, 125.99, 125.95, 124.96, 123.95.

Preparation of single crystals of *rac*-**2-TH**: 10 mg of *rac*-**2-TH** was dissolved in 1 mL of CH_2Cl_2 in a small tube which was placed in a closed bottle with 50 mL of pentane. Yellow tabular crystals of *rac*-**2-TH**, suitable for single crystal X-ray diffraction analysis, were obtained at the bottom of the tube upon solvent diffusion within two days.

Preparation of single crystals of *P*-**2-TH**: 10 mg of *P*-**2-TH** was dissolved in 1 mL of CH_2Cl_2 in a small tube which was placed in a closed bottle with 50 mL of pentane. Greenish-yellow tabular crystals of *P*-**2-TH**, suitable for single crystal X-ray diffraction analysis, were obtained at the bottom of the tube upon solvent diffusion within two days.

4-(1,2,2-triphenylvinyl)[6]helicene (**4-TH**):

rac-**4-TH**: Starting with 40.7 mg of *rac*-4-bromo[6]helicene (0.1 mmol) to obtain 42.2 mg of the product as yellow solid (yield: 72%).

P-**4-TH**: Starting with 40.7 mg of *P*-4-bromo[6]helicene (0.1 mmol) to obtain 46.0 mg of the product as yellow solid (yield: 79%).

M-**4-TH**: Starting with 40.7 mg of *M*-4-bromo[6]helicene (0.1 mmol) to obtain 47.0 mg of the product as yellow solid (yield: 81%).

^{1}H NMR (500 MHz, DMSO-d_6, 303 K): **4-TH** has two distinguished rotamers (**4-TH^1** 60% and **4-TH^2** 40%) in DMSO-d_6 solution. δ 8.35 (d, J = 8.8 Hz, 0.4H, $H_{\textbf{4-TH}^2}$), 8.20 – 8.09 (m, 3.6H), 8.09 – 7.96 (m, 4H), 7.94 – 7.87 (m, 1H), 7.38 – 7.09 (m, 13.4H), 7.04 – 6.96 (m, 1.8H), 6.92 – 6.82 (m, 3.8H), 6.65 (ddd, J = 8.7 Hz, J = 6.9 Hz, J = 1.3 Hz, 0.6H, $H_{\textbf{4-TH}^1}$), 6.56 (dd, J = 7.1 Hz, J = 8.5 Hz, 0.4H, $H_{\textbf{4-TH}^2}$), 6.52 (ddd, J = 8.6 Hz, J = 6.9 Hz, J = 1.4 Hz, 0.6H, $H_{\textbf{4-TH}^2}$), 6.47 (dd, J = 7.1 Hz, J = 8.5 Hz, 0.4H, $H_{\textbf{4-TH}^1}$).

Preparation of single crystals of *rac*-**4-TH**: 10 mg of *rac*-**4-TH** was dissolved in 1 mL of CH_2Cl_2 in a small tube which was placed in a closed bottle with 50 mL of pentane. Colorless prismatic crystals

of *rac*-**4-TH**, suitable for single crystal X-ray diffraction analysis, were obtained at the bottom of the tube upon solvent diffusion within two days.

4,13-bis(1,2,2-triphenylvinyl)[6]helicene (**4,13-BTH**):

rac-**4,13-BTH**: Starting with 24.3 mg of *rac*-4,13-dibromo[6]helicene (0.05 mmol) to obtain 25.2 mg of the product as white solid (yield: 60%).

P-**4,13-BTH**: Starting with 24.3 mg of *P*-4,13-dibromo[6]helicene (0.05 mmol) to obtain 20.4 mg of the product as white solid (yield: 49%).

M-**4,13-BTH**: Starting with 24.3 mg of *M*-4,13-dibromo[6]helicene (0.05 mmol) to obtain 26.7 mg of the product as white solid (yield: 64%).

^{1}H NMR (500 MHz, DMSO-d_6, 298 K): **4,13-BTH** has three distinguished rotamers (two symmetric rotamers: **4,13-BTH^1** 42% and **4,13-BTH^2** 13%, and non-symmetric rotamer: **4,13-BTH^3** 45%) in DMSO-d_6 solution. δ 8.37 – 8.31 (m, 0.7 H), 8.17 – 7.93 (m, 7.3H), 7.28 – 6.82 (m, 34H), 6.54 (dd, J = 7.4 Hz, J = 8.5 Hz, 0.45H, $H_{\mathbf{4,13\text{-}BTH^3}}$), 6.45 (dd, J = 7.4 Hz, J = 8.5 Hz, 0.84H, $H_{\mathbf{4,13\text{-}BTH^1}}$), 6.37 (dd, J = 7.4 Hz, J = 8.5 Hz, 0.28H, $H_{\mathbf{4,13\text{-}BTH^2}}$), 6.31 (dd, J = 7.4 Hz, J = 8.5 Hz, 0.45H, $H_{\mathbf{4,13\text{-}BTH^3}}$).

2,15-bis(1,2,2-triphenylvinyl)[6]helicene (**2,15-BTH**):

Because of the low yield via the general procedure due to the dibromonation caused from the steric hindrance, we adopted 2,15-bis(pinacolatoboryl)[6]helicene and 1-bromo-1,2,2-triphenylethene to synthesize **2,15-BTH**. 29.0 mg of 2,15-bis(pinacolatoboryl)[6]helicene (0.05 mmol), 40.2 mg of 1-bromo-1,2,2-triphenylethene (0.12 mmol) , 11.6 mg of $Pd(PPh_3)_4$ (20 mol %) and 27.6 mg of K_2CO_3 (0.2 mmol) were suspended in 3 mL of mixed solvent (toluene/THF/H_2O = 1/1/1, *v*/*v*/*v*) under argon. The reaction was stirred at 80 °C for 24 hours. Then, another 11.6 mg of $Pd(PPh_3)_4$ (20 mol %) was added, and the reaction was stirred at 80 °C for another 24 hours. After the reaction, the reaction mixture was extracted by CH_2Cl_2 and the organic layer was collected and dried over Na_2SO_4. The solvent was then removed and the residue was purified by silica column chromatography (heptane : ethyl acetate = 15 : 1) to obtain the final product.

rac-**2,15-BTH**: Starting with 29.0 mg of *rac*-2,15-bis(pinacolatoboryl)[6]helicene to obtain 18.2 mg of the product as greenish-yellow solid (yield: 43%).

P-**2,15-BTH**: Starting with 29.0 mg of *P*-2,15-bis(pinacolatoboryl)[6]helicene to obtain 16.6 mg of the product as greenish-yellow solid (yield: 40%).

M-**2,15-BTH**: Starting with 29.0 mg of *M*-2,15-bis(pinacolatoboryl)[6]helicene to obtain 17.3 mg of the product as greenish-yellow solid (yield: 41%).

^{1}H NMR (500 MHz, $CDCl_3$, 298 K): δ 7.79 (d, J = 8.2 Hz, 2H), 7.76 (d, J = 8.2 Hz, 2H), 7.70 (d, J = 8.5 Hz, 2H), 7.65 (d, J = 8.5 Hz, 2H), 7.56 (d, J = 8.3 Hz, 2H), 7.40 (d, J = 1.0 Hz, 2H), 7.02 (t, J =

7.4 Hz, 2H), 7.00 – 6.95 (m, 8H), 6.88 (t, J = 7.7 Hz, 4H), 6.74 – 6.70 (m, 4H), 6.59 – 6.53 (m, 6H), 6.51 (d, J = 7.8 Hz, 4H), 6.40 (m, 4H). $^{13}C\{^{1}H\}$ NMR (125 MHz, $CDCl_3$, 298 K): δ 143.96, 143.25, 142.94, 141.20, 141.08, 139.53, 132.35, 131.73, 131.38, 131.01, 130.79, 130.51, 130.45, 129.51, 128.27, 128.26, 127.80, 127.48, 127.34, 127.26, 126.89, 126.66, 126.08, 126.06, 126.05, 125.79, 125.60, 123.50.

Preparation of single crystals of *rac*-**2,15-BTH**: 10 mg of *rac*-**2,15-BTH** was dissolved in 1 mL of CH_2Cl_2 in a small tube which was placed in a closed bottle with 50 mL of pentane. Greenish-yellow prismatic crystals of *rac*-**2,15-BTH**, suitable for single crystal X-ray diffraction analysis, were obtained at the bottom of the tube upon solvent diffusion within two days.

Table S1. Crystal data and structure refinement for *rac*-2,15-bis(pinacolatoboryl)[6]helicene (*rac*-2,15-BPH), *rac*-**2-TEH** and *rac*-**4-TEH**.

	rac-2,15-BPH	*rac*-**2-TEH**	*rac*-**4-TEH**
Empirical formula	$C_{38}H_{38}B_2O_4$	$C_{48}H_{30}$	$C_{48}H_{30}$
Formula weight	580.30	606.72	606.72
Temperature (K)	150.0	293.15	173.0
Crystal system	Monoclinic	Orthorhombic	Triclinic
Space group	$P2_1/c$	*Pbca*	*P*-1
a (Å)	19.9117(16)	9.2316(10)	9.5706(4)
b (Å)	11.8108(10)	17.9626(17)	10.1978(4)
c (Å)	14.5211(11)	38.228(5)	17.0183(7)
α (deg)	90	90	102.247(2)
β (deg)	108.076(2)	90	90.604(2)
γ (deg)	90	90	96.768(2)
Volume (Å^3)	3246.4(5)	6339.1(12)	1610.78(11)
Z	4	8	2
ρ_{cal} (g·cm^{-3})	1.187	1.271	1.251
μ (mm^{-1})	0.074	0.547	0.538
F(000)	1232.0	2544.0	636.0
Crystal size (mm^3)	0.2 × 0.15 × 0.15	0.22 × 0.16 × 0.11	0.2 × 0.1 × 0.05
Radiation	Mo K_α (λ = 0.71073)	Cu K_α (λ = 1.54178)	Cu K_α (λ = 1.54184)
2θ range for data collection (deg)	4.538 – 52.802	9.254 – 158.308	5.32 – 130.34
Index ranges	$-24 \le h \le 24$ $-14 \le k \le 14$ $-18 \le l \le 18$	$-11 \le h \le 11$ $-22 \le k \le 22$ $-48 \le l \le 48$	$-11 \le h \le 11$ $-11 \le k \le 11$ $-19 \le l \le 20$
Reflections collected	44199	121858	36707
Independent reflection	6634 R_{int} = 0.0835 R_σ = 0.0463	6830 R_{int} = 0.0572 R_σ = 0.0178	5470 R_{int} = 0.0572 R_σ = 0.0333
Data/restraints/parameters	6634/0/405	6830/0/433	5470/0/434
Goodness-of-fit on F^2	1.050	1.039	1.007
Final *R* indexes [$I \ge 2\theta_I$]	R_1 = 0.0716 wR_2 = 0.1748	R_1 = 0.0529 wR_2 = 0.1411	R_1 = 0.1166 wR_2 = 0.3442
Final *R* indexes [all data]	R_1 = 0.1233 wR_2 = 0.2199	R_1 = 0.0605 wR_2 = 0.1474	R_1 = 0.1260 wR_2 = 0.3484
Largest difference peak/hole (e·Å^{-3})	0.70/−0.49	0.66/−0.24	0.55/−0.43
Flack parameter			

Table S2. Crystal data and structure refinement for *P*-**2,15-BTEH**, *M*-**4,13-BTEH** and *rac*-**2-TH**.

	***P*-2,15-BTEH**	***M*-4,13-BTEH**	***rac*-2-TH**
Empirical formula	$C_{70}H_{44}$	$C_{71}H_{46}Cl_2$	$C_{46}H_{30}$
Formula weight	885.05	969.98	582.70
Temperature (K)	150.0	290.64	150.0
Crystal system	Monoclinic	Monoclinic	Monoclinic
Space group	*C*2	$P2_1$	$P2_1/c$
a (Å)	28.3898(11)	9.5228(3)	20.1900(11)
b (Å)	9.4926(4)	16.7998(5)	16.7921(8)
c (Å)	9.0611(3)	17.1815(5)	18.4805(8)
α (deg)	90	90	90
β (deg)	99.148(2)	105.316(2)	91.1650(10)
γ (deg)	90	90	90
Volume (Å^3)	2410.84(16)	2651.09(14)	6264.2(5)
Z	2	2	8
ρ_{cal} (g·cm^{-3})	1.219	1.215	1.236
μ (mm^{-1})	0.524	1.425	0.070
F(000)	928.0	1012.0	2448.0
Crystal size (mm^3)	0.2 × 0.2 × 0.05	0.2 × 0.1 × 0.04	0.2 × 0.2 × 0.15
Radiation	Cu K$_\alpha$ (λ = 1.54178)	Cu K$_\alpha$ (λ = 1.54178)	Mo K$_\alpha$ (λ = 0.71073)
2θ range for data collection (deg)	6.306 – 155.798	5.332 – 136.886	4.708 – 52.834
Index ranges	$-35 \le h \le 35$ $-11 \le k \le 11$ $-10 \le l \le 8$	$-10 \le h \le 11$ $-20 \le k \le 20$ $-20 \le l \le 20$	$-25 \le h \le 25$ $-21 \le k \le 21$ $-23 \le l \le 23$
Reflections collected	15019	26898	88339
Independent reflection	4978 R_{int} = 0.0564 R_σ = 0.0639	9481 R_{int} = 0.0411 R_σ = 0.0436	12818 R_{int} = 0.1116 R_σ = 0.0569
Data/restraints/parameters	4978/1/439	9481/1/658	12818/0/829
Goodness-of-fit on F^2	1.047	1.058	1.043
Final *R* indexes [$I \ge 2\theta_I$]	R_1 = 0.0505 wR_2 = 0.1322	R_1 = 0.0573 wR_2 = 0.1335	R_1 = 0.0495 wR_2 = 0.0959
Final *R* indexes [all data]	R_1 = 0.0585 wR_2 = 0.1390	R_1 = 0.0785 wR_2 = 0.1487	R_1 = 0.0979 wR_2 = 0.1168
Largest difference peak/hole (e·Å^{-3})	0.18/−0.15	0.24/−0.41	0.37/−0.26
Flack parameter	−1.7(10)	0.157(10)	

Table S3. Crystal data and structure refinement for *rac*-**4-TH**, *rac*-**2,15-BTH** and *P*-**2-TH**.

	rac-**4-TH**	*rac*-**2,15-BTH**	*P*-**2-TH**
Empirical formula	$C_{46}H_{30}$	$C_{66}H_{44}$	$C_{46}H_{30}$
Formula weight	582.70	837.01	582.70
Temperature (K)	173.0	172.99	150.0
Crystal system	Monoclinic	Triclinic	Monoclinic
Space group	$P2_1/c$	P-1	$P2_1$
a (Å)	14.937(3)	9.9178(2)	9.6304(3)
b (Å)	9.0510(14)	13.4025(2)	13.5032(5)
c (Å)	23.053(3)	18.3363(3)	12.9444(4)
α (deg)	90	75.1790(10)	90
β (deg)	97.336(9)	75.4010(10)	111.485(2)
γ (deg)	90	78.5690(10)	90
Volume (Å^3)	3091.2(9)	2256.75(7)	1566.34(9)
Z	4	2	2
ρ_{cal} (g·cm^{-3})	1.252	1.232	1.235
μ (mm^{-1})	0.538	0.528	0.531
F(000)	1224.0	880.0	612.0
Crystal size (mm^3)	0.22 × 0.14 × 0.11	0.16 × 0.15 × 0.11	0.2 × 0.2 × 0.1
Radiation	Cu K$_\alpha$ (λ = 1.54178)	Cu K$_\alpha$ (λ = 1.54178)	Cu K$_\alpha$ (λ = 1.54178)
2θ range for data collection (deg)	7.732 – 136.778	5.102 – 136.55	7.34 – 149.6
Index ranges	$-19 \le h \le 17$ $-9 \le k \le 10$ $-27 \le l \le 27$	$-11 \le h \le 11$ $-16 \le k \le 15$ $-22 \le l \le 22$	$-12 \le h \le 12$ $-15 \le k \le 16$ $-16 \le l \le 16$
Reflections collected	30414	41740	18901
Independent reflection	5631 R_{int} = 0.0423 R_σ = 0.0257	8227 R_{int} = 0.0380 R_σ = 0.0242	6083 R_{int} = 0.0679 R_σ = 0.0667
Data/restraints/parameters	5631/0/409	8227/0/595	6083/1/415
Goodness-of-fit on F^2	1.084	1.043	1.058
Final R indexes [$I \ge 2\theta_I$]	R_1 = 0.0561 wR_2 = 0.1346	R_1 = 0.0389 wR_2 = 0.0935	R_1 = 0.0564 wR_2 = 0.1220
Final R indexes [all data]	R_1 = 0.0725 wR_2 = 0.1456	R_1 = 0.0515 wR_2 = 0.1005	R_1 = 0.0807 wR_2 = 0.1360
Largest difference peak/hole (e·Å^{-3})	0.46/−0.33	0.24/−0.20	0.20/−0.26
Flack parameter			0(2)

Table S4. Energies of four most reasonable conformations of *P*-**2-TEH** and their occupancies at 298.15 K.

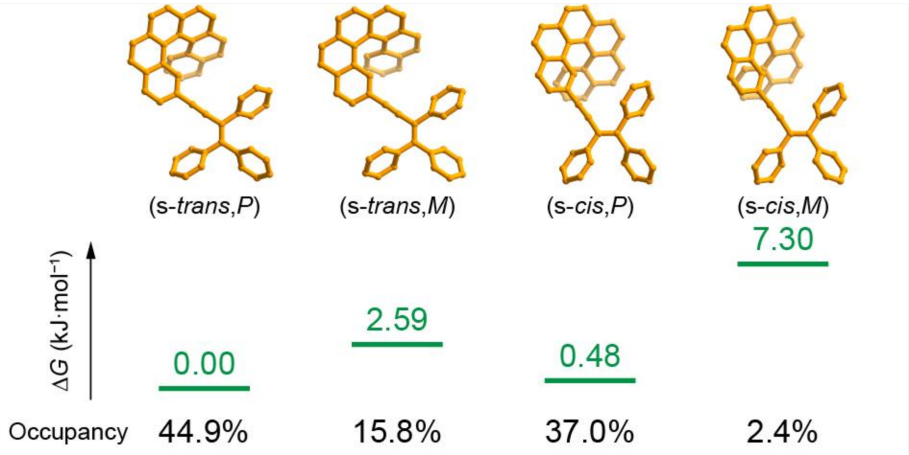

Conformations	*EE*[a]	*EE* + *ZPE*[a]	*H*[a]	*G*[a]	Δ*G*[b]	*p*
(s-*trans*,*P*),*P*-**2-TEH**	-1847.623519	-1847.006028	-1846.969025	-1847.078373	0.00	44.9%
(s-*trans*,*M*),*P*-**2-TEH**	-1847.623333	-1847.005854	-1846.968887	-1847.077385	2.59	15.8%
(s-*cis*,*P*),*P*-**2-TEH**	-1847.623229	-1847.005702	-1846.968667	-1847.078192	0.48	37.0%
(s-*cis*,*M*),*P*-**2-TEH**	-1847.622127	-1847.004502	-1846.967555	-1847.075594	7.30	2.4%

(a) in Hartree. (b) in kJ·mol^{-1}, relative to (s-*trans*,*P*),*P*-**2-TEH**.

Table S5. Energies of four most reasonable conformations of *P*-**4-TEH** and their occupancies at 298.15 K.

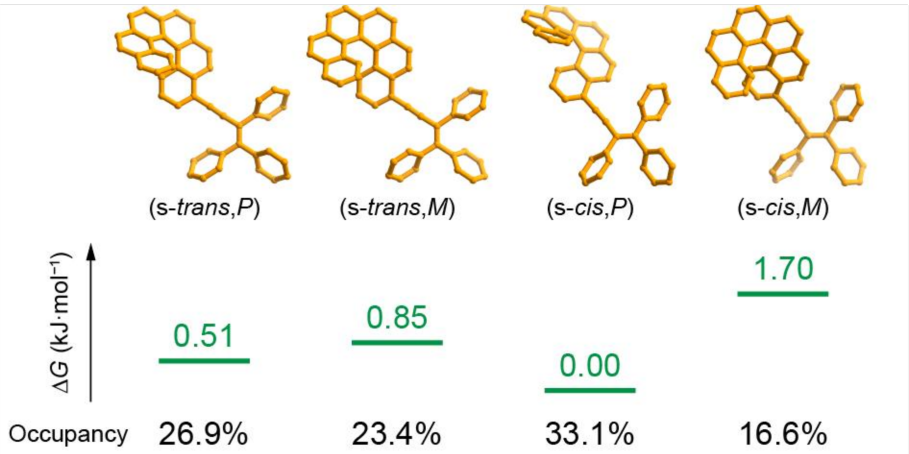

Conformations	*EE*[a]	*EE* + *ZPE*[a]	*H*[a]	*G*[a]	Δ*G*[b]	*p*
(s-*trans*,*P*),*P*-**4-TEH**	-1847.622433	-1847.004837	-1846.967862	-1847.076886	0.51	26.9%
(s-*trans*,*M*),*P*-**4-TEH**	-1847.622442	-1847.004802	-1846.967835	-1847.076756	0.85	23.4%
(s-*cis*,*P*),*P*-**4-TEH**	-1847.622124	-1847.004561	-1846.967537	-1847.077081	0.00	33.1%
(s-*cis*,*M*),*P*-**4-TEH**	-1847.622063	-1847.004442	-1846.967469	-1847.076433	1.70	16.6%

(a) in Hartree. (b) in kJ·mol^{-1}, relative to (s-*cis*,*P*),*P*-**4-TEH**.

Table S6. Energies of ten most reasonable conformations of *P*-**2,15-BTEH** and their occupancies at 298.15 K.

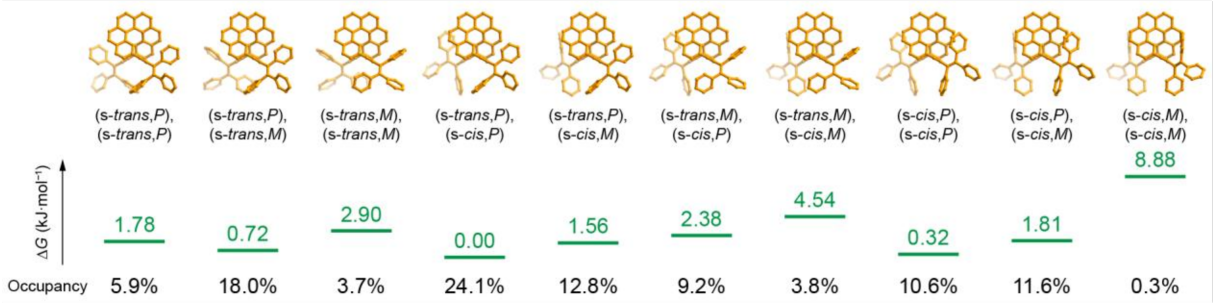

Conformations	*EE*[a]	*EE* + *ZPE*[a]	*H*[a]	*G*[a]	Δ*G*[b]	*p*
(s-*trans*,*P*),(s-*trans*,*P*), *P*-**2,15-BTEH**	-2694.556444	-2693.654306	-2693.598717	-2693.752590	1.78	5.9%
(s-*trans*,*P*),(s-*trans*,*M*), *P*-**2,15-BTEH**	-2694.556251	-2693.654275	-2693.598649	-2693.752991	0.72	18.0%[c]
(s-*trans*,*M*),(s-*trans*,*M*), *P*-**2,15-BTEH**	-2694.555865	-2693.653819	-2693.598204	-2693.752162	2.90	3.7%
(s-*trans*,*P*),(s-*cis*,*P*), *P*-**2,15-BTEH**	-2694.556282	-2693.654300	-2693.598675	-2693.753267	0.00	24.1%[c]
(s-*trans*,*P*),(s-*cis*,*M*), *P*-**2,15-BTEH**	-2694.555098	-2693.653272	-2693.597588	-2693.752672	1.56	12.8%[c]
(s-*trans*,*M*),(s-*cis*,*P*), *P*-**2,15-BTEH**	-2694.556031	-2693.654050	-2693.598442	-2693.752362	2.38	9.2%[c]
(s-*trans*,*M*),(s-*cis*,*M*), *P*-**2,15-BTEH**	-2694.554659	-2693.652767	-2693.597106	-2693.751536	4.54	3.8%[c]
(s-*cis*,*P*),(s-*cis*,*P*), *P*-**2,15-BTEH**	-2694.556060	-2693.654205	-2693.598548	-2693.753145	0.32	10.6%
(s-*cis*,*P*),(s-*cis*,*M*), *P*-**2,15-BTEH**	-2694.554754	-2693.652745	-2693.597092	-2693.752576	1.81	11.6%[c]
(s-*cis*,*M*),(s-*cis*,*M*), *P*-**2,15-BTEH**	-2694.553454	-2693.651393	-2693.595779	-2693.749886	8.88	0.3%

(a) in Hartree. (b) in kJ·mol^{-1}, relative to (s-*trans*,*P*),(s-*trans*,*P*),*P*-**2,15-BTEH**. (c) degeneracy $g = 2$.

Table S7. Energies of ten most reasonable conformations of *P*-**4,13-BTEH** and their occupancies at 298.15 K.

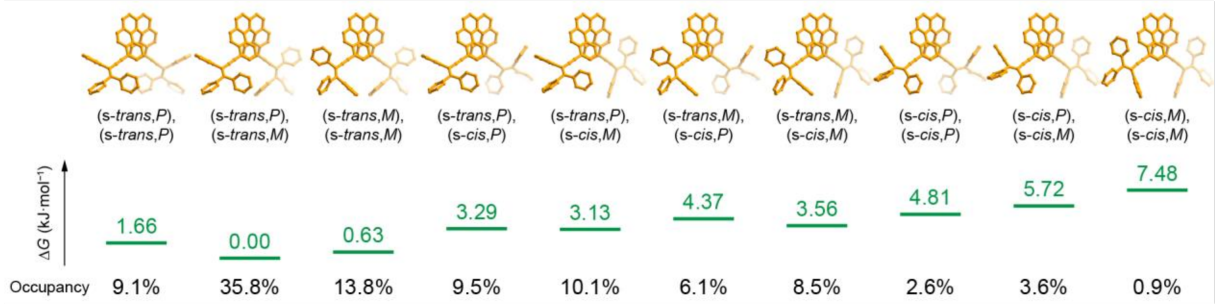

Conformations	*EE*[a]	*EE* + *ZPE*[a]	*H*[a]	*G*[a]	Δ*G*[b]	*p*
(s-*trans*,*P*),(s-*trans*,*P*), *P*-**4,13-BTEH**	-2694.554309	-2693.652148	-2693.596528	-2693.751057	1.66	5.9%
(s-*trans*,*P*),(s-*trans*,*M*), *P*-**4,13-BTEH**	-2694.554268	-2693.652144	-2693.596511	-2693.751690	0.00	18.0%[c]
(s-*trans*,*M*),(s-*trans*,*M*), *P*-**4,13-BTEH**	-2694.554258	-2693.652102	-2693.596493	-2693.751449	0.63	3.7%
(s-*trans*,*P*),(s-*cis*,*P*), *P*-**4,13-BTEH**	-2694.553973	-2693.651871	-2693.596266	-2693.750438	3.29	24.1%[c]
(s-*trans*,*P*),(s-*cis*,*M*), *P*-**4,13-BTEH**	-2694.553865	-2693.651618	-2693.596032	-2693.750498	3.13	12.8%[c]
(s-*trans*,*M*),(s-*cis*,*P*), *P*-**4,13-BTEH**	-2694.554029	-2693.651859	-2693.596297	-2693.750027	4.37	9.2%[c]
(s-*trans*,*M*),(s-*cis*,*M*), *P*-**4,13-BTEH**	-2694.553898	-2693.651672	-2693.596096	-2693.750334	3.56	3.8%[c]
(s-*cis*,*P*),(s-*cis*,*P*), *P*-**4,13-BTEH**	-2694.553673	-2693.651595	-2693.595999	-2693.749859	4.81	10.6%
(s-*cis*,*P*),(s-*cis*,*M*), *P*-**4,13-BTEH**	-2694.553597	-2693.651345	-2693.595782	-2693.749512	5.72	11.6%[c]
(s-*cis*,*M*),(s-*cis*,*M*), *P*-**4,13-BTEH**	-2694.553614	-2693.651252	-2693.595773	-2693.748841	7.48	0.3%

(a) in Hartree. (b) in kJ·mol^{-1}, relative to (s-*trans*,*M*),(s-*trans*,*M*),*P*-**4,13-BTEH**. (c) degeneracy $g = 2$.

Table S8. Energies of four most reasonable conformations of *P*-**2-TH** and their occupancies at 298.15 K.

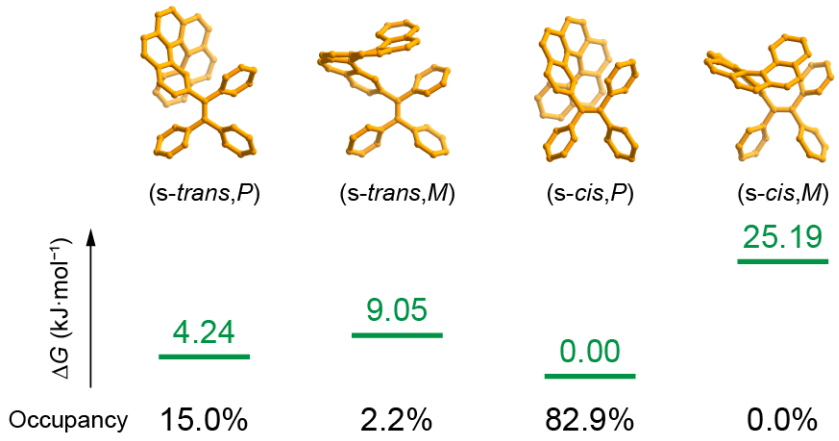

Conformations	*EE*[a]	*EE* + *ZPE*[a]	*H*[a]	*G*[a]	Δ*G*[b]	*p*
(s-*trans*,*P*),*P*-**2-TH**	-1771.439627	-1770.832176	-1770.797284	-1770.898883	4.24	17.6%
(s-*trans*,*M*),*P*-**2-TH**	-1771.436464	-1770.829525	-1770.794467	-1770.897053	9.05	3.2%
(s-*cis*,*P*),*P*-**2-TH**	-1771.440302	-1770.833054	-1770.798063	-1770.900499	0.00	79.2%
(s-*cis*,*M*),*P*-**2-TH**	-1771.431077	-1770.823909	-1770.788940	-1770.890906	25.19	0.0%

(a) in Hartree. (b) in kJ·mol^{-1}, relative to (s-*cis*,*P*),*P*-**2-TH**.

Table S9. Energies of four most reasonable conformations of *P*-**4-TH** and their occupancies at 298.15 K.

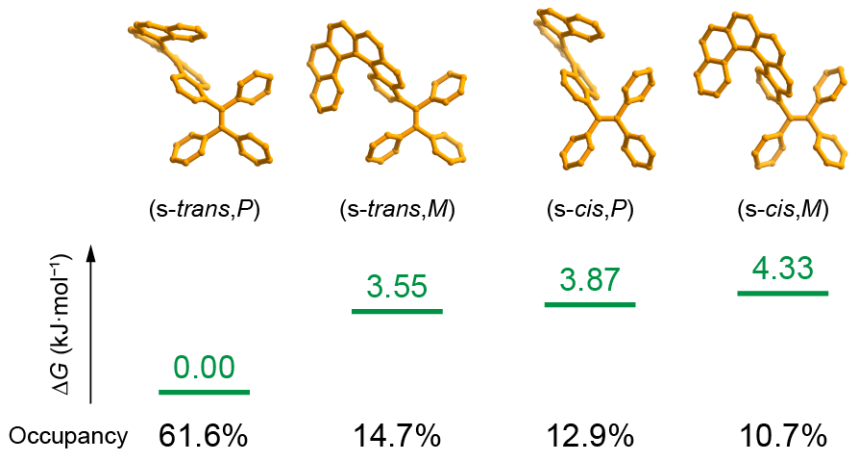

Conformations	*EE*[a]	*EE* + *ZPE*[a]	*H*[a]	*G*[a]	Δ*G*[b]	*p*
(s-*trans*,*P*),*P*-**4-TH**	-1771.436468	-1770.829125	-1770.794173	-1770.896457	0.00	61.6%
(s-*trans*,*M*),*P*-**4-TH**	-1771.434932	-1770.827671	-1770.792672	-1770.895103	3.55	14.7%
(s-*cis*,*P*),*P*-**4-TH**	-1771.434489	-1770.827271	-1770.792250	-1770.894983	3.87	12.9%
(s-*cis*,*M*),*P*-**4-TH**	-1771.434649	-1770.827350	-1770.792366	-1770.894806	4.33	10.7%

(a) in Hartree. (b) in kJ·mol^{-1}, relative to (s-*trans*,*P*),*P*-**4-TH**.

Table S10. Energies of ten most reasonable conformations of *P*-**2,15-BTH** and their occupancies at 298.15 K.

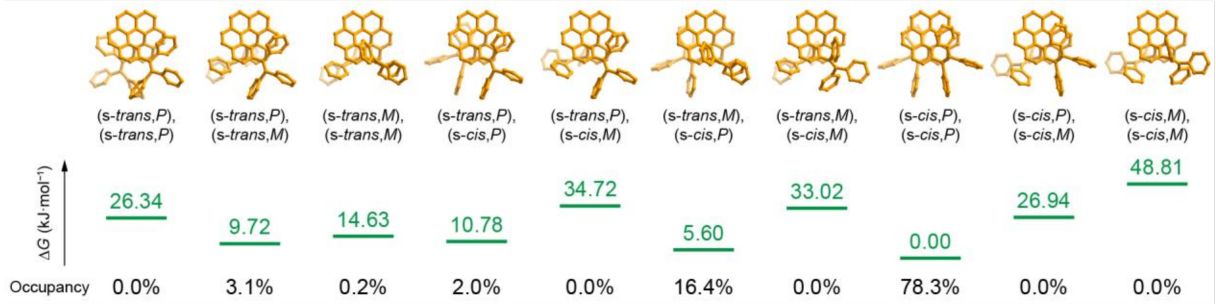

Conformations	*EE*[a]	*EE* + *ZPE*[a]	*H*[a]	*G*[a]	Δ*G*[b]	*p*
(s-*trans*,*P*),(s-*trans*,*P*), *P*-**2,15-BTH**	-2542.180382	-2541.298712	-2541.247279	-2541.387143	26.34	0.0%
(s-*trans*,*P*),(s-*trans*,*M*), *P*-**2,15-BTH**	-2542.184187	-2541.302974	-2541.251339	-2541.393474	9.72	3.1%[c]
(s-*trans*,*M*),(s-*trans*,*M*), *P*-**2,15-BTH**	-2542.182977	-2541.301921	-2541.250260	-2541.391601	14.63	0.2%
(s-*trans*,*P*),(s-*cis*,*P*), *P*-**2,15-BTH**	-2542.185417	-2541.304079	-2541.252520	-2541.393068	10.78	2.0%[c]
(s-*trans*,*P*),(s-*cis*,*M*), *P*-**2,15-BTH**	-2542.175419	-2541.294420	-2541.242799	-2541.383950	34.72	0.0%[c]
(s-*trans*,*M*),(s-*cis*,*P*), *P*-**2,15-BTH**	-2542.186086	-2541.304951	-2541.253269	-2541.395043	5.60	16.4%[c]
(s-*trans*,*M*),(s-*cis*,*M*), *P*-**2,15-BTH**	-2542.177653	-2541.296089	-2541.244627	-2541.384598	33.02	0.0%[c]
(s-*cis*,*P*),(s-*cis*,*P*), *P*-**2,15-BTH**	-2542.189312	-2541.307786	-2541.256220	-2541.397175	0.00	78.3%
(s-*cis*,*P*),(s-*cis*,*M*), *P*-**2,15-BTH**	-2542.179348	-2541.297967	-2541.246413	-2541.386913	26.94	0.0%[c]
(s-*cis*,*M*),(s-*cis*,*M*), *P*-**2,15-BTH**	-2542.169794	-2541.288825	-2541.237201	-2541.378586	48.81	0.0%

(a) in Hartree. (b) in kJ·mol^{-1}, relative to (s-*cis*,*P*),(s-*cis*,*P*),*P*-**2,15-BTH**. (c) degeneracy $g = 2$.

Table S11. Energies of ten most reasonable conformations of *P*-**4,13-BTH** and their occupancies at 298.15 K.

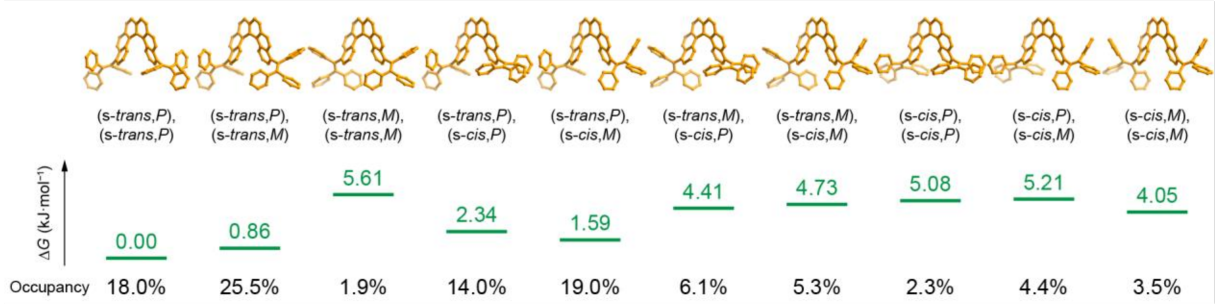

Conformations	*EE*[a]	*EE* + *ZPE*[a]	*H*[a]	*G*[a]	Δ*G*[b]	*p*
(s-*trans*,*P*),(s-*trans*,*P*), *P*-**4,13-BTH**	-2542.182268	-2541.300314	-2541.248827	-2541.390012	0.00	18.0%
(s-*trans*,*P*),(s-*trans*,*M*), *P*-**4,13-BTH**	-2542.180827	-2541.299256	-2541.247639	-2541.389685	0.86	25.5%[c]
(s-*trans*,*M*),(s-*trans*,*M*), *P*-**4,13-BTH**	-2542.179011	-2541.297445	-2541.245799	-2541.387877	5.61	1.9%
(s-*trans*,*P*),(s-*cis*,*P*), *P*-**4,13-BTH**	-2542.180417	-2541.298826	-2541.247189	-2541.389122	2.34	14.0%[c]
(s-*trans*,*P*),(s-*cis*,*M*), *P*-**4,13-BTH**	-2542.180570	-2541.299114	-2541.247494	-2541.389408	1.59	19.0%[c]
(s-*trans*,*M*),(s-*cis*,*P*), *P*-**4,13-BTH**	-2542.178911	-2541.297398	-2541.245705	-2541.388333	4.41	6.1%[c]
(s-*trans*,*M*),(s-*cis*,*M*), *P*-**4,13-BTH**	-2542.178985	-2541.297427	-2541.245773	-2541.388212	4.73	5.3%[c]
(s-*cis*,*P*),(s-*cis*,*P*), *P*-**4,13-BTH**	-2542.178577	-2541.297098	-2541.245386	-2541.388076	5.08	2.3%
(s-*cis*,*P*),(s-*cis*,*M*), *P*-**4,13-BTH**	-2542.178651	-2541.297149	-2541.245476	-2541.388026	5.21	4.4%[c]
(s-*cis*,*M*),(s-*cis*,*M*), *P*-**4,13-BTH**	-2542.178634	-2541.297193	-2541.245516	-2541.388471	4.05	3.5%

(a) in Hartree. (b) in kJ·mol^{-1}, relative to (s-*trans*,*P*),(s-*trans*,*P*),*P*-**4,13-BTH**. (c) degeneracy $g = 2$.

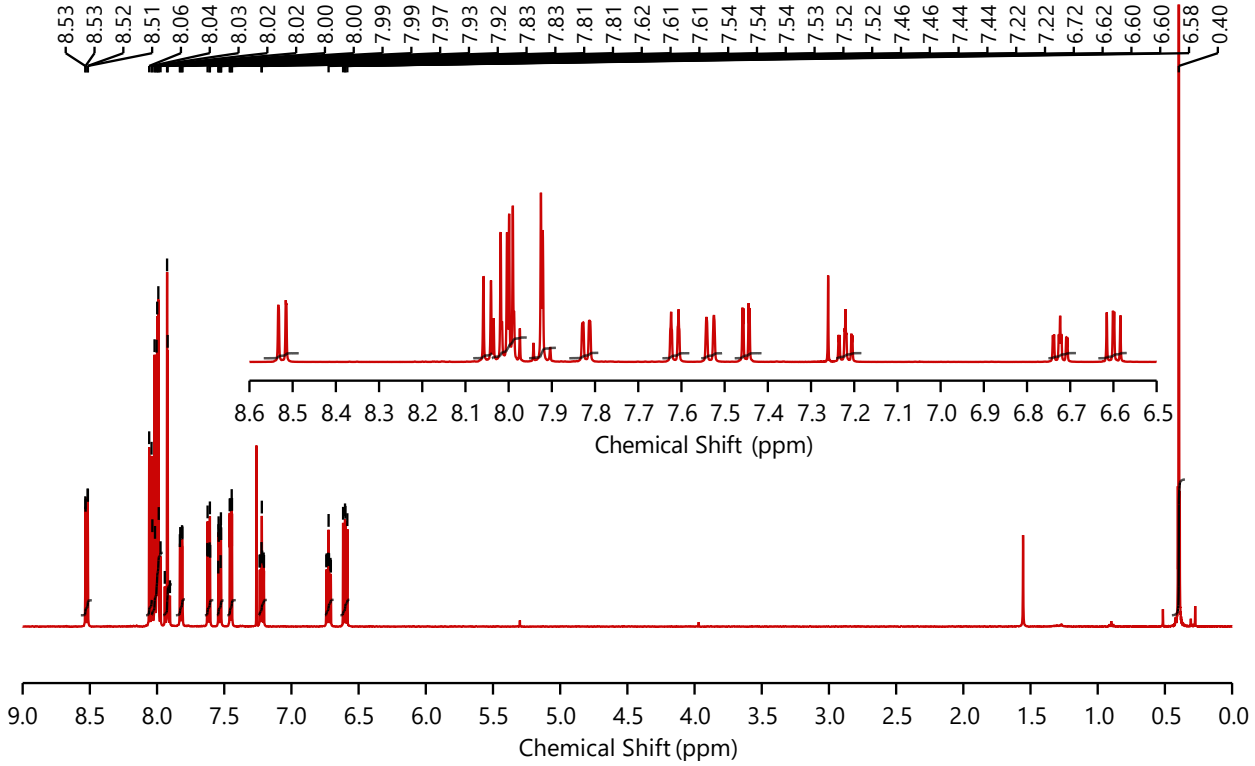

Figure S1. ^{1}H NMR of 4-(trimethylsilylethynyl)[6]helicene (500 MHz, $CDCl_3$, 298 K).

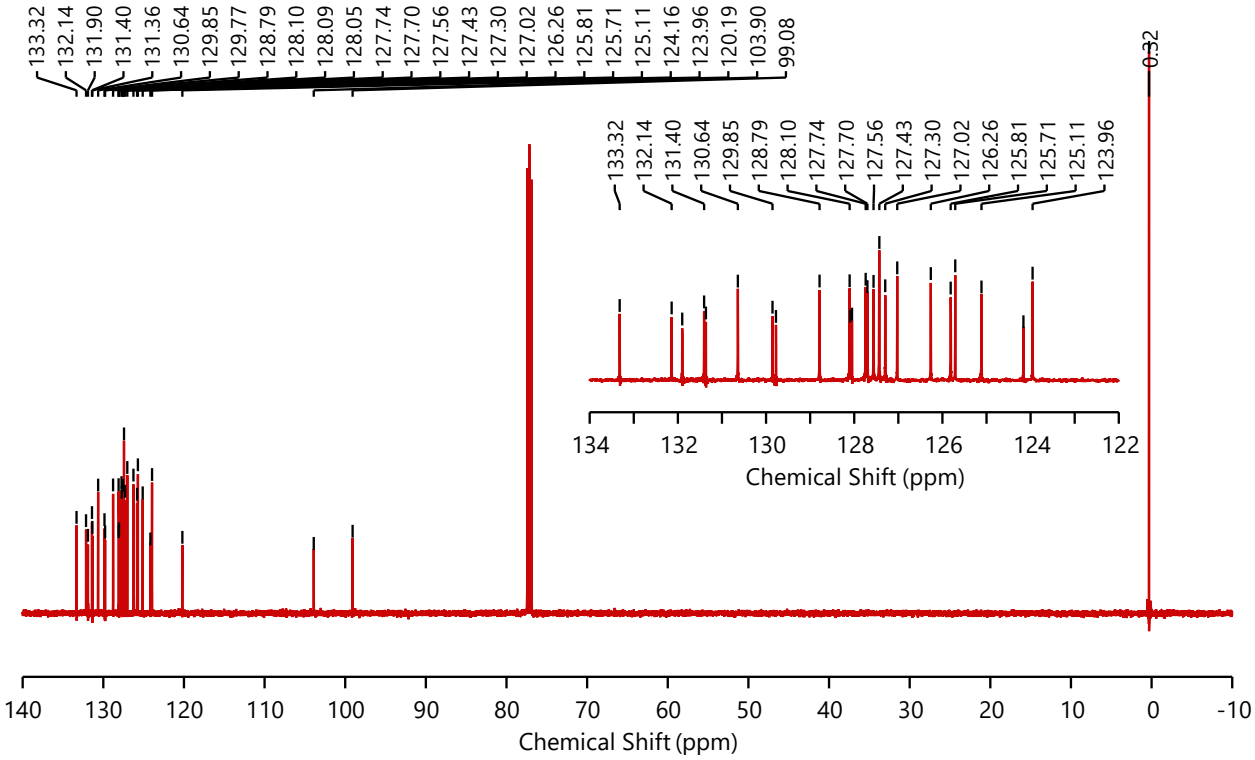

Figure S2. ^{13}C{^{1}H} NMR of 4-(trimethylsilylethynyl)[6]helicene (125 MHz, $CDCl_3$, 298 K).

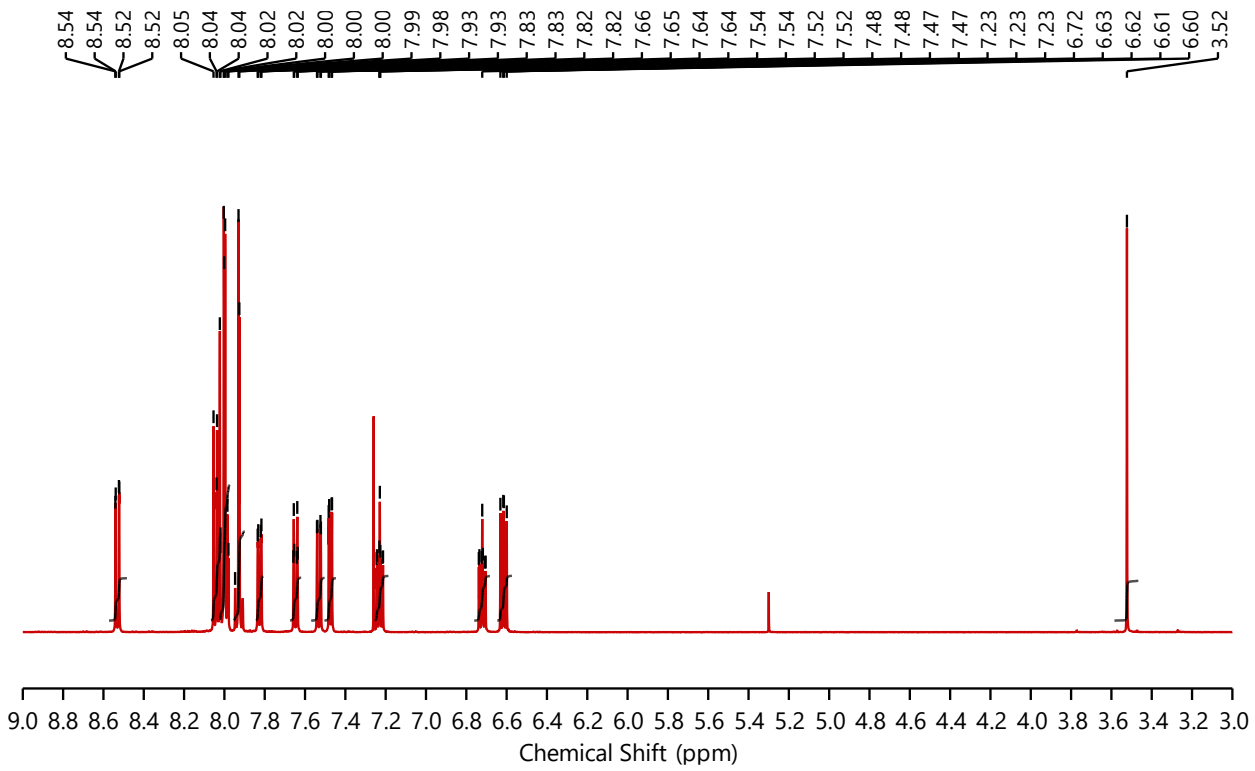

Figure S3. ^{1}H NMR of 4-ethynyl[6]helicene (500 MHz, $CDCl_3$, 298 K).

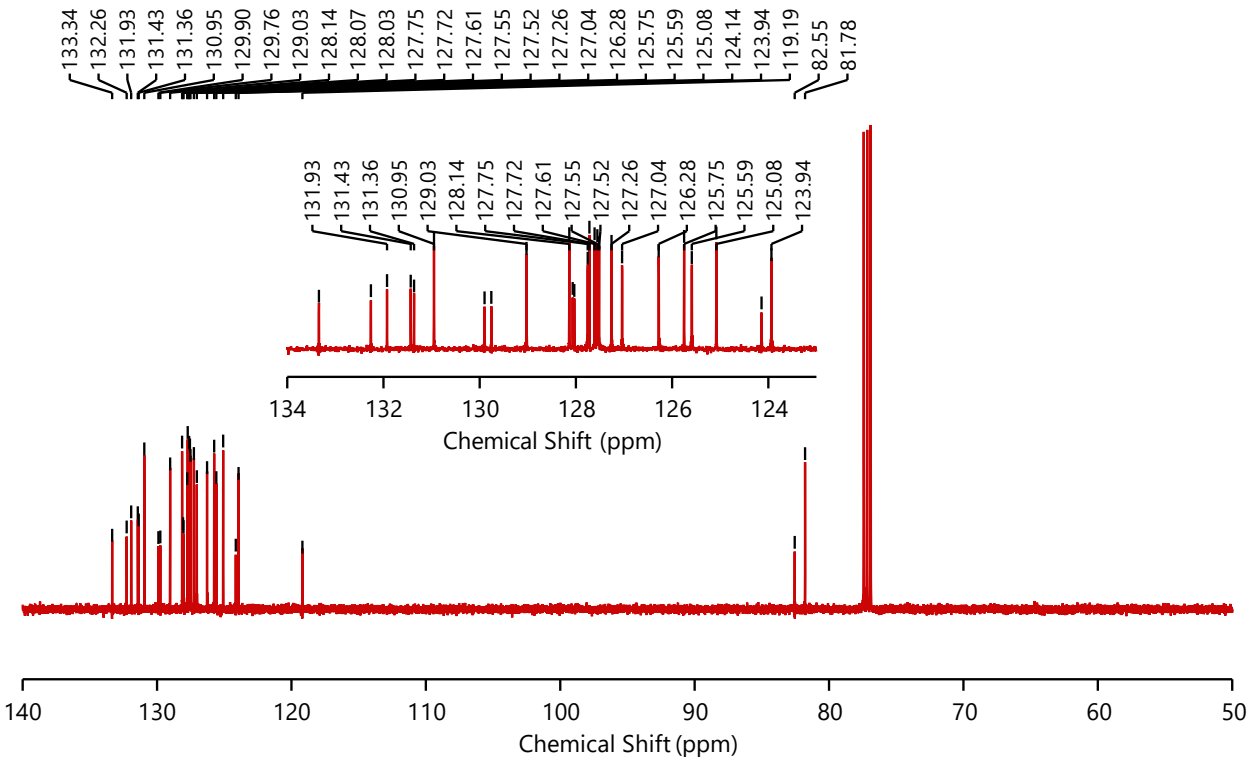

Figure S4. $^{13}C\{^{1}H\}$ NMR of 4-ethynyl[6]helicene (125 MHz, $CDCl_3$, 298 K).

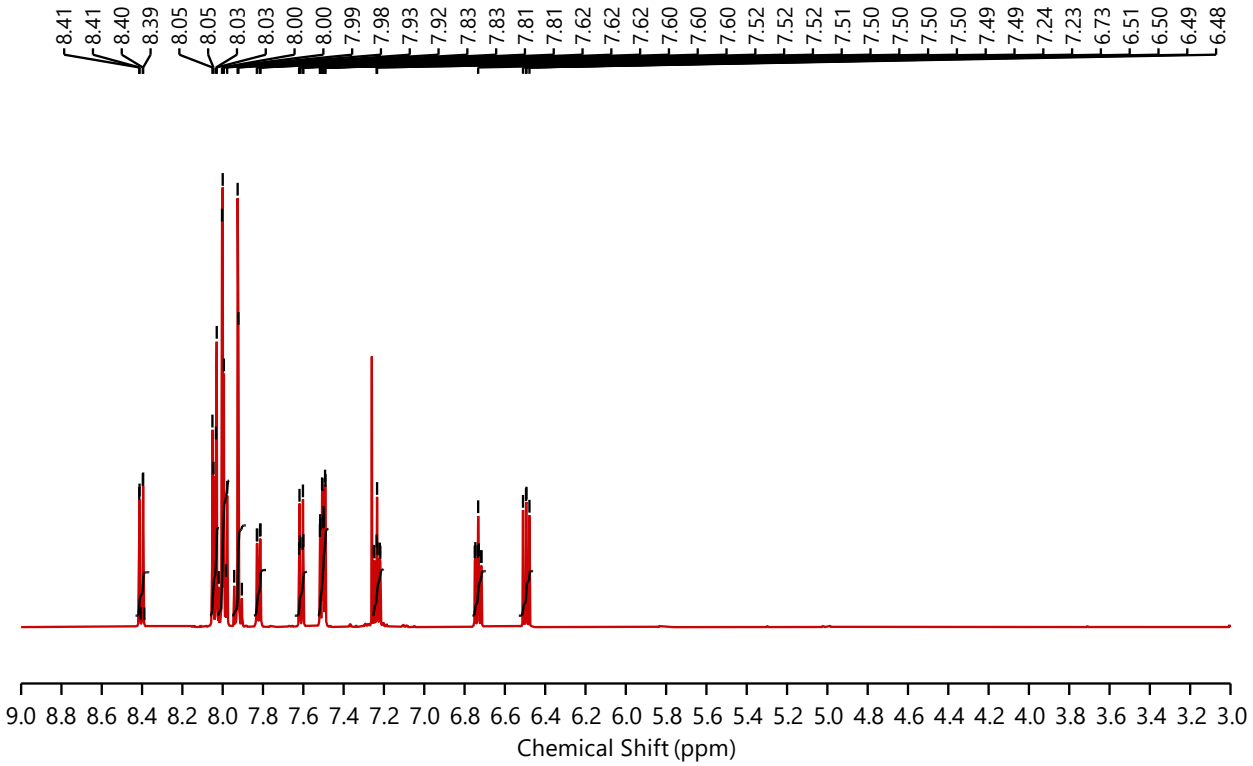

Figure S5. ^{1}H NMR of 4-bromo[6]helicene (500 MHz, $CDCl_3$, 298 K).

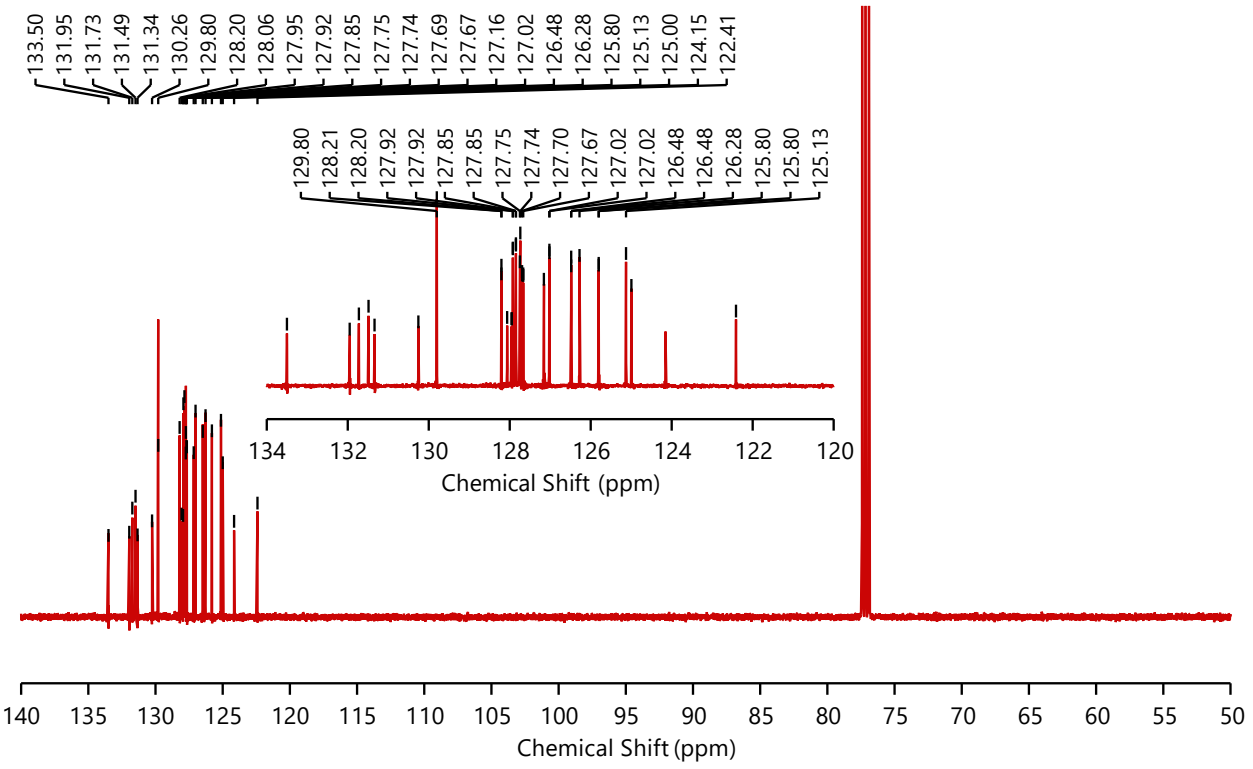

Figure S6. $^{13}C\{^{1}H\}$ NMR of 4-bromo[6]helicene (125 MHz, $CDCl_3$, 298 K).

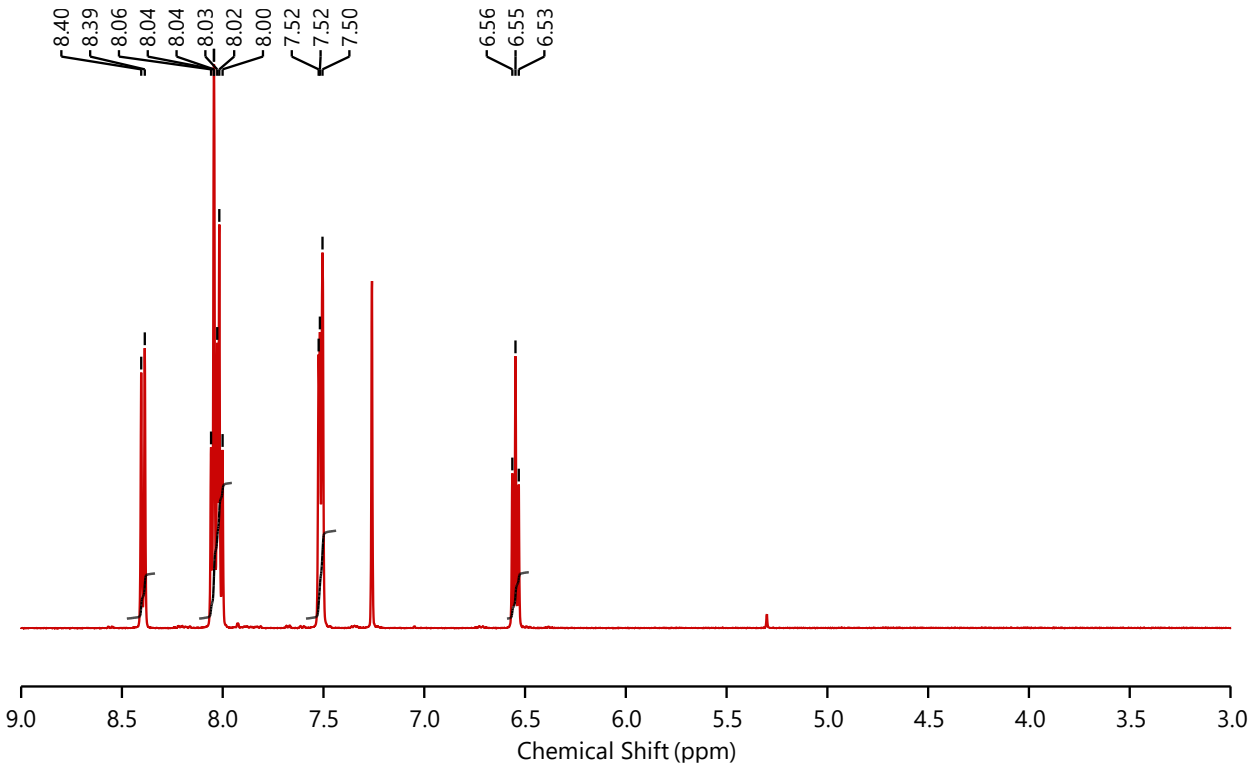

Figure S7. ^{1}H NMR of 4,13-dibromo[6]helicene (500 MHz, $CDCl_3$, 298 K).

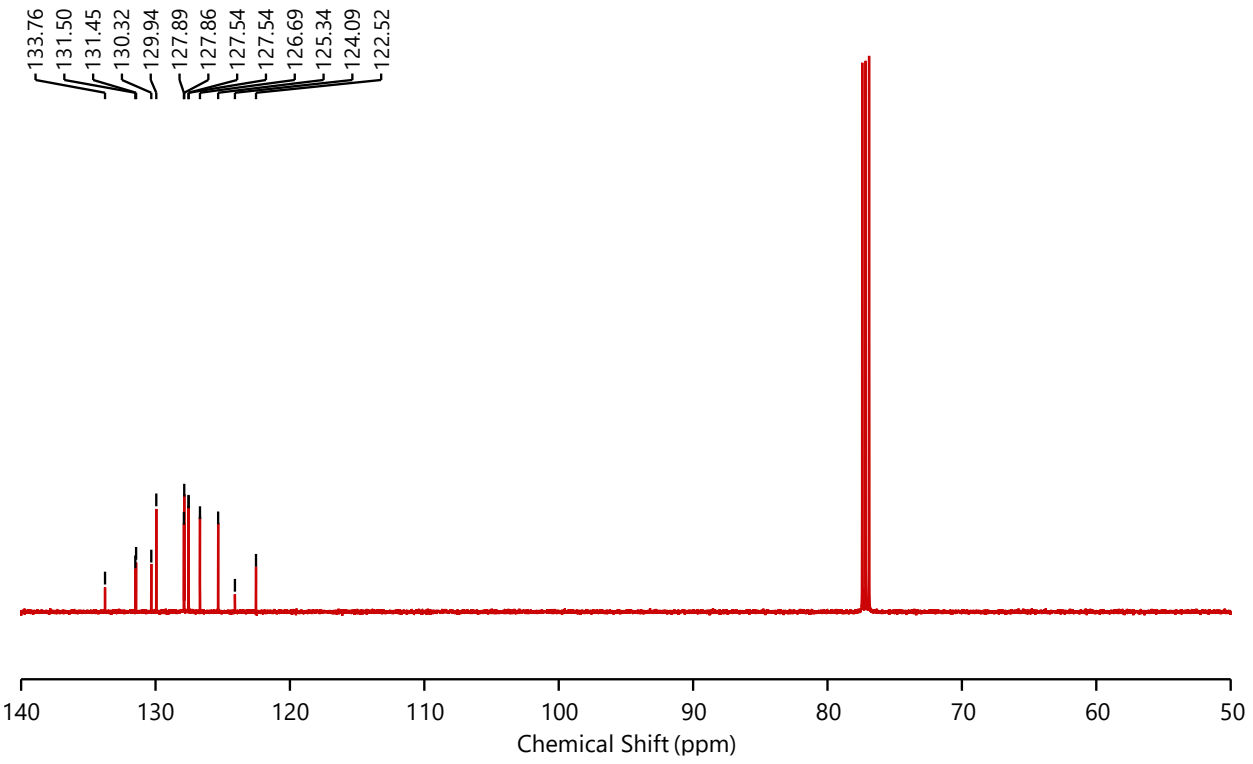

Figure S8. $^{13}C\{^{1}H\}$ NMR of 4,13-dibromo[6]helicene (125 MHz, $CDCl_3$, 298 K).

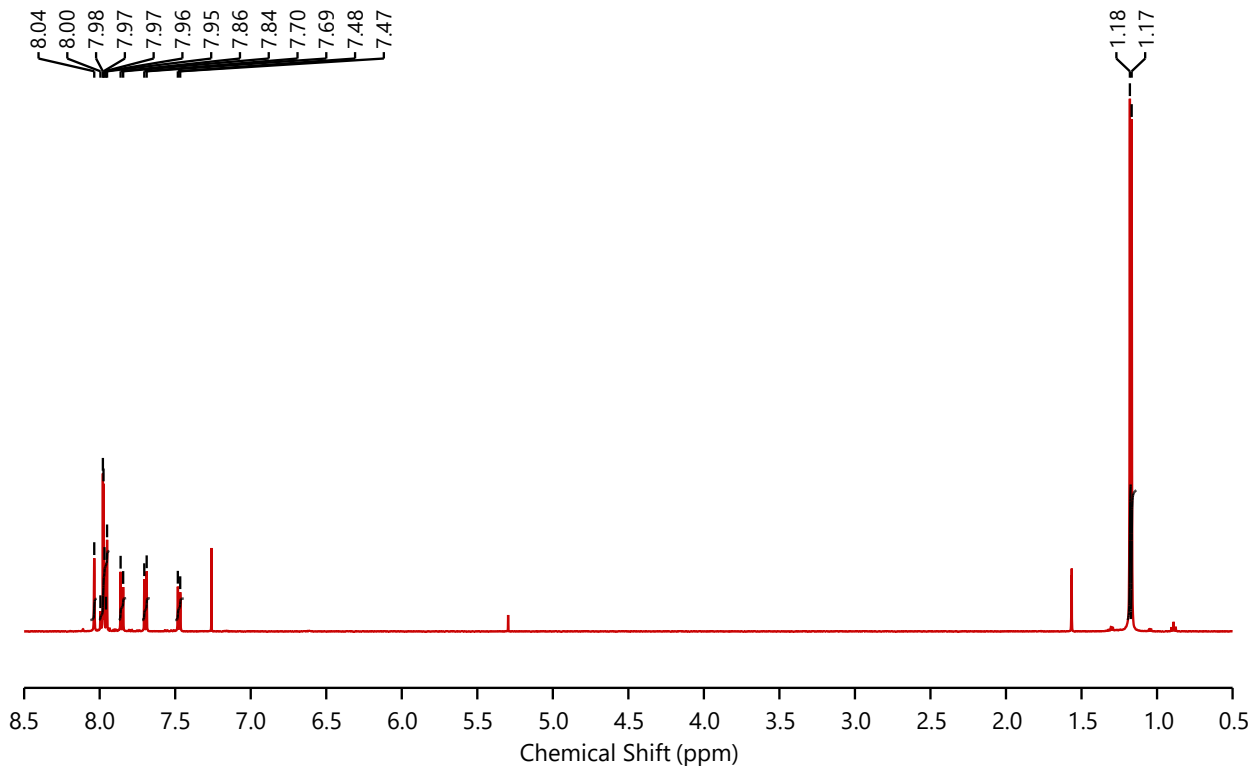

Figure S9. ^{1}H NMR of *rac*-2,15-bis(pinacolatoboryl)[6]helicene (500 MHz, $CDCl_3$, 298 K).

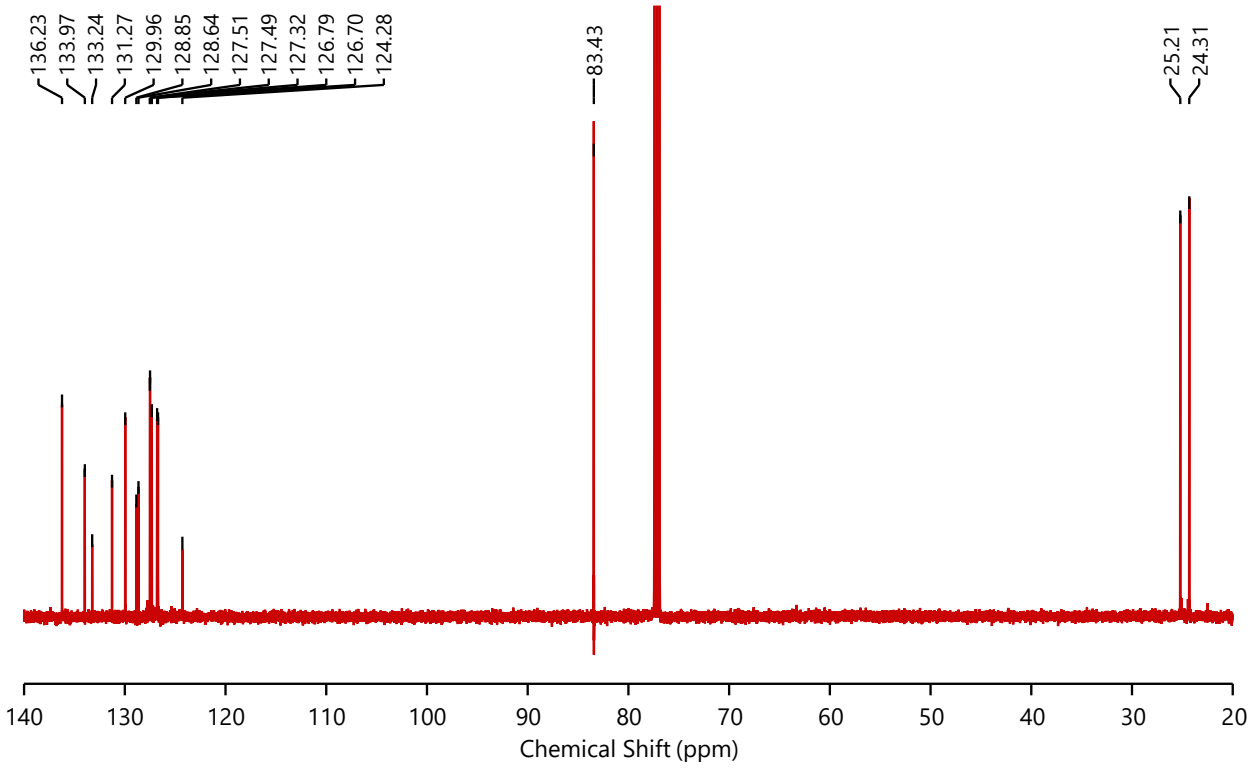

Figure S10. $^{13}C\{^{1}H\}$ NMR of *rac*-2,15-bis(pinacolatoboryl)[6]helicene (125 MHz, $CDCl_3$, 298 K).

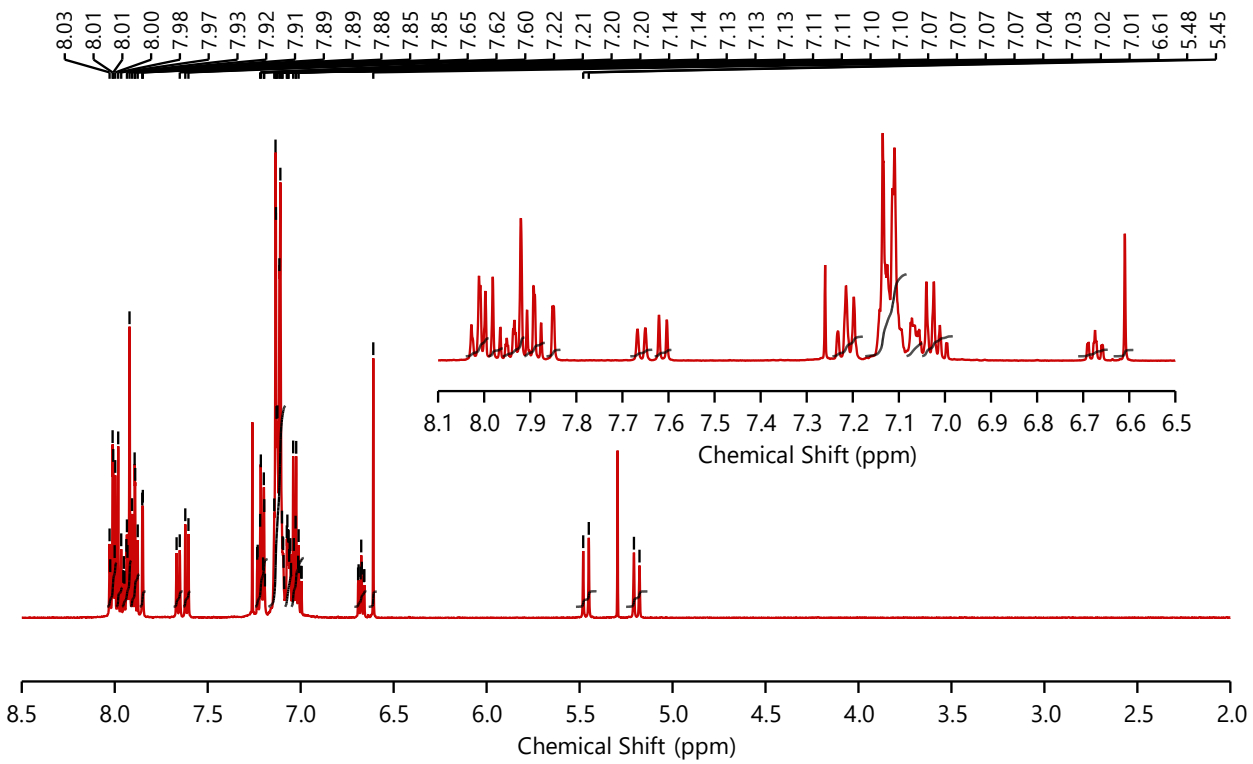

Figure S11. ^{1}H NMR of *rac*-**2-TBTH** (500 MHz, $CDCl_3$, 298 K).

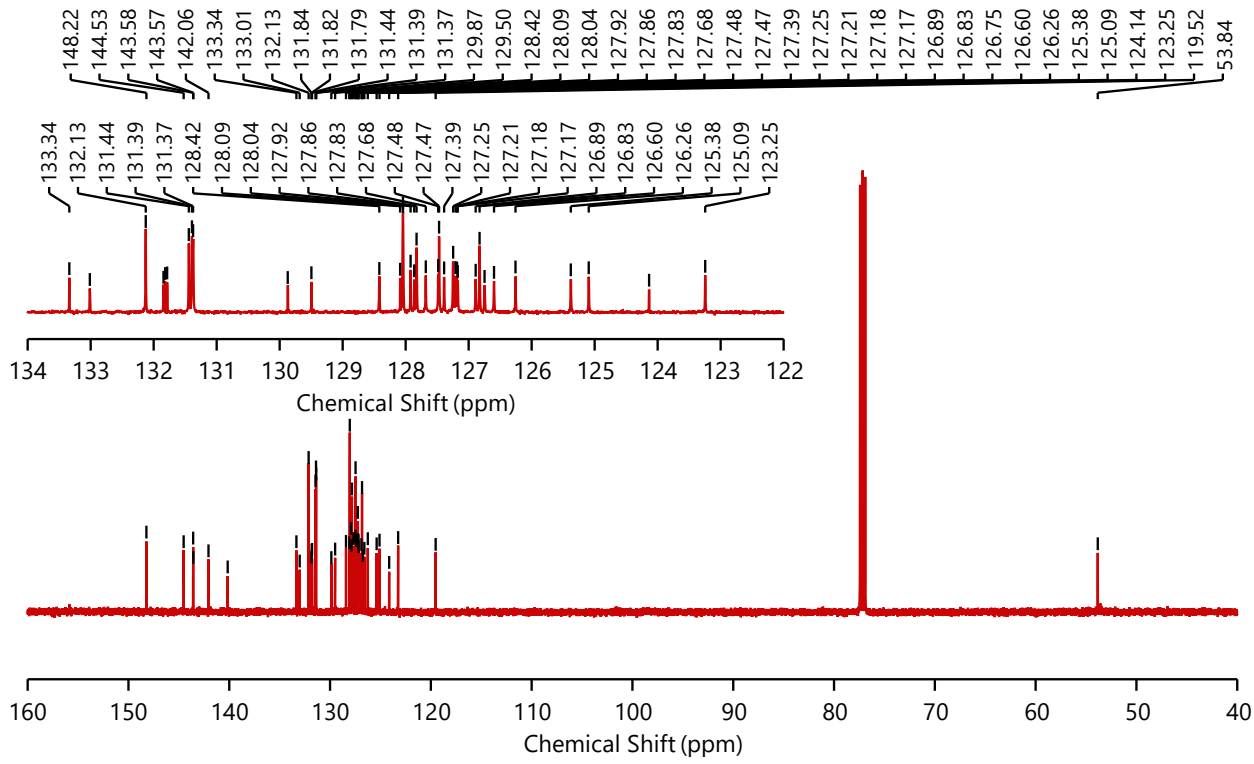

Figure S12. $^{13}C\{^{1}H\}$ NMR of *rac*-**2-TBTH** (125 MHz, $CDCl_3$, 298 K).

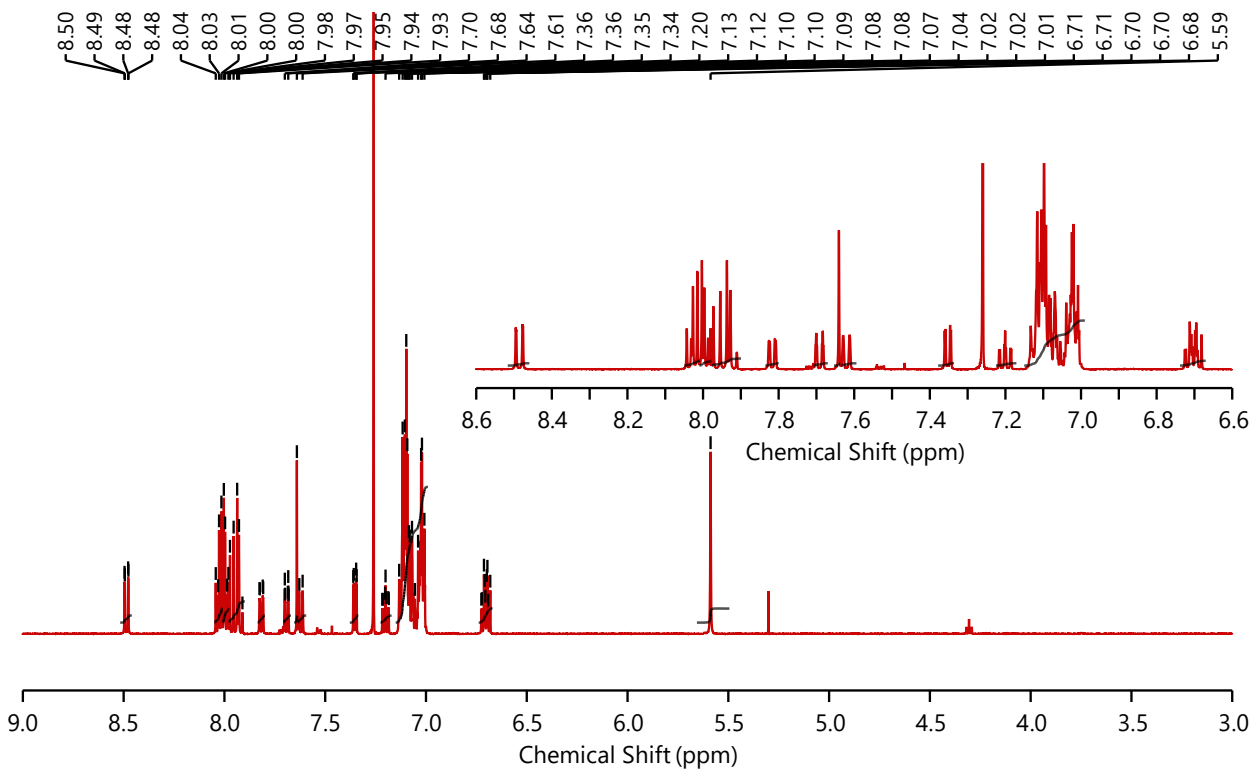

Figure S13. ^{1}H NMR of *rac*-**4-TBTH** (500 MHz, $CDCl_3$, 298 K).

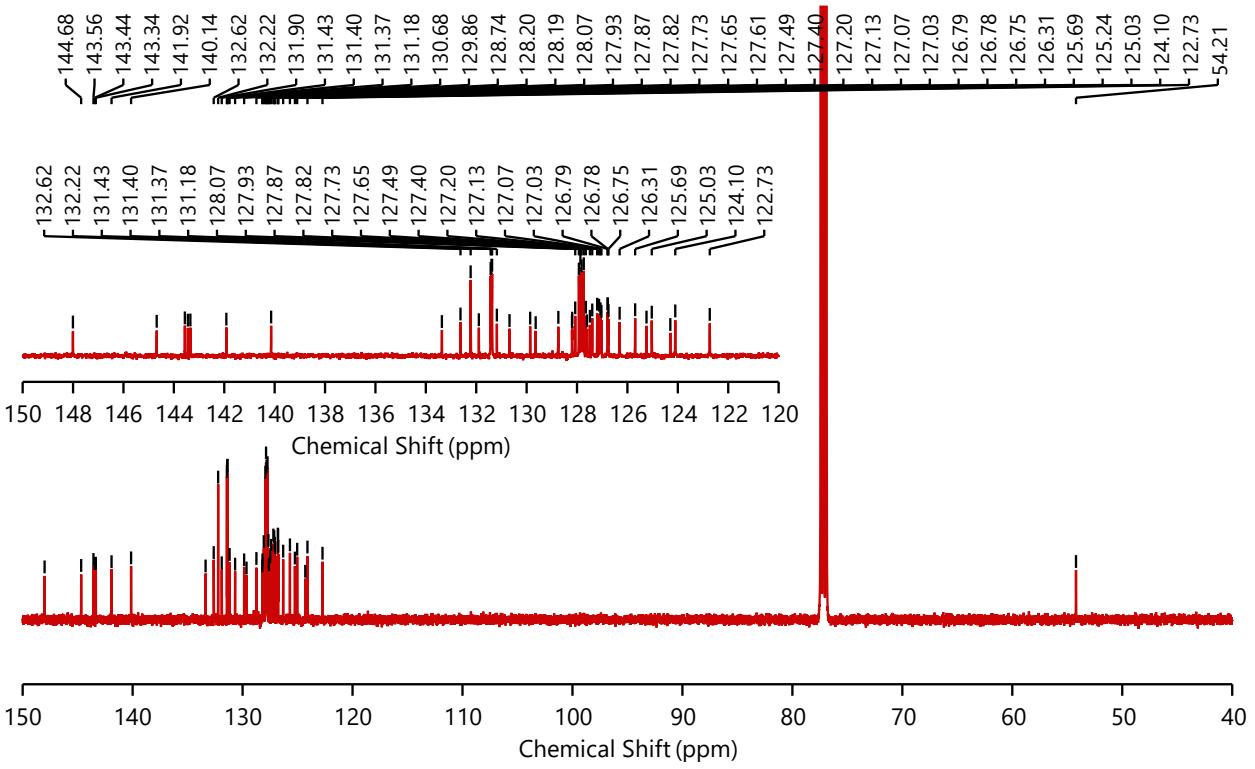

Figure S14. ^{13}C{^{1}H} NMR of *rac*-**4-TBTH** (125 MHz, $CDCl_3$, 298 K).

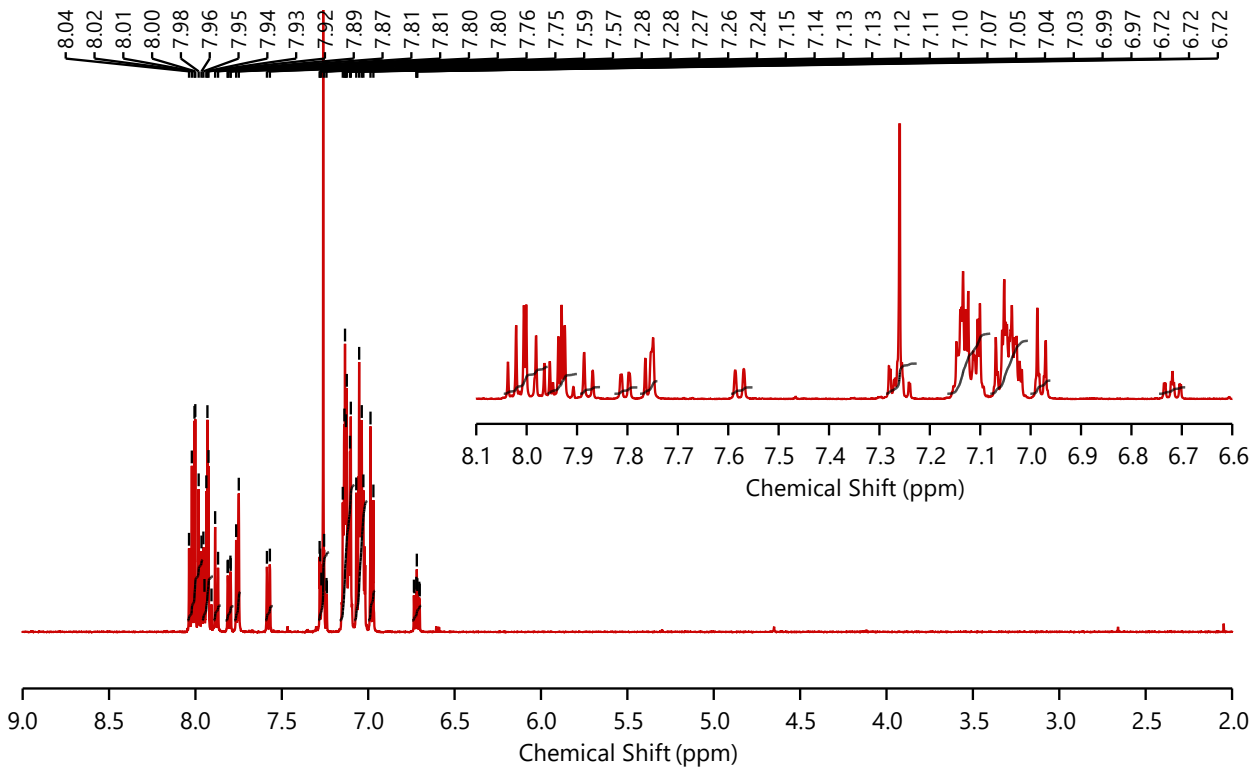

Figure S15. ^{1}H NMR of *rac*-**2-TPEH** (500 MHz, $CDCl_3$, 298 K).

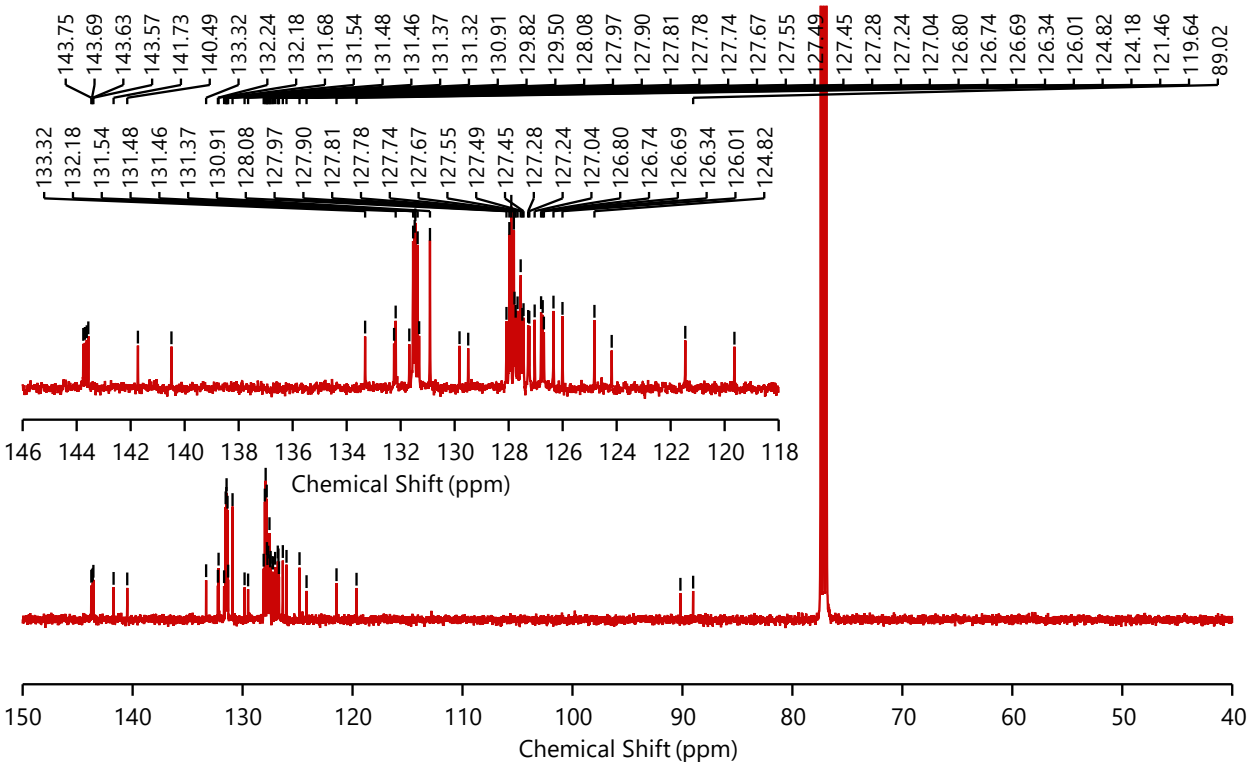

Figure S16. ^{13}C{^{1}H} NMR of *rac*-**2-TPEH** (125 MHz, $CDCl_3$, 298 K).

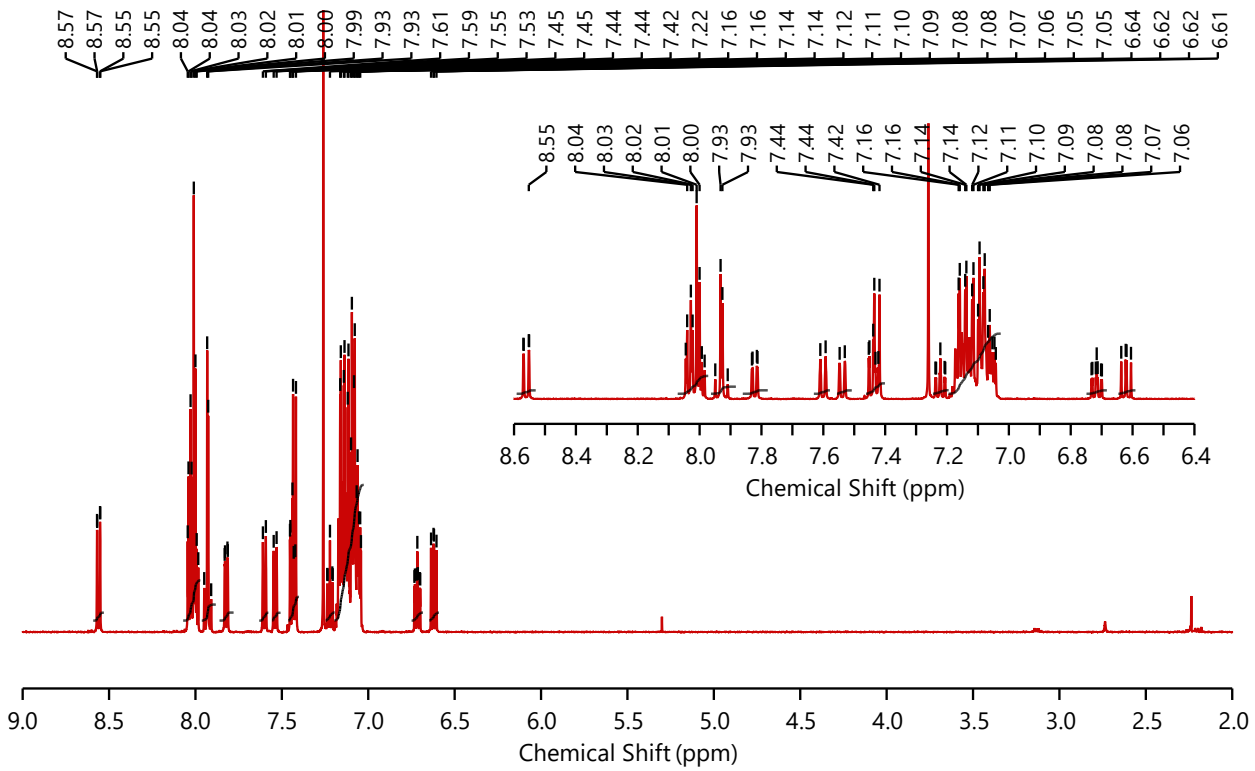

Figure S17. ^{1}H NMR of *rac*-**4-TPEH** (500 MHz, $CDCl_3$, 298 K).

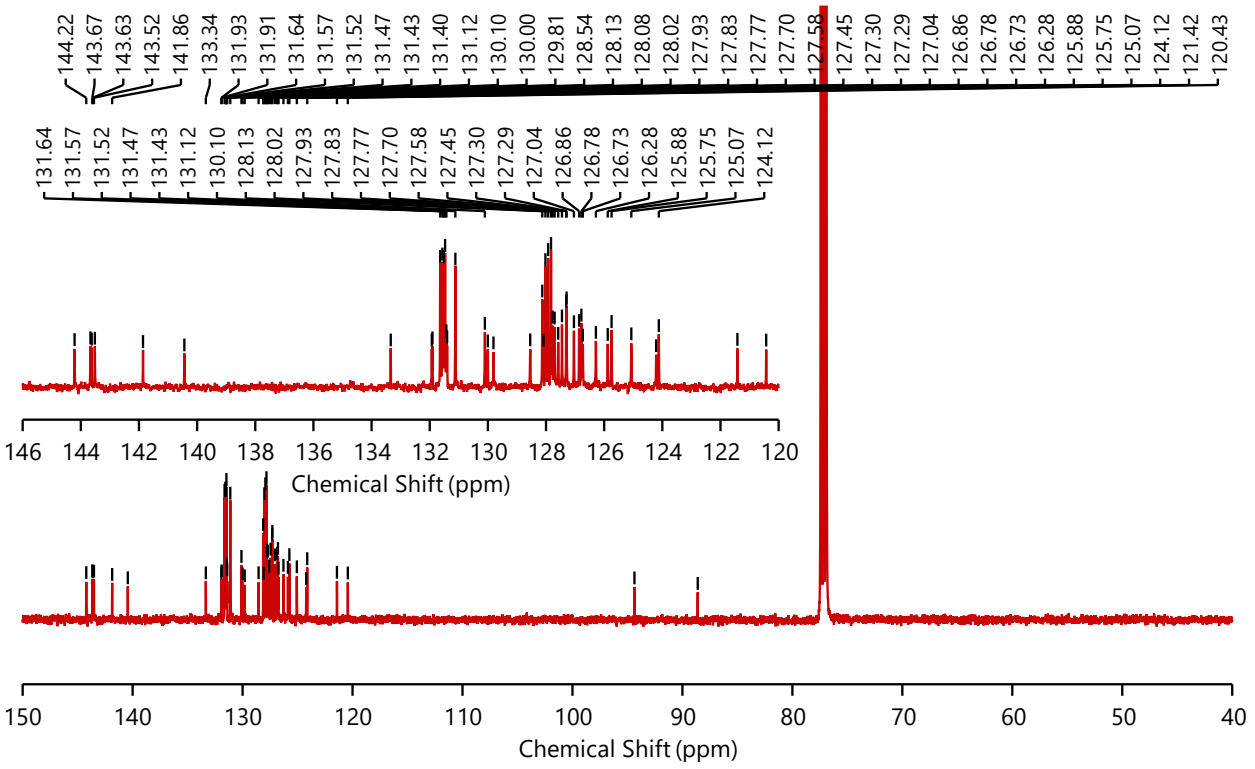

Figure S18. $^{13}C\{^{1}H\}$ NMR of *rac*-**4-TPEH** (125 MHz, $CDCl_3$, 298 K).

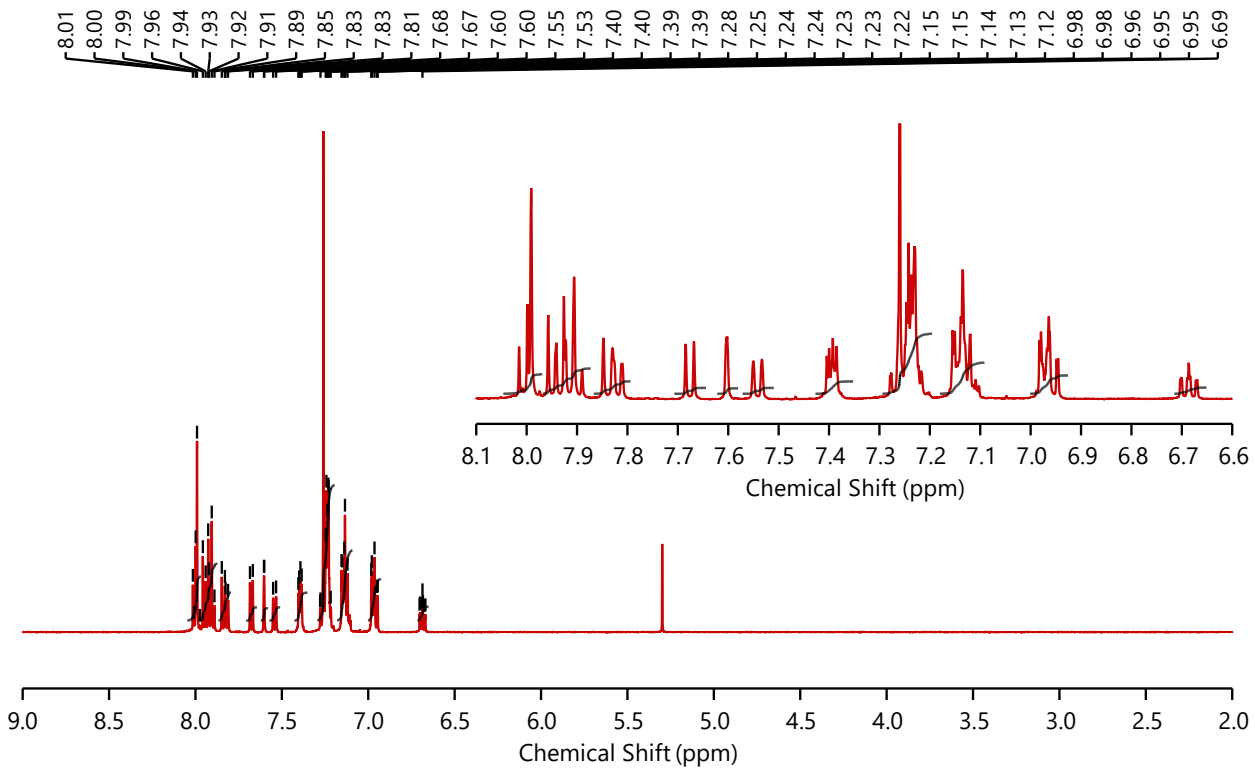

Figure S19. ^{1}H NMR of *rac*-**2-TEH** (500 MHz, $CDCl_3$, 298 K).

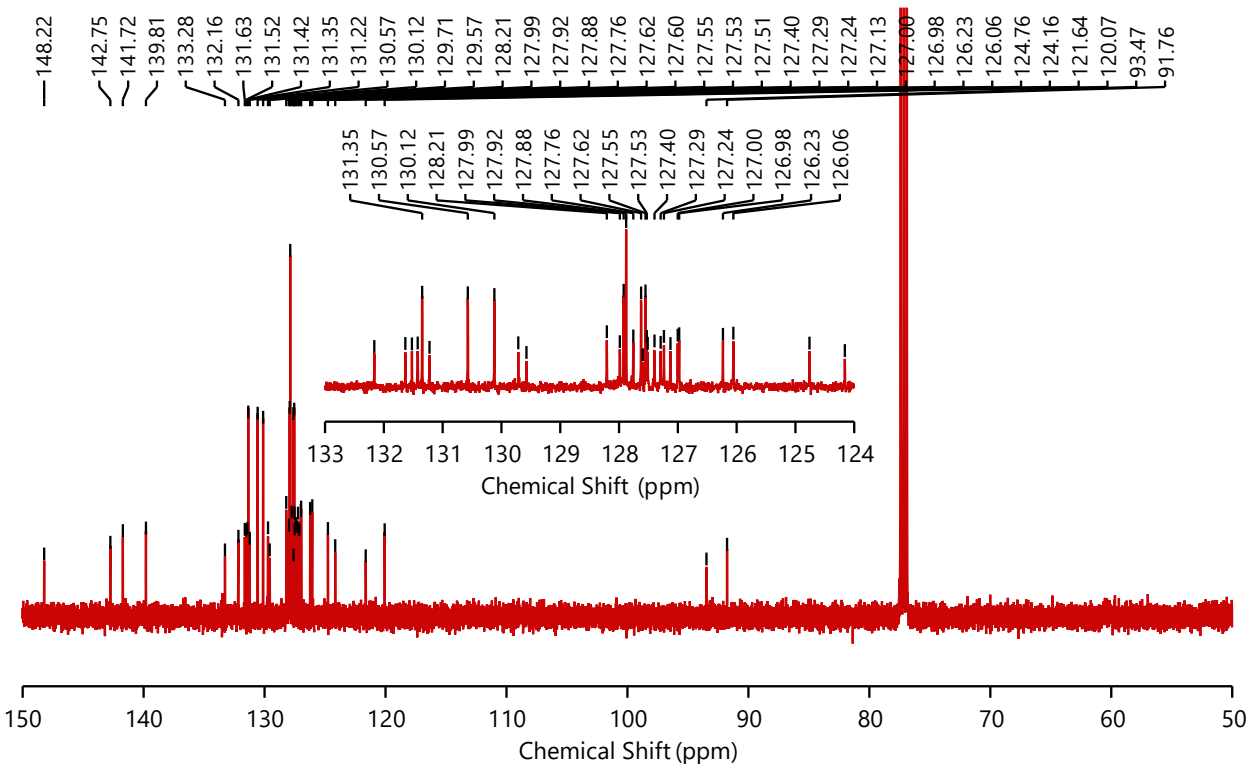

Figure S20. ^{13}C{^{1}H} NMR of *rac*-**2-TEH** (125 MHz, $CDCl_3$, 298 K).

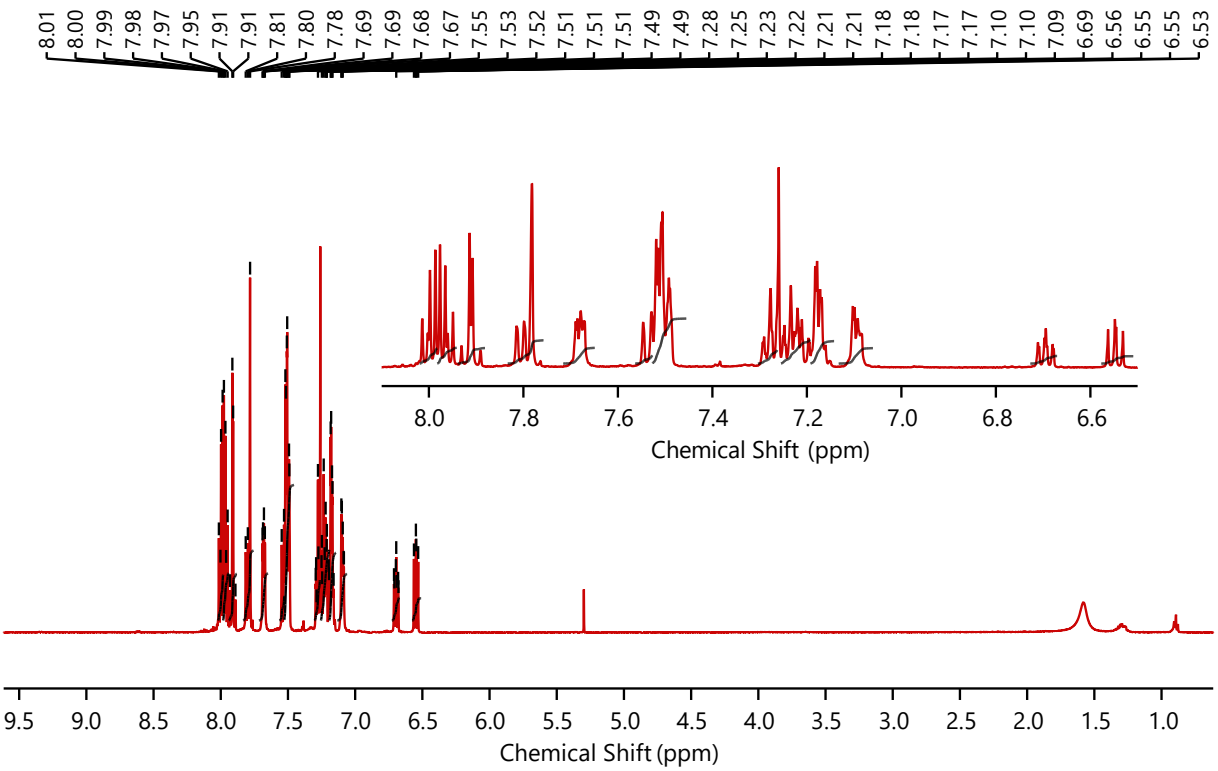

Figure S21. ^{1}H NMR of *rac*-**4-TEH** (500 MHz, $CDCl_3$, 298 K).

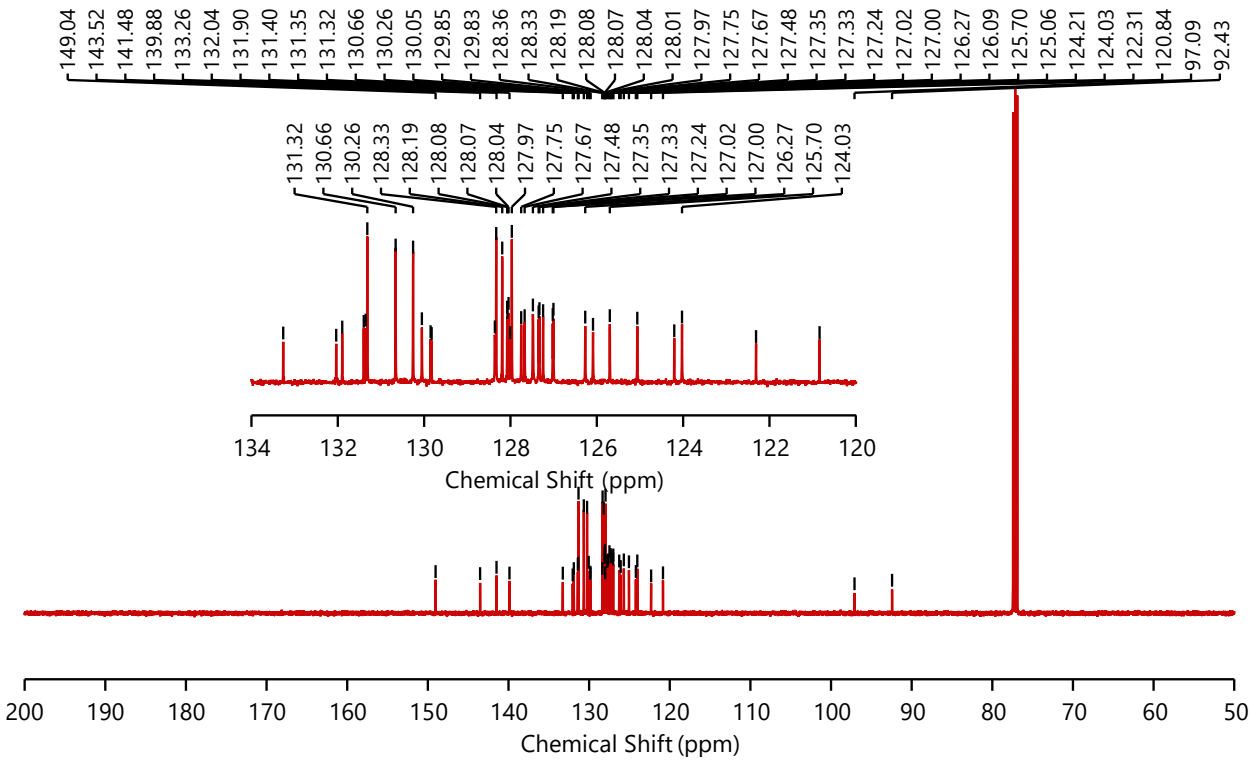

Figure S22. ^{13}C{^{1}H} NMR of *rac*-**4-TEH** (125 MHz, $CDCl_3$, 298 K).

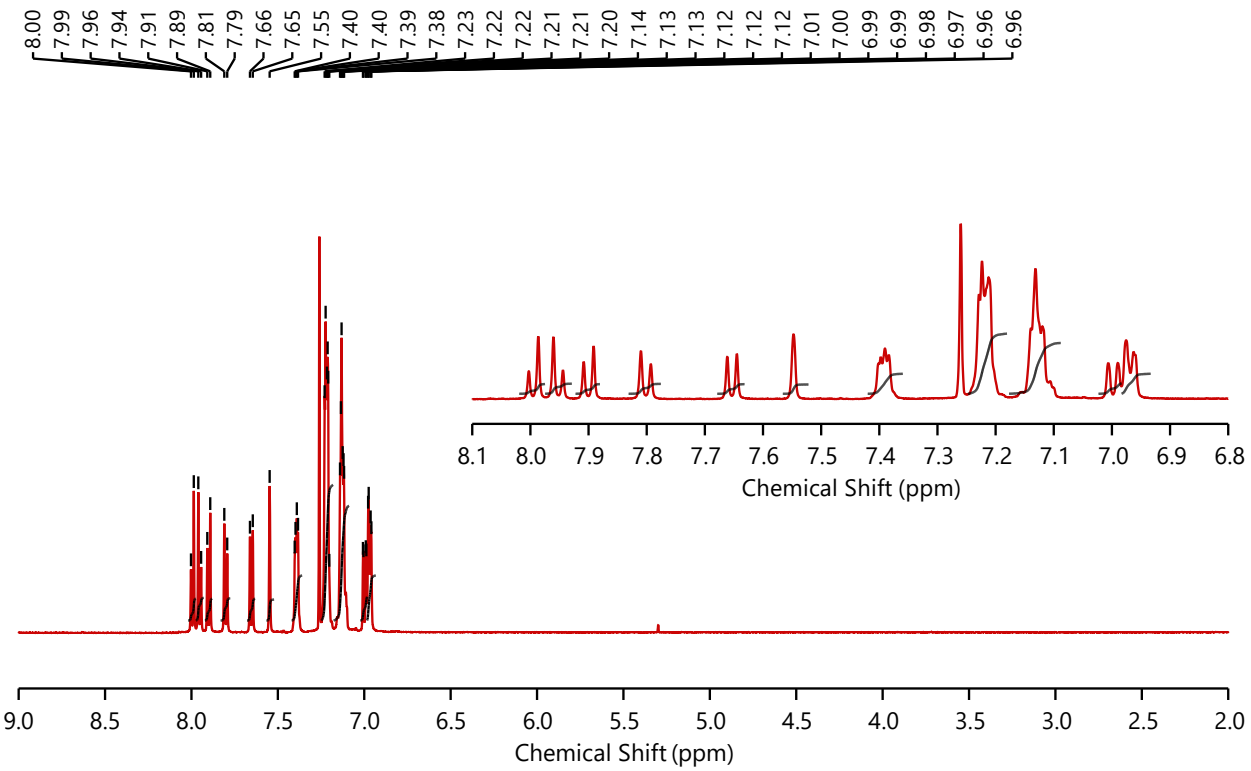

Figure S23. ^{1}H NMR of *P*-**2,15-BTEH** (500 MHz, $CDCl_3$, 298 K).

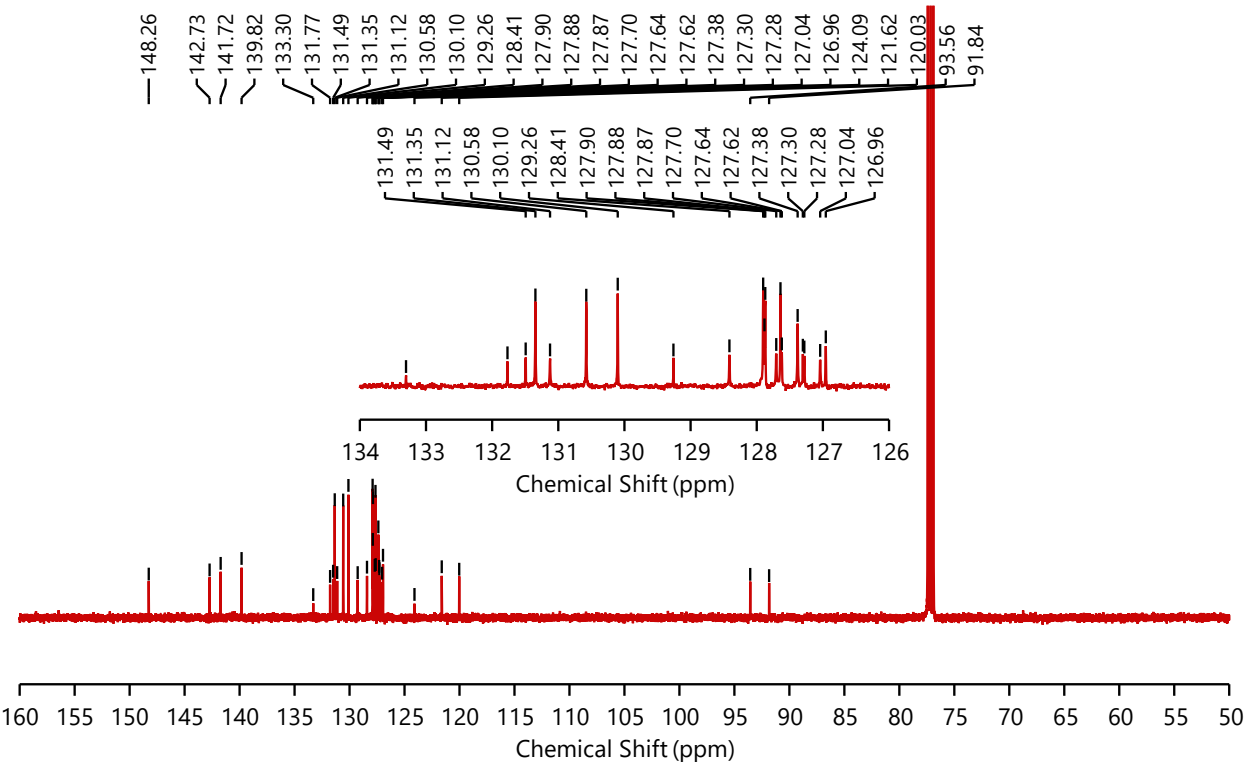

Figure S24. ^{13}C{^{1}H} NMR of *P*-**2,15-BTEH** (125 MHz, $CDCl_3$, 298 K).

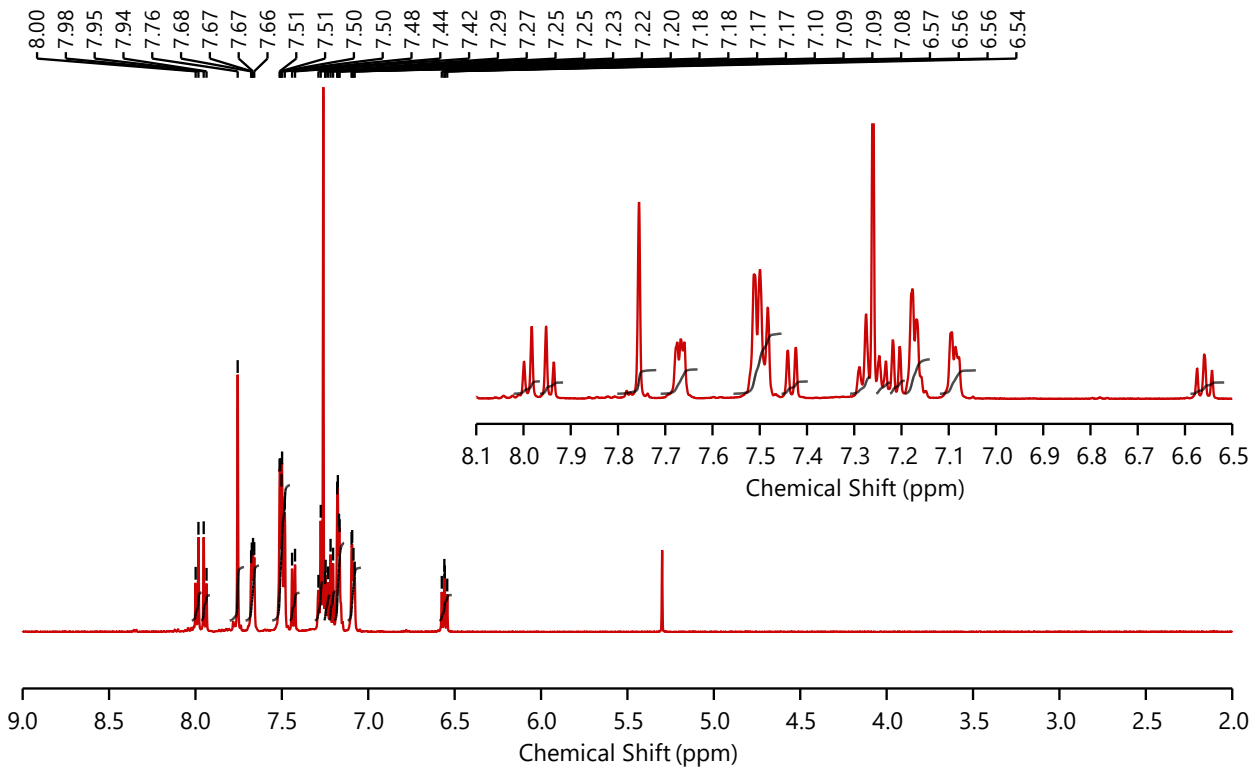

Figure S25. ^{1}H NMR of *P*-**4,13-BTEH** (500 MHz, $CDCl_3$, 298 K).

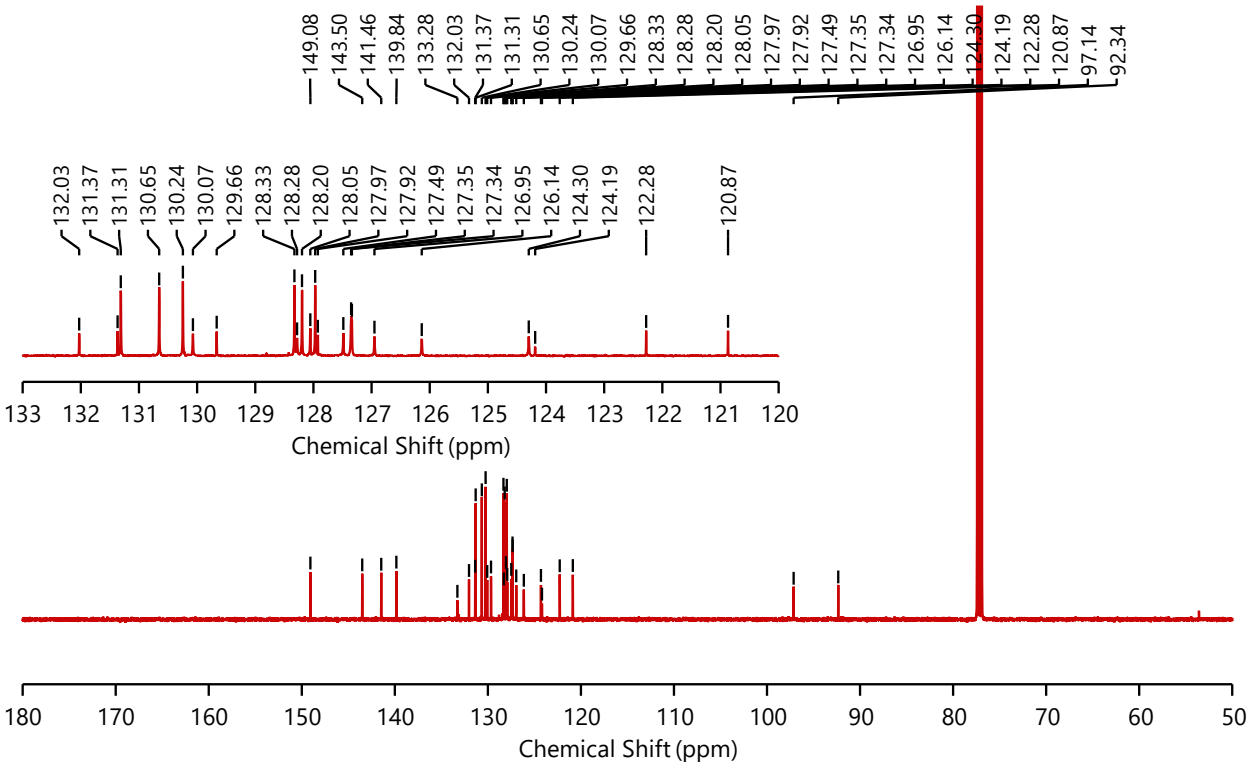

Figure S26. $^{13}C\{^{1}H\}$ NMR of *P*-**4,13-BTEH** (125 MHz, $CDCl_3$, 298 K).

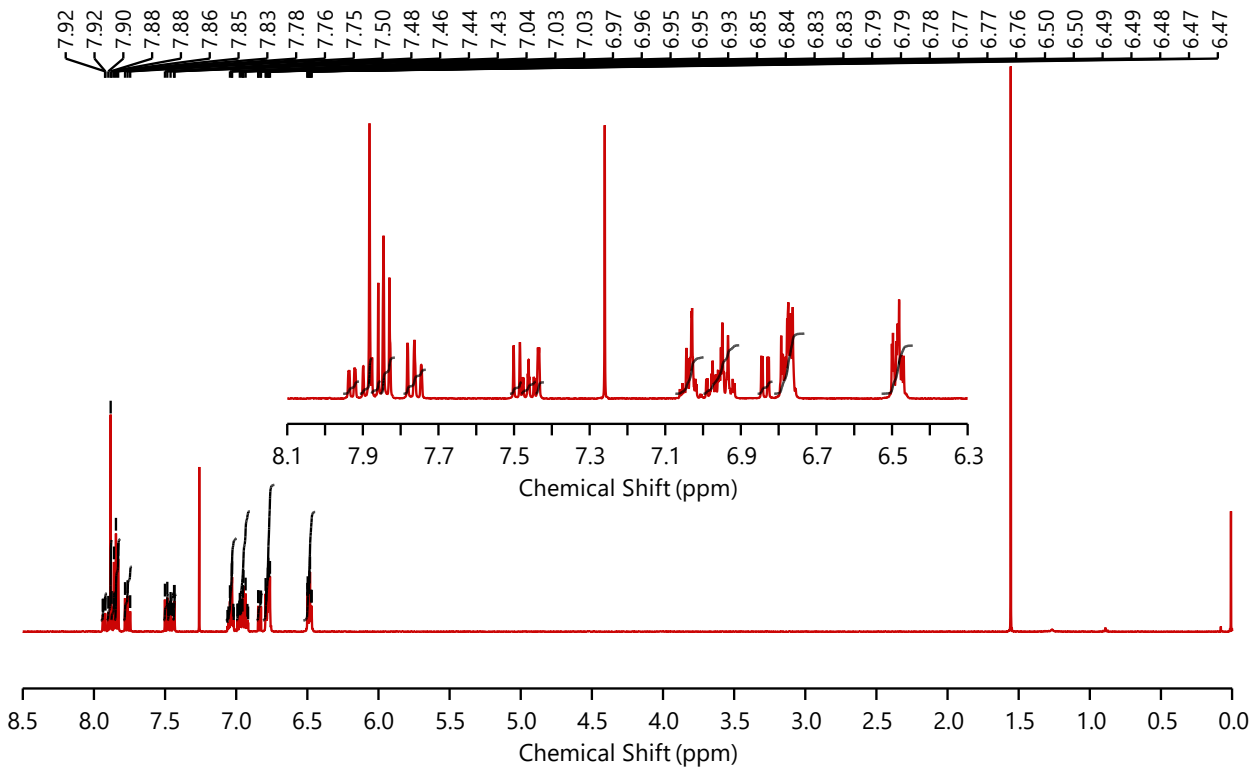

Figure S27. ^{1}H NMR of *rac*-**2-TH** (500 MHz, $CDCl_3$, 298 K).

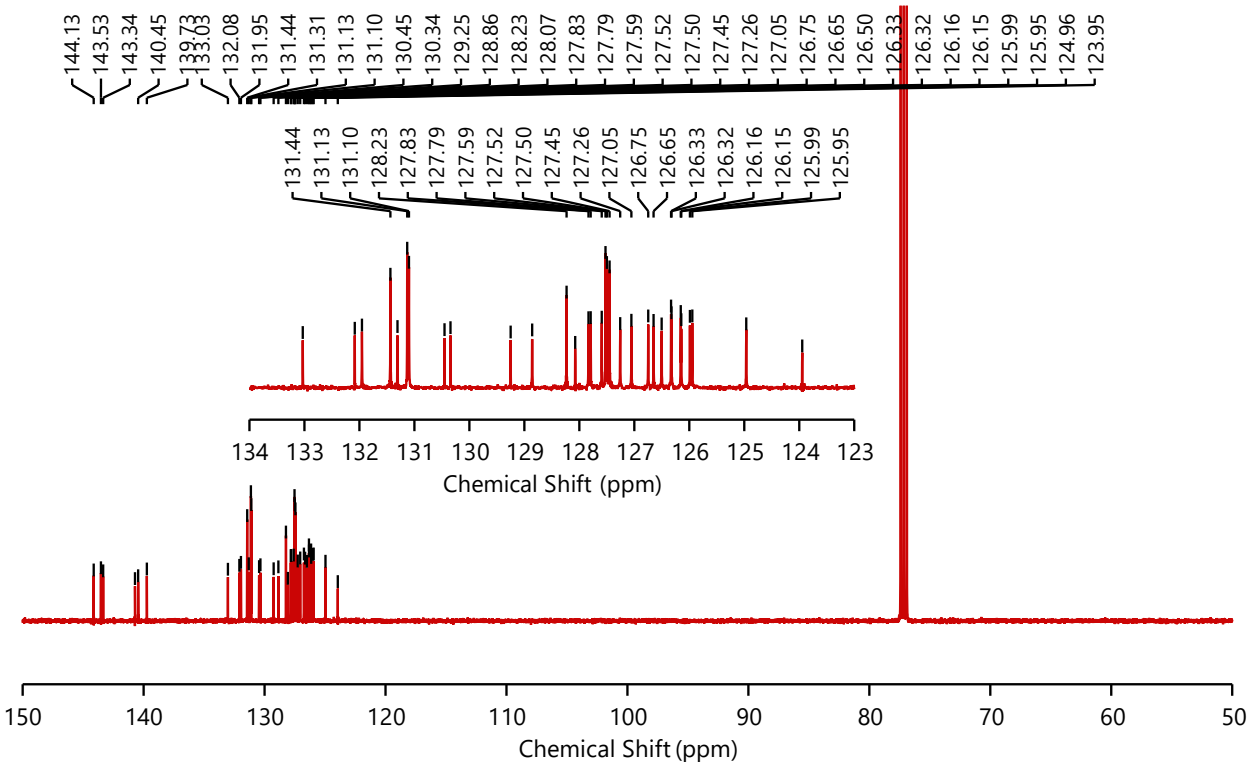

Figure S28. ^{13}C{^{1}H} NMR of *rac*-**2-TH** (125 MHz, $CDCl_3$, 298 K).

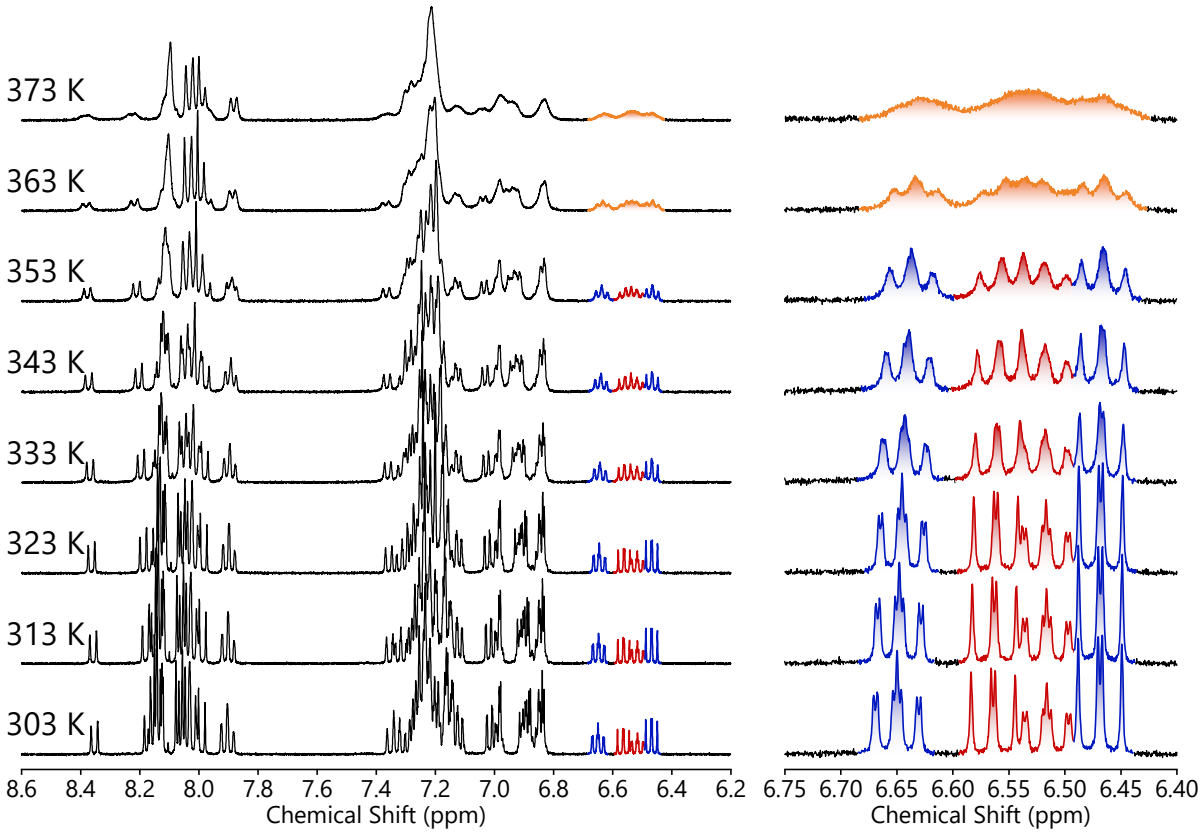

Figure S29. Variable temperature ^{1}H NMR spectra of *rac*-**4-TH** (400 MHz, DMSO-d_6). Notably, the ^{1}H NMR spectrum of **4-TH** obtained at 298 K showed two sets of signals (**4-TH^{1}** (60%, in blue) vs **4-TH^{2}** (40%, in red)), which gradually merged with an increasing in temperature. This might be attributed to the huge steric hindrance between the helicene and AIE moieties.

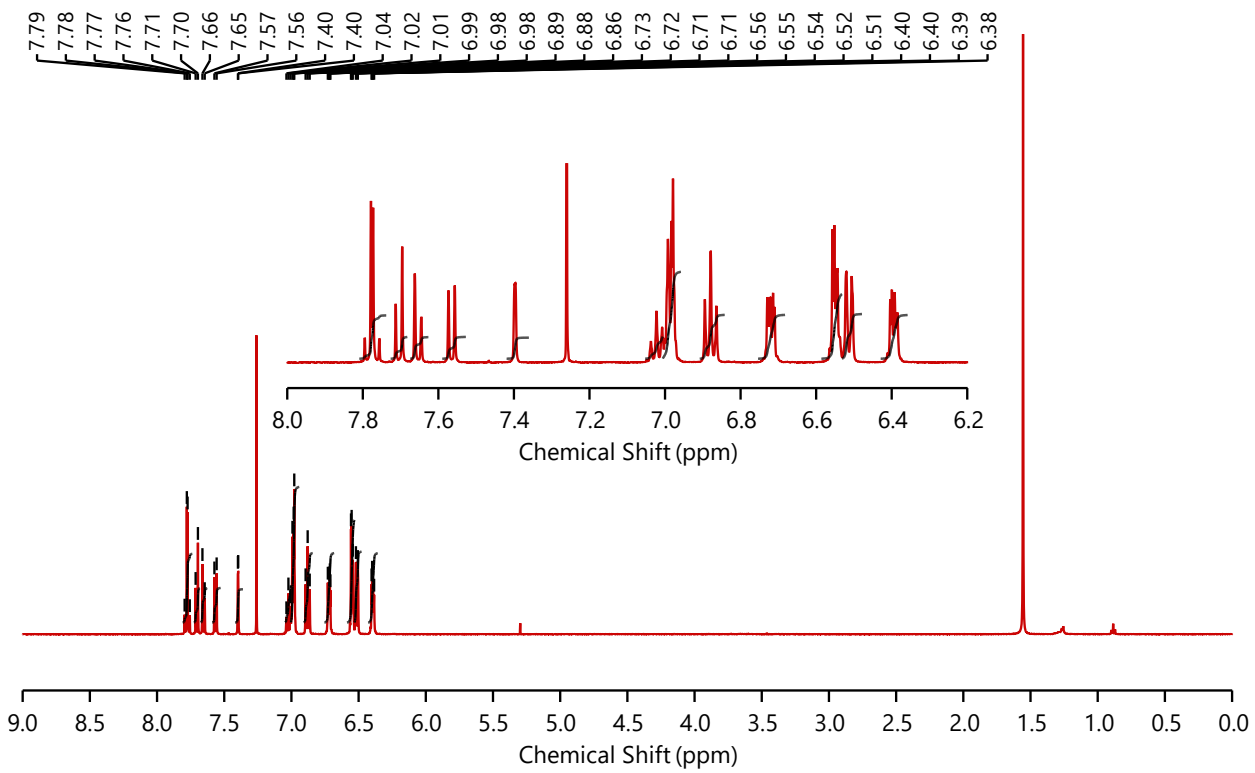

Figure S30. ^{1}H NMR of *rac*-**2,15-BTH** (500 MHz, $CDCl_3$, 298 K).

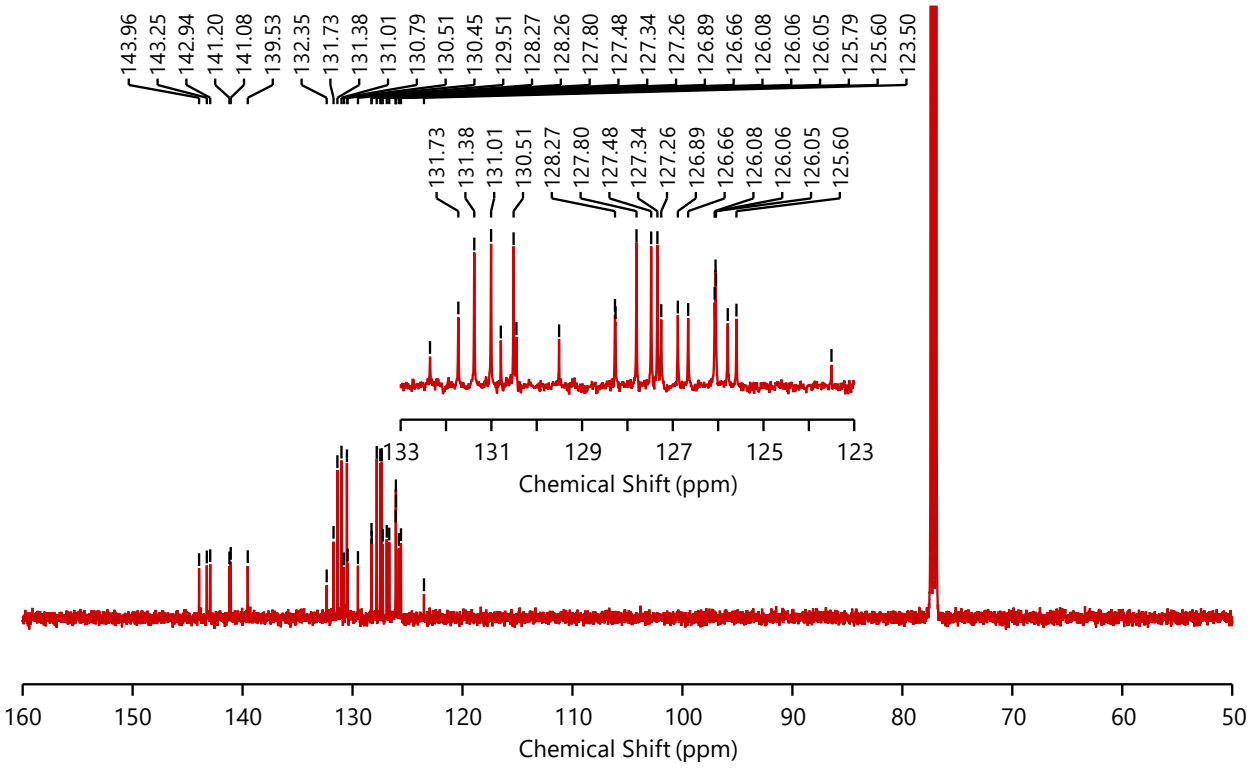

Figure S31. $^{13}C\{^{1}H\}$ NMR of *rac*-**2,15-BTH** (125 MHz, $CDCl_3$, 298 K).

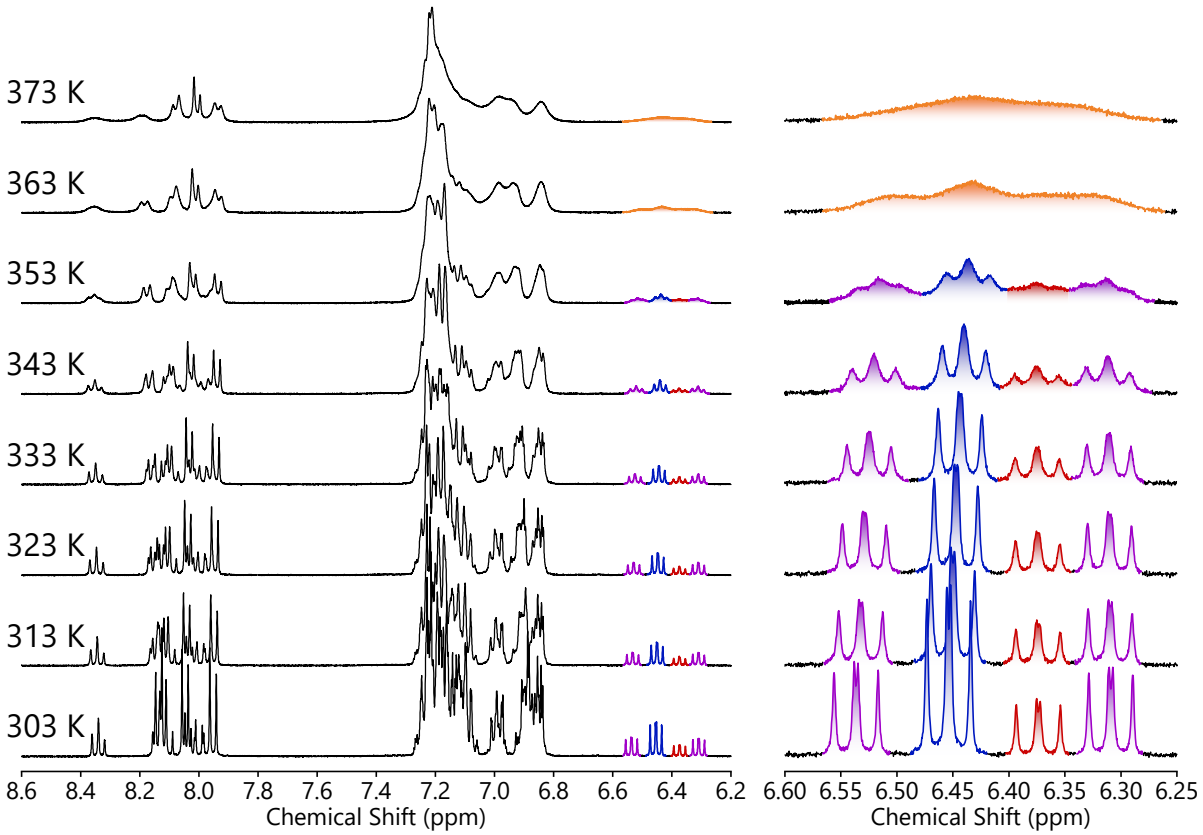

Figure S32. Variable temperature ^{1}H NMR spectra of *rac*-**4,13-BTH** (400 MHz, DMSO-d_6). Notably, the ^{1}H NMR spectrum of **4-TH** obtained at 298 K showed three sets of signals (two symmetric rotamers: **4,13-BTH^{1}** (42%, in blue) and **4,13-BTH^{2}** (13%, in red), and non-symmetric rotamer: **4,13-BTH^{3}** (45%, in purple)), which gradually merged with an increasing in temperature. This might be attributed to the huge steric hindrance between the helicene and AIE moieties.

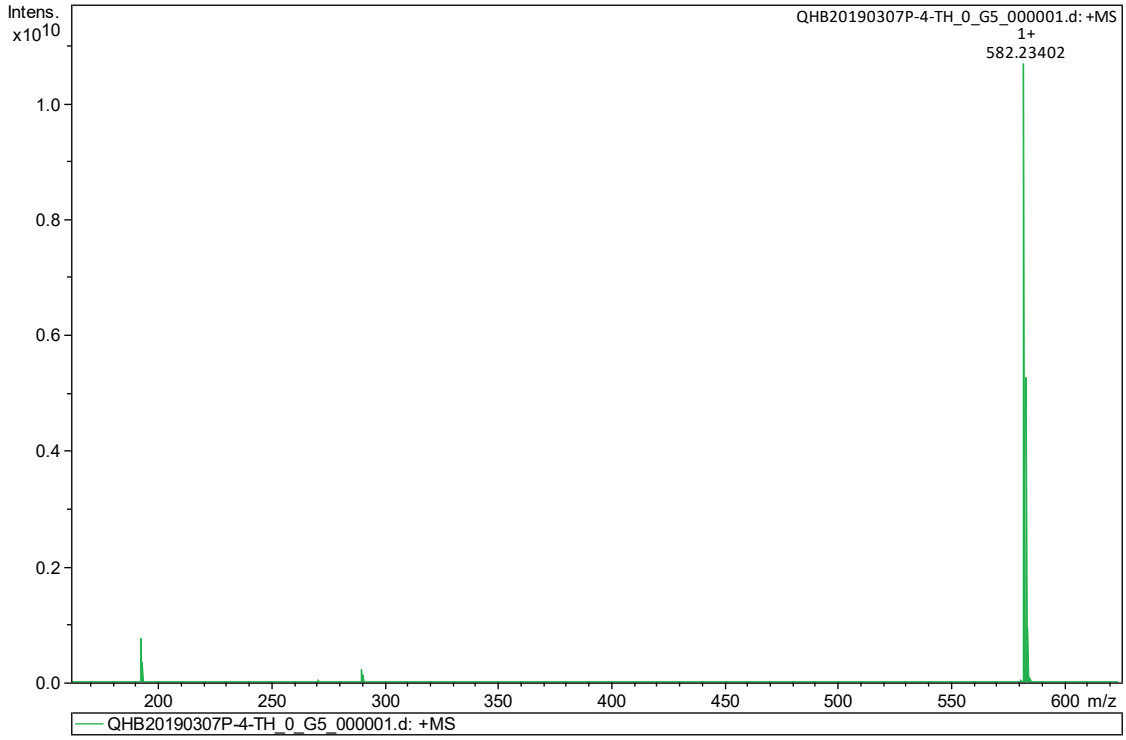

Figure S33. EI-MS spectrum of **4-TH**. Mass peak at *m*/*z* = 582.23402 for [M^+]; calculated mass for [M^+] is 582.23420.

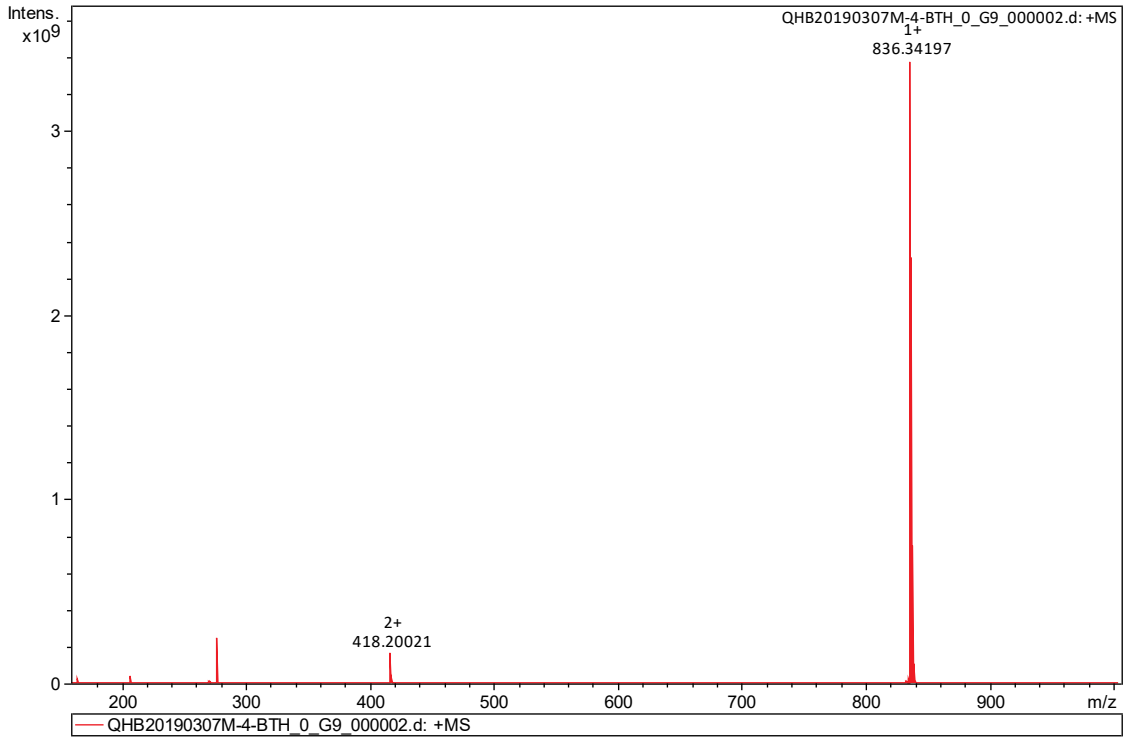

Figure S34. EI-MS spectrum of **4,13-BTH**. Mass peak at *m*/*z* = 836.34197 for [M^+]; calculated mass for [M^+] is 836.34375.

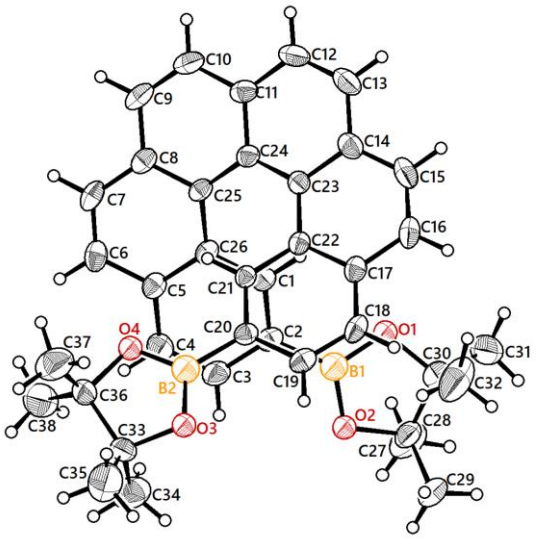

Figure S35. X-ray crystallographic structure of *rac*-2,15-bis(pinacolatoboryl)[6]helicene (only *P* enantiomer is shown). Thermal ellipsoids are shown at the 50% probability level.

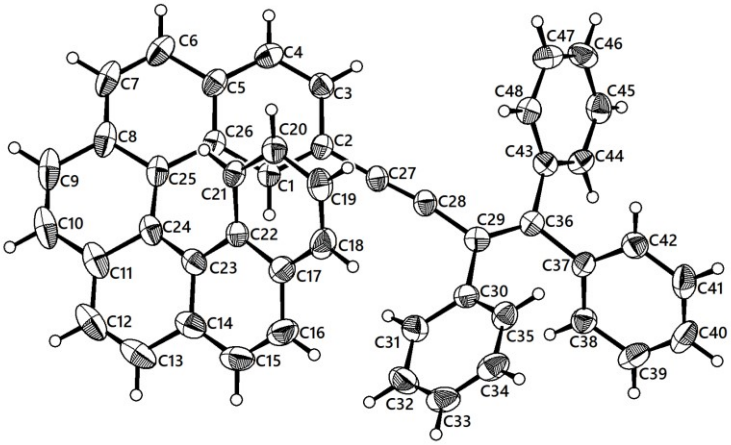

Figure S36. X-ray crystallographic structure of *rac*-**2-TEH** (only *P* enantiomer is shown). Thermal ellipsoids are shown at the 50% probability level.

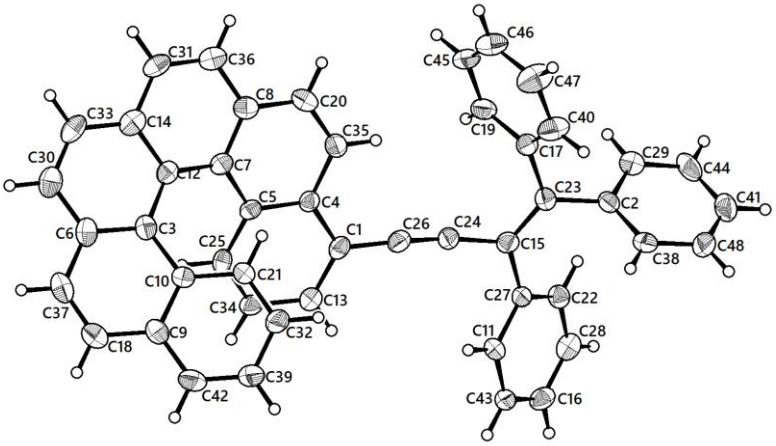

Figure S37. X-ray crystallographic structure of *rac*-**4-TEH** (only *P* enantiomer is shown). Thermal

ellipsoids are shown at the 50% probability level.

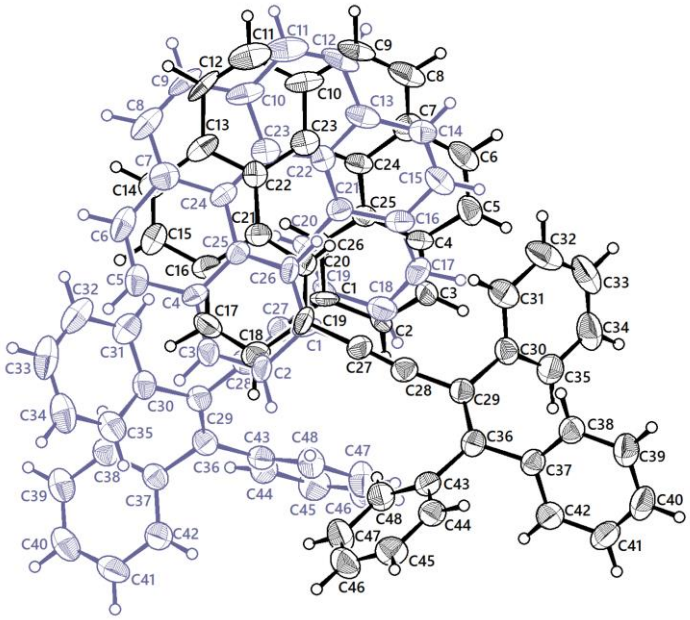

Figure S38. X-ray crystallographic structure of *P*-**2,15-BTEH**. Thermal ellipsoids are shown at the 50% probability level. The symmetric part is shown in blue color and the occupancy of atoms at the helicene unit (C1 to C26) is 0.5.

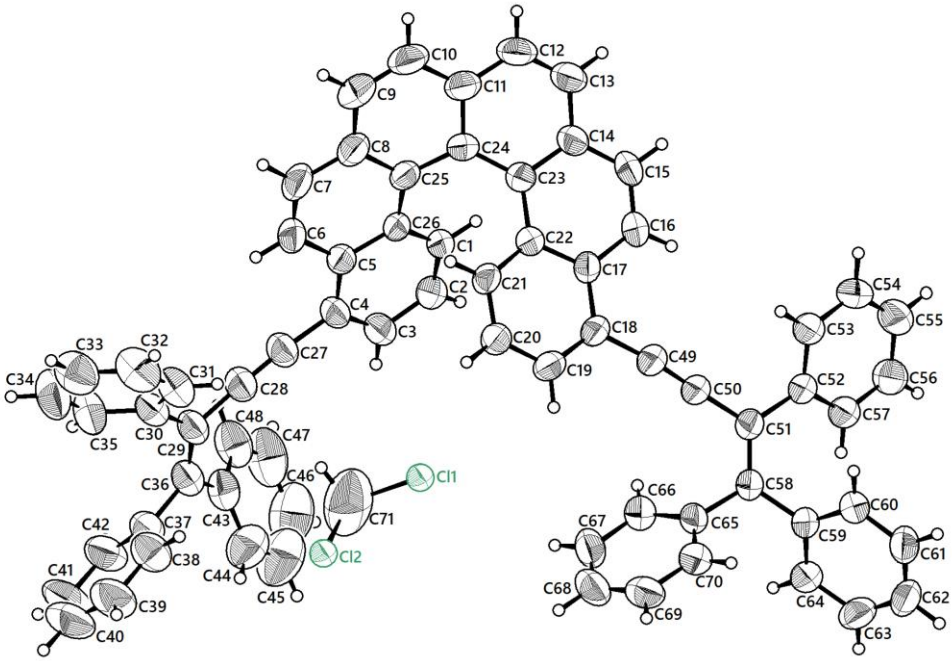

Figure S39. X-ray crystallographic structure of *M*-**4,13-BTEH**. Thermal ellipsoids are shown at the 50% probability level.

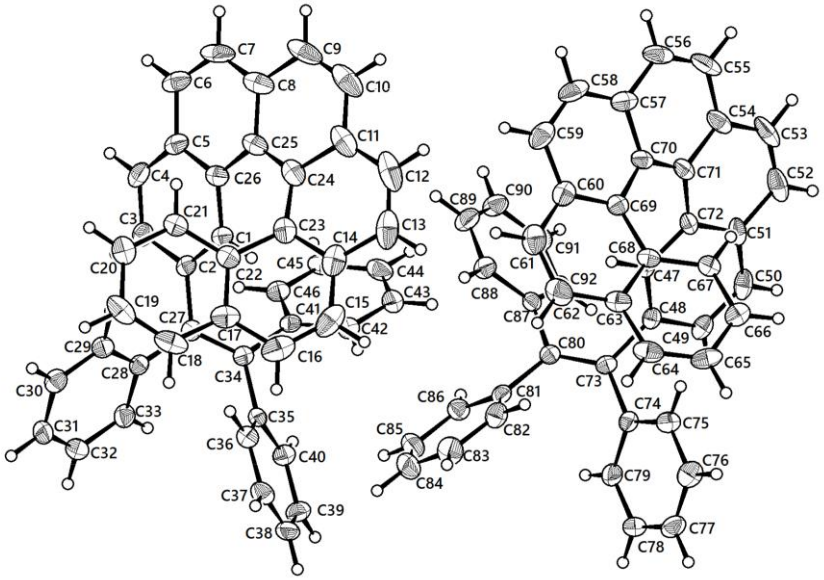

Figure S40. X-ray crystallographic structure of *rac*-**2-TH**. Thermal ellipsoids are shown at the 50% probability level.

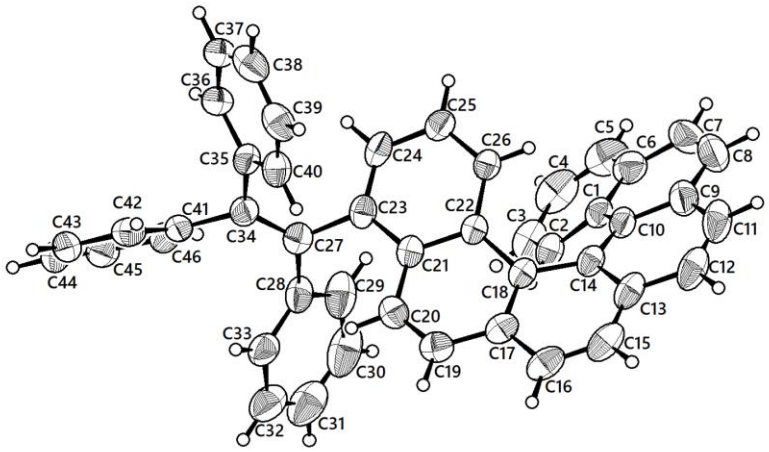

Figure S41. X-ray crystallographic structure of *rac*-**4-TH** (only *M* enantiomer is shown). Thermal ellipsoids are shown at the 50% probability level.

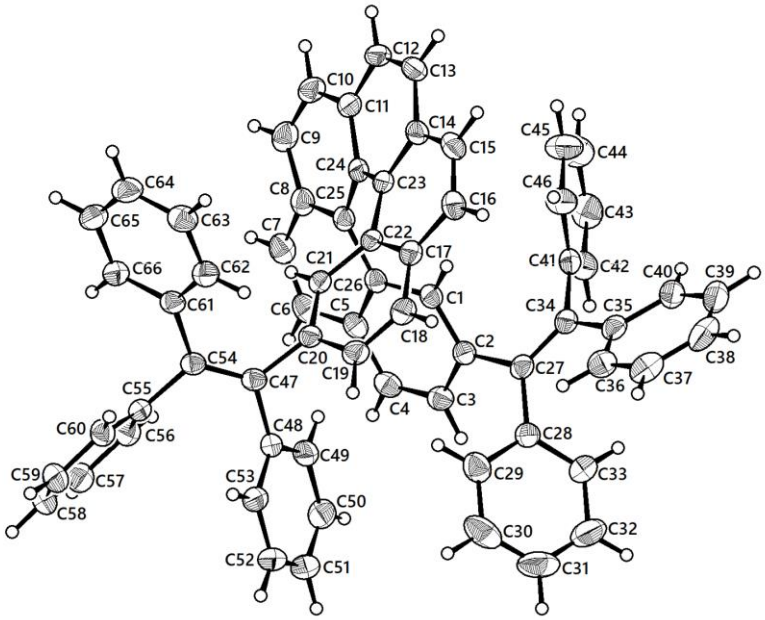

Figure S42. X-ray crystallographic structure of *rac*-**2,15-BTH** (only *M* enantiomer is shown). Thermal ellipsoids are shown at the 50% probability level.

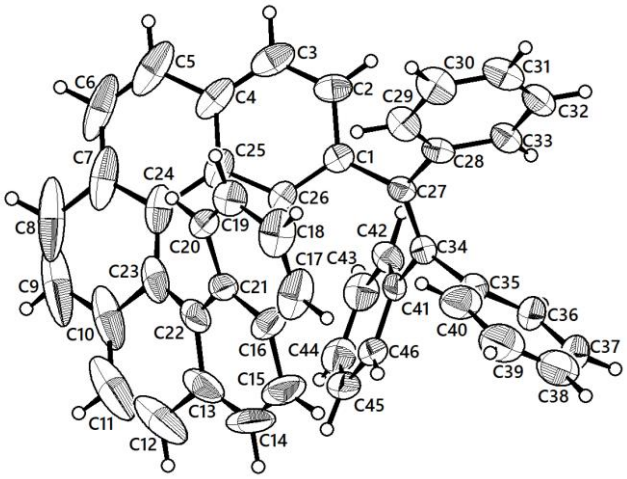

Figure S43. X-ray crystallographic structure of *P*-**2-TH**. Thermal ellipsoids are shown at the 50% probability level.

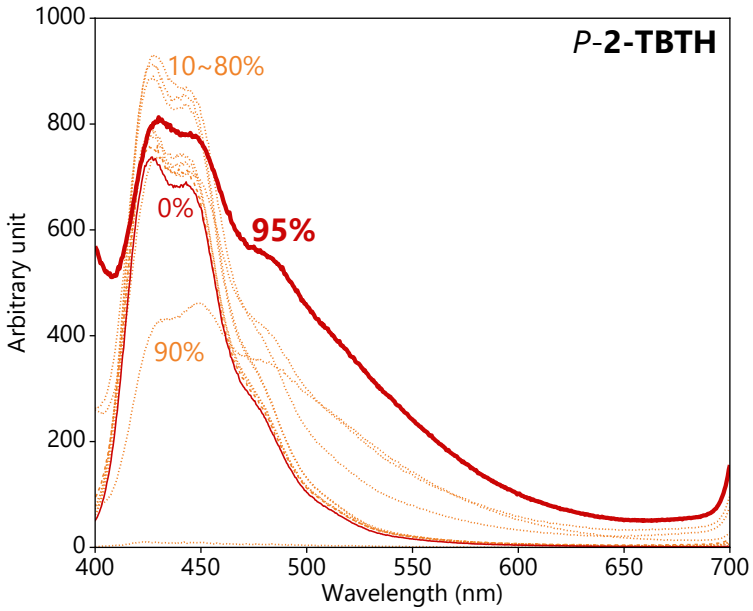

Figure S44. Emission spectra of *P*-**2-TBTH** in various mixtures of THF and water with volume fraction of water varying from 0% to 95% (λ_{ex} = 365 nm).

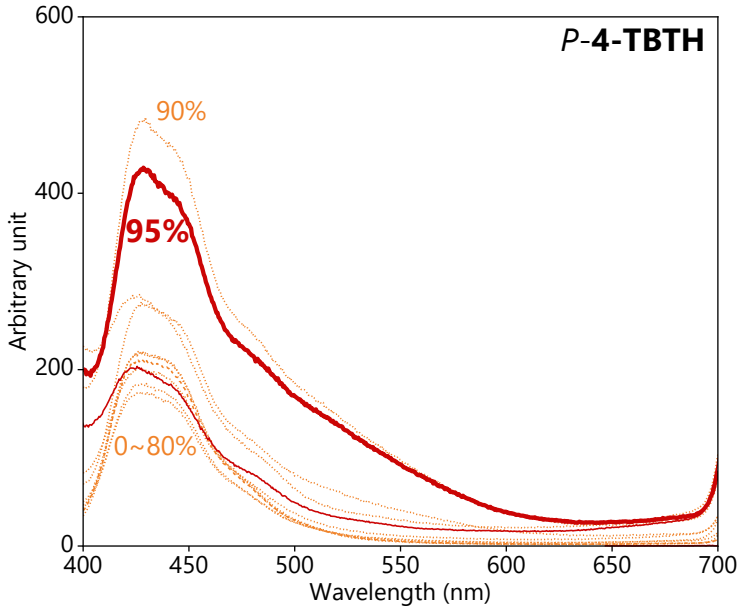

Figure S45. Emission spectra of *P*-**4-TBTH** in various mixtures of THF and water with volume fraction of water varying from 0% to 95% (λ_{ex} = 365 nm).

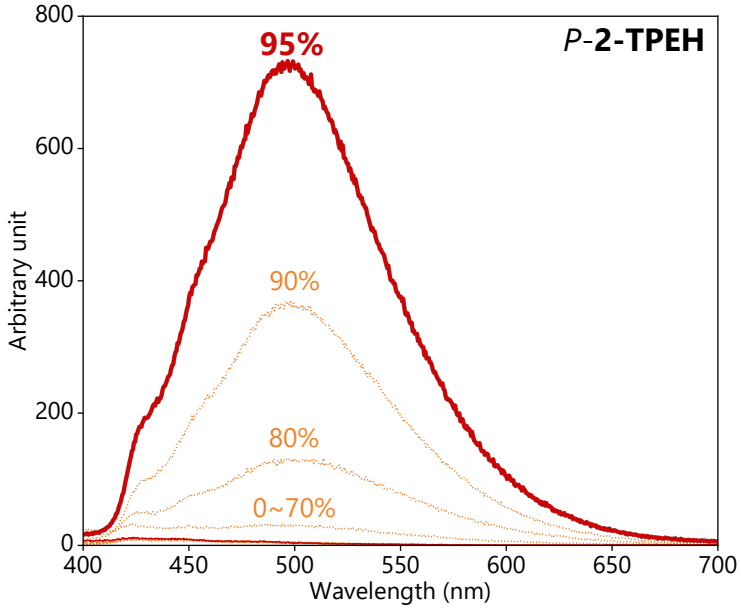

Figure S46. Emission spectra of *P*-**2-TPEH** in various mixtures of THF and water with volume fraction of water varying from 0% to 95% (λ_{ex} = 365 nm).

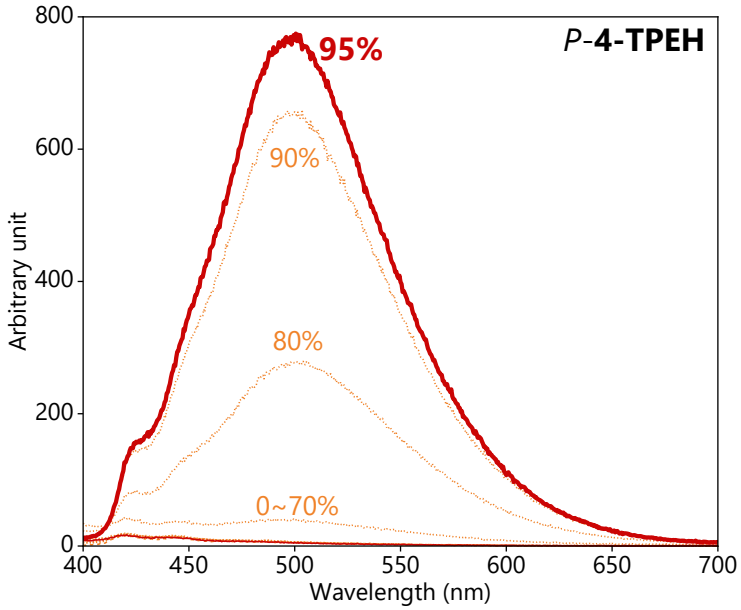

Figure S47. Emission spectra of *P*-**4-TPEH** in various mixtures of THF and water with volume fraction of water varying from 0% to 95% (λ_{ex} = 365 nm).

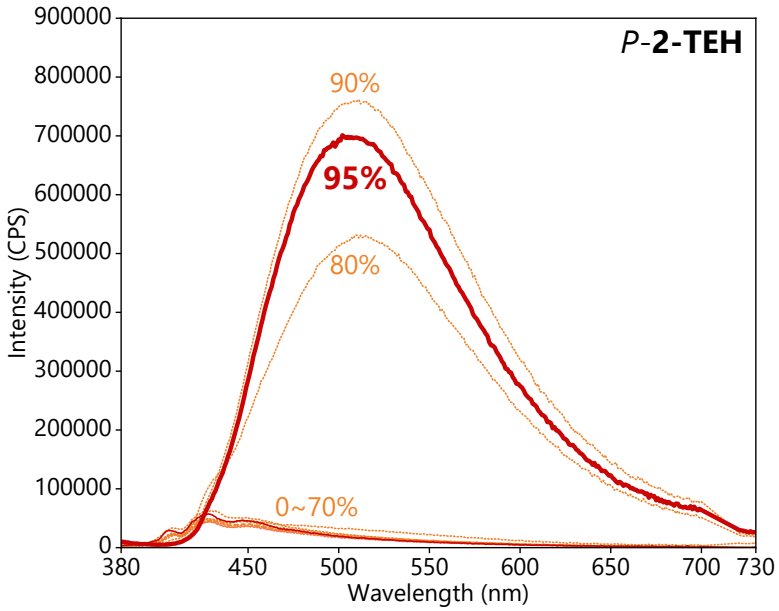

Figure S48. Emission spectra of *P*-**2-TEH** in various mixtures of THF and water with volume fraction of water varying from 0% to 95% (λ_{ex} = 365 nm).

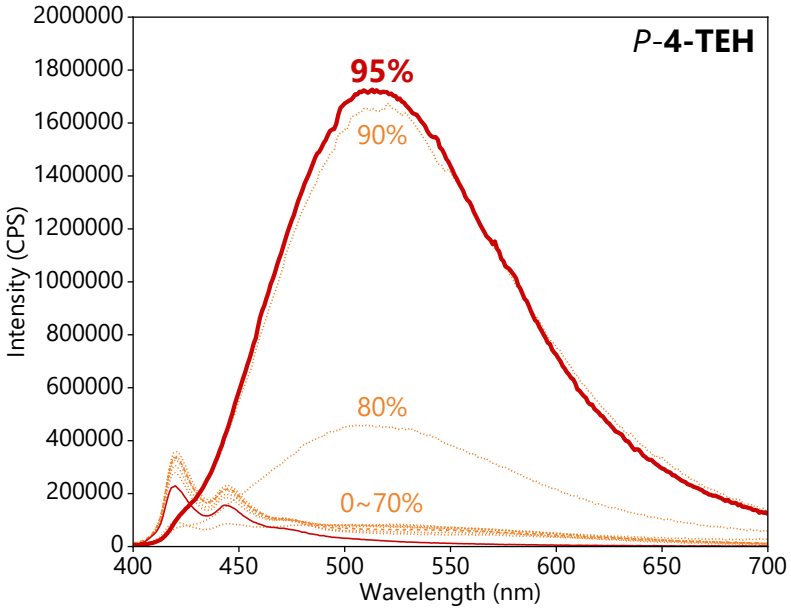

Figure S49. Emission spectra of *P*-**4-TEH** in various mixtures of THF and water with volume fraction of water varying from 0% to 95% (λ_{ex} = 365 nm).

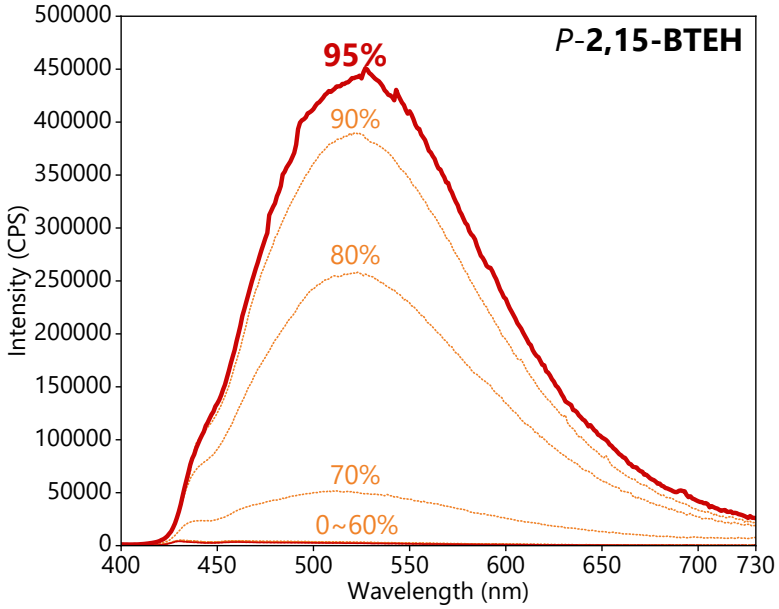

Figure S50. Emission spectra of *P*-**2,15-BTEH** in various mixtures of THF and water with volume fraction of water varying from 0% to 95% (λ_{ex} = 365 nm).

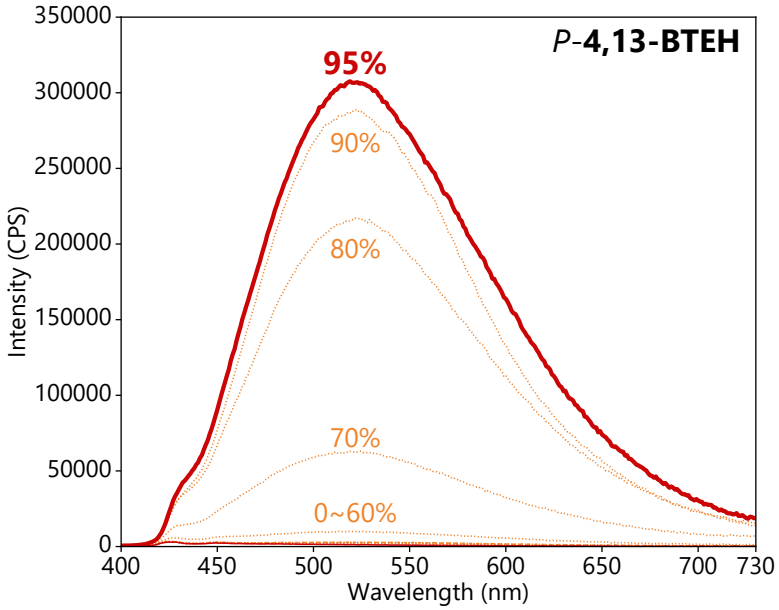

Figure S51. Emission spectra of *P*-**4,13-BTEH** in various mixtures of THF and water with volume fraction of water varying from 0% to 95% (λ_{ex} = 365 nm).

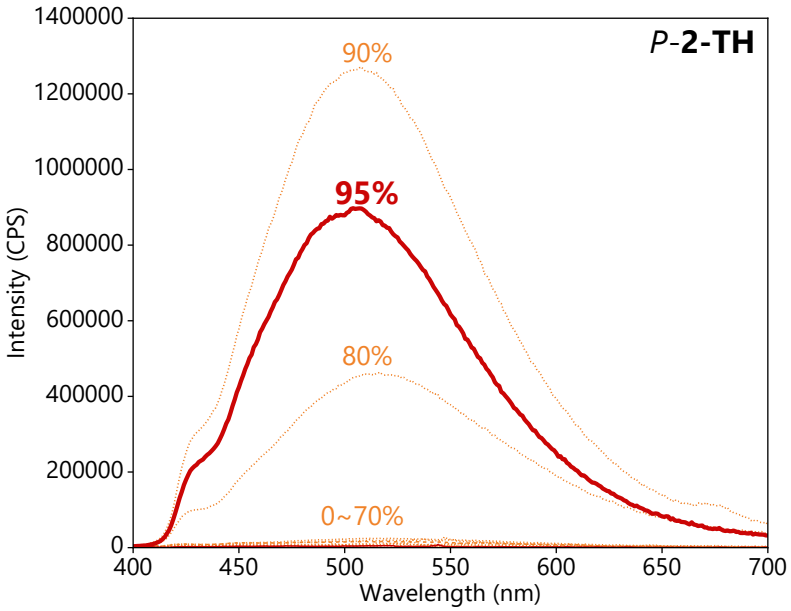

Figure S52. Emission spectra of *P*-**2-TH** in various mixtures of THF and water with volume fraction of water varying from 0% to 95% (λ_{ex} = 365 nm).

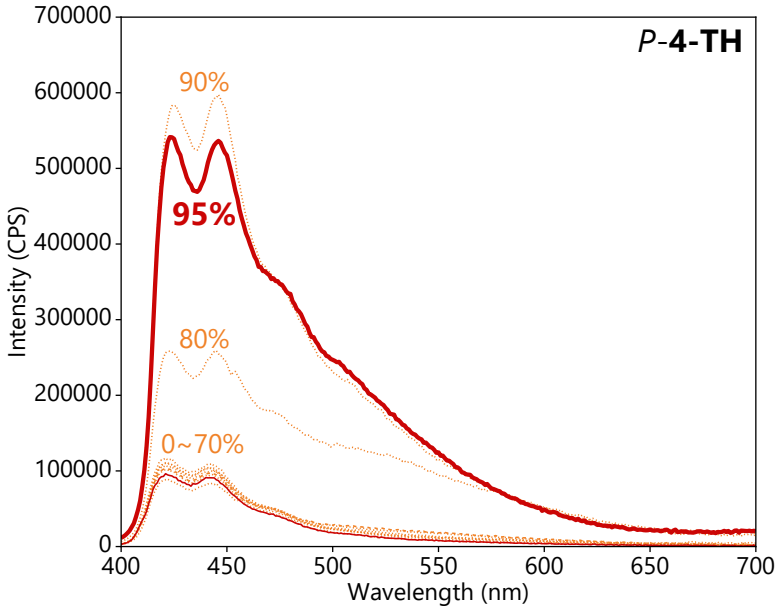

Figure S53. Emission spectra of *P*-**4-TH** in various mixtures of THF and water with volume fraction of water varying from 0% to 95% (λ_{ex} = 365 nm).

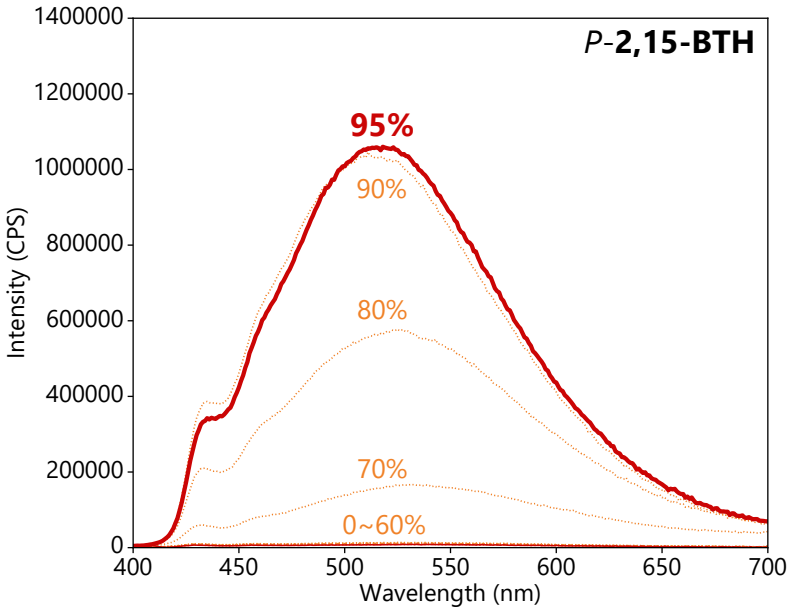

Figure S54. Emission spectra of *P*-**2,15-BTH** in various mixtures of THF and water with volume fraction of water varying from 0% to 95% (λ_{ex} = 365 nm).

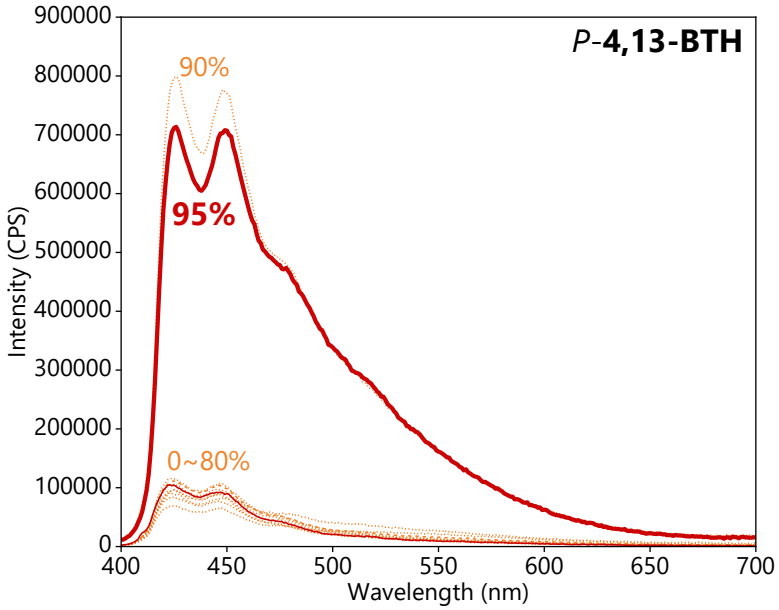

Figure S55. Emission spectra of *P*-**4,13-BTH** in various mixtures of THF and water with volume fraction of water varying from 0% to 95% (λ_{ex} = 365 nm).

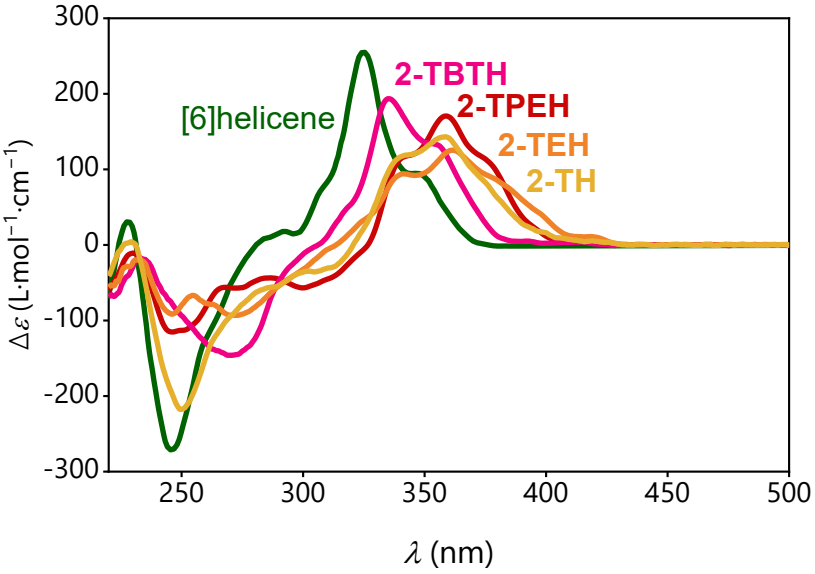

Figure S56. Comparison of ECD curves of **2-TBTH**, **2-TPEH**, **2-TEH**, **2-TH** (in THF) and carbo[6]helicene (in acetonitrile).[9] Only the curves of *P* enantiomers are shown.

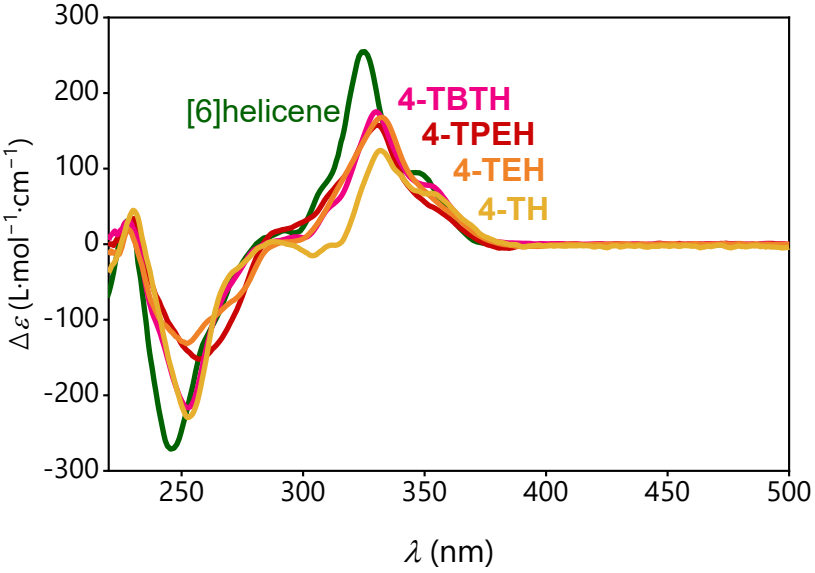

Figure S57. Comparison of ECD curves of **4-TBTH**, **4-TPEH**, **4-TEH**, **4-TH** (in THF) and carbo[6]helicene (in acetonitrile).[9] Only the curves of *P* enantiomers are shown.

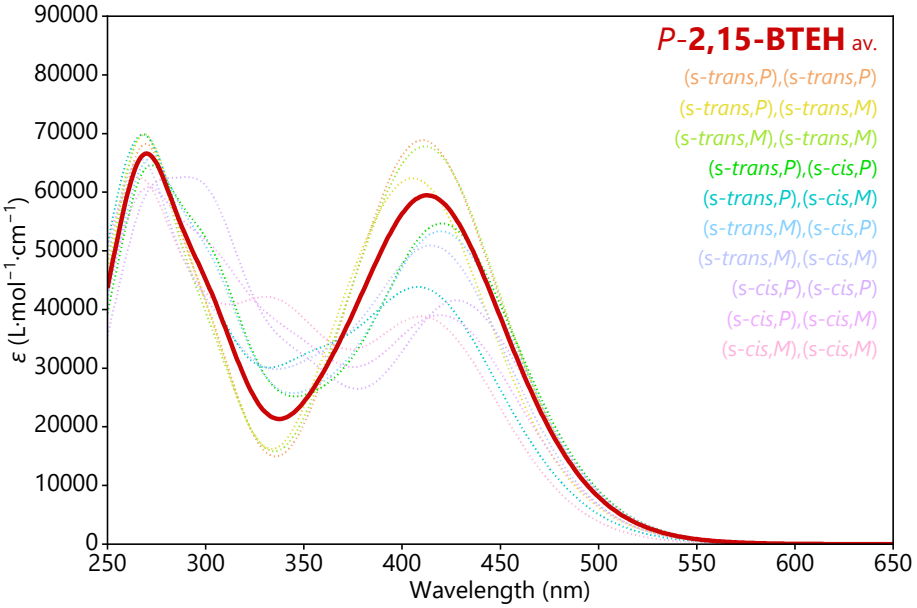

Figure S58. Boltzmann-averaged simulated absorption spectra of *P*-**2,15-BTEH**. Spectra were simulated following a Gaussian function centered at vertical excitation energies with a half-width at half height of 0.25 eV.

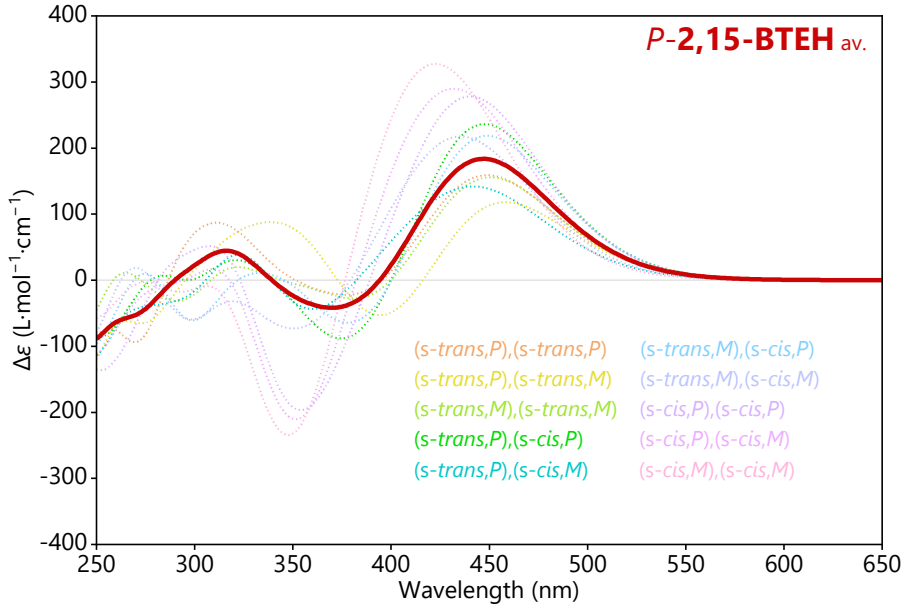

Figure S59. Boltzmann-averaged simulated ECD spectra of *P*-**2,15-BTEH**. Spectra were simulated following a Gaussian function centered at vertical excitation energies with a half-width at half height of 0.25 eV.

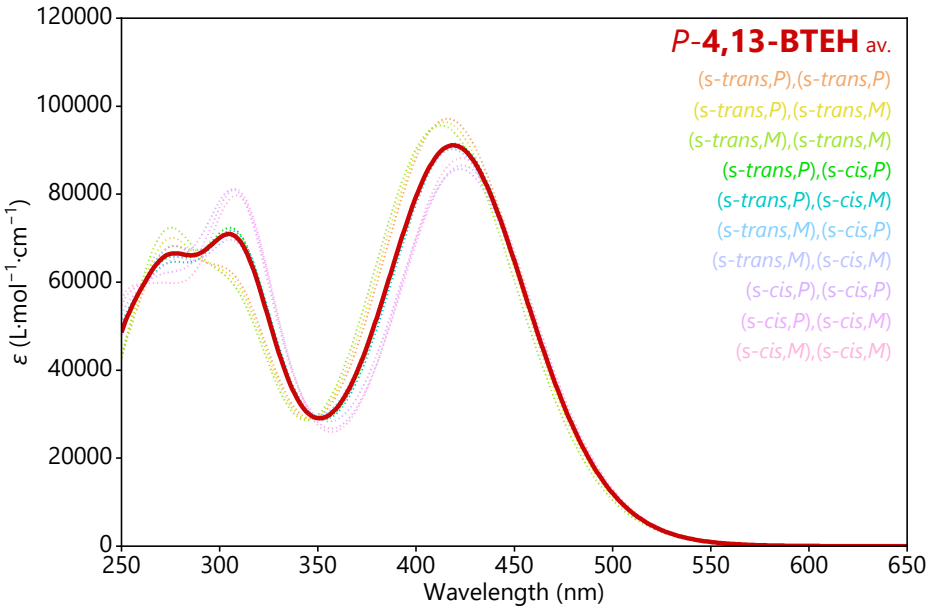

Figure S60. Boltzmann-averaged simulated absorption spectra of *P*-**4,13-BTEH**. Spectra were simulated following a Gaussian function centered at vertical excitation energies with a half-width at half height of 0.25 eV.

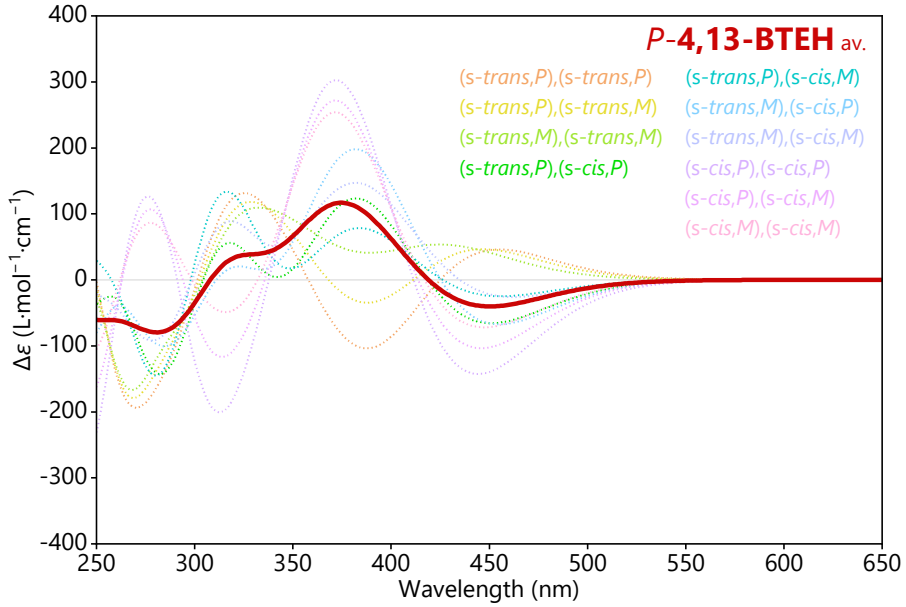

Figure S61. Boltzmann-averaged simulated ECD spectra of *P*-**4,13-BTEH**. Spectra were simulated following a Gaussian function centered at vertical excitation energies with a half-width at half height of 0.25 eV.

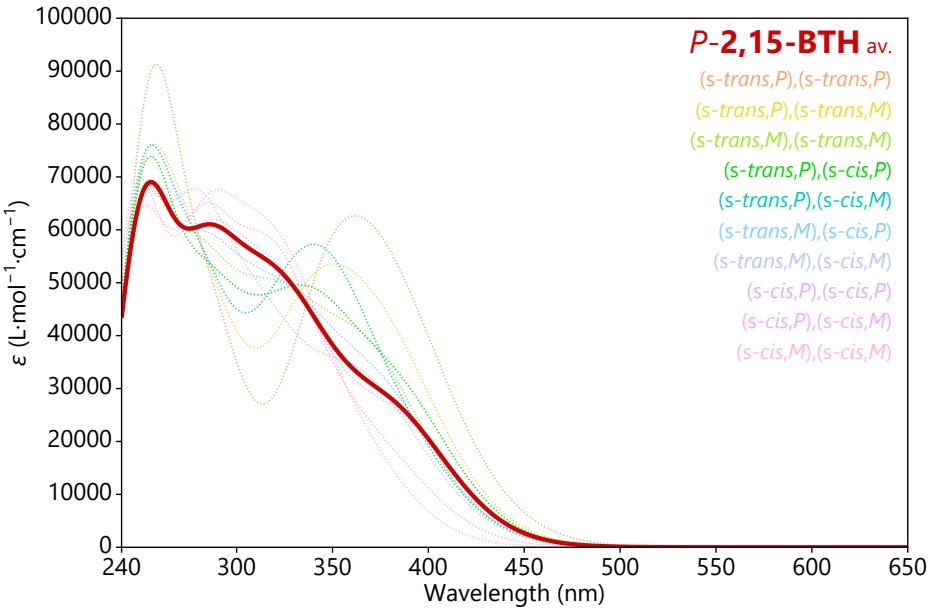

Figure S62. Boltzmann-averaged simulated absorption spectra of *P*-**2,15-BTH**. Spectra were simulated following a Gaussian function centered at vertical excitation energies with a half-width at half height of 0.25 eV.

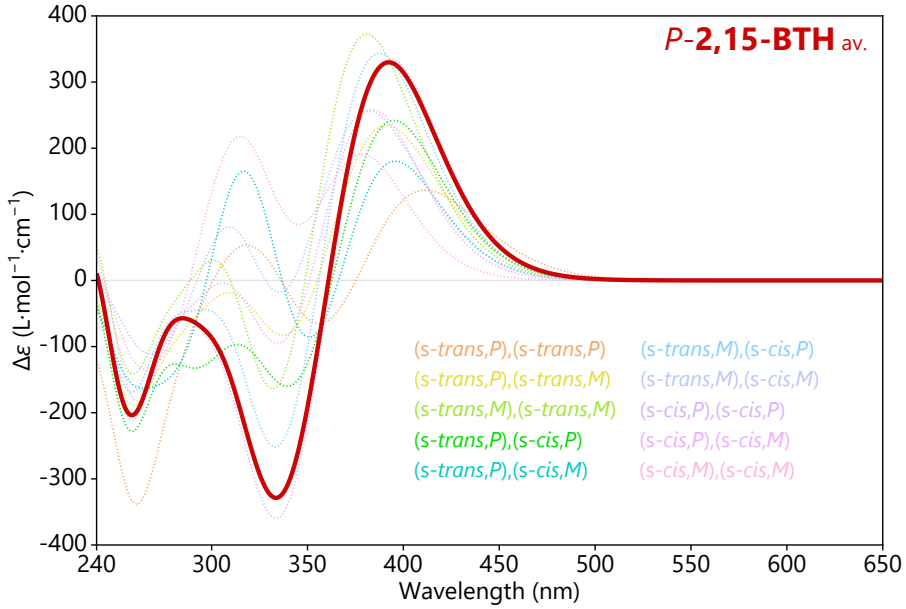

Figure S63. Boltzmann-averaged simulated ECD spectra of *P*-**2,15-BTH**. Spectra were simulated following a Gaussian function centered at vertical excitation energies with a half-width at half height of 0.25 eV.

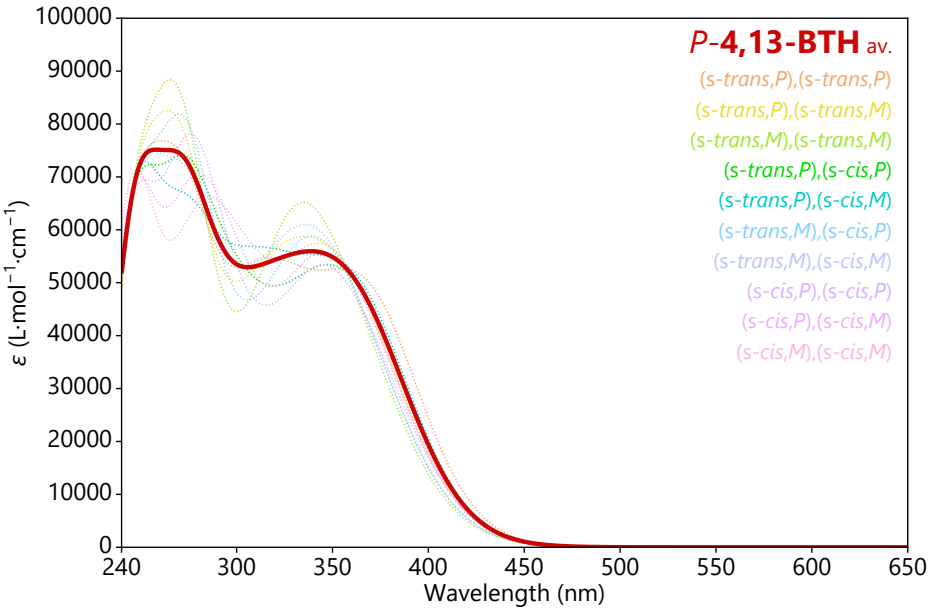

Figure S64. Boltzmann-averaged simulated absorption spectra of *P*-**4,13-BTH**. Spectra were simulated following a Gaussian function centered at vertical excitation energies with a half-width at half height of 0.25 eV.

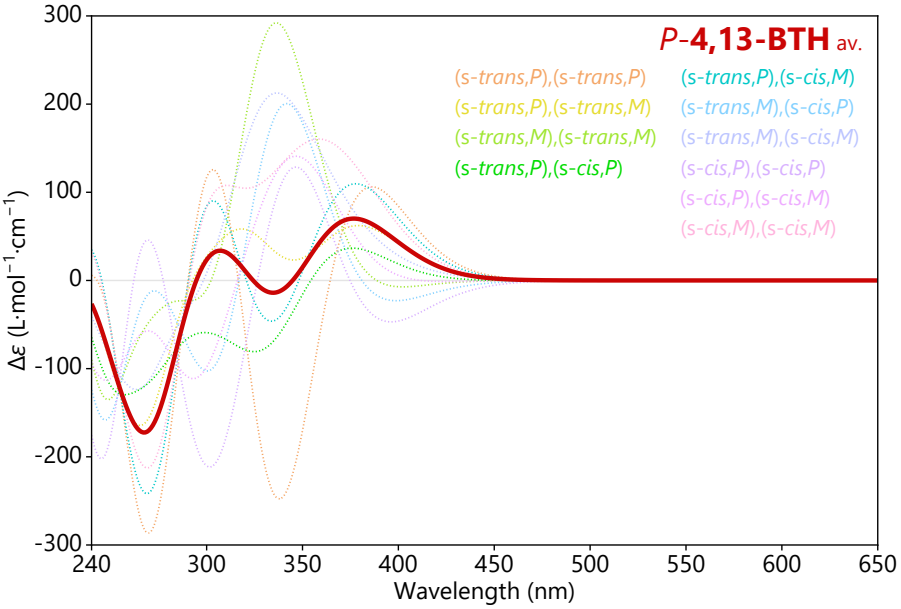

Figure S65. Boltzmann-averaged simulated ECD spectra of *P*-**4,13-BTH**. Spectra were simulated following a Gaussian function centered at vertical excitation energies with a half-width at half height of 0.25 eV.

References

(1) Frisch, M. J.; Trucks, G. W.; Schlegel, H. B.; Scuseria, G. E.; Robb, M. A.; Cheeseman, J. R.; Scalmani, G.; Barone, V.; Mennucci, B.; Petersson, G. A.; Nakatsuji, H.; Caricato, M.; Li, X.; Hratchian, H. P.; Izmaylov, A. F.; Bloino, J.; Zheng, G.; Sonnenberg, J. L.; Hada, M.; Ehara, M.; Toyota, K.; Fukuda, R.; Hasegawa, J.; Ishida, M.; Nakajima, T.; Honda, Y.; Kitao, O.; Nakai, H.; Vreven, T.; Montgomery, J. A., Jr.; Peralta, J. E.; Ogliaro, F.; Bearpark, M.; Heyd, J. J.; Brothers, E.; Kudin, K. N.; Staroverov, V. N.; Kobayashi, R.; Normand, J.; Raghavachari, K.; Rendell, A.; Burant, J. C.; Iyengar, S. S.; Tomasi, J.; Cossi, M.; Rega, N.; Millam, J. M.; Klene, M.; Knox, J. E.; Cross, J. B.; Bakken, V.; Adamo, C.; Jaramillo, J.; Gomperts, R.; Stratmann, R. E.; Yazyev, O.; Austin, A. J.; Cammi, R.; Pomelli, C.; Ochterski, J. W.; Martin, R. L.; Morokuma, K.; Zakrzewski, V. G.; Voth, G. A.; Salvador, P.; Dannenberg, J. J.; Dapprich, S.; Daniels, A. D.; Farkas, Ö.; Foresman, J. B.; Ortiz, J. V.; Cioslowski, J.; Fox, D. J. *Gaussian, Inc., Wallingford CT,* **2009**.

(2) Lee, C.; Yang, W.; Parr, R. G. *Phys. Rev. B: Condens. Matter Mater. Phys.* **1988**, *37*, 785.

(3) Marenich, A. V.; Cramer, C. J.; Truhlar, D. G. *J. Phys. Chem. B* **2009**, *113*, 6378.

(4) Lightner, D. A.; Hefelfinger, D. T.; Powers, T. W.; Frank G. W.; Trueblodd, K. N. *J. Am. Chem. Soc.* **1972**, *94*, 3492.

(5) Nakazaki, M.; Yamamoto, K.; Ikeda, T.; Kitsuki, T.; Okamoto, Y. *J. Chem. Soc., Chem. Commun.* **1983**, 787.

(6) Anger, E.; Srebro, M.; Vanthuyne, N.; Toupet, L.; Rigaut, S.; Roussel, C.; Autschbach, J.; Crassous, J. *J. Am. Chem. Soc.* **2012**, *134*, 15628.

(7) Malik, A. U.; Gan, F.; Shen, C.; Yu, N.; Wang, R.; Crassous, J.; Shu, M.; Qiu, H. *J. Am. Chem. Soc.* **2018**, *140*, 2769.

(8) Jana, D.; Ghorai, B. K. *Tetrahedron* **2012**, *68*, 7309.

(9) Nakai, Y.; Mori, T.; Inoue, Y. *J. Phys. Chem. A* **2012,** *116*, 7372.